

Analysis and Optimization of A Double-IRS Cooperatively Assisted System with A Quasi-Static Phase Shift Design

Gengfa Ding, Feng Yang, Lianghui Ding, and Ying Cui

Abstract

The analysis and optimization of single intelligent reflecting surface (IRS)-assisted systems have been extensively studied, whereas little is known regarding multiple-IRS-assisted systems. This paper investigates the analysis and optimization of a double-IRS cooperatively assisted downlink system, where a multi-antenna base station (BS) serves a single-antenna user with the help of two multi-element IRSs, connected by an inter-IRS channel. The channel between any two nodes is modeled with Rician fading. The BS adopts the instantaneous CSI-adaptive maximum-ratio transmission (MRT) beamformer, and the two IRSs adopt a cooperative quasi-static phase shift design. The goal is to maximize the average achievable rate, which can be reflected by the average channel power of the equivalent channel between the BS and user, at a low phase adjustment cost and computational complexity. First, we obtain tractable expressions of the average channel power of the equivalent channel in the general Rician factor, pure line of sight (LoS), and pure non-line of sight (NLoS) regimes, respectively. Then, we jointly optimize the phase shifts of the two IRSs to maximize the average channel power of the equivalent channel in these regimes. The optimization problems are challenging non-convex problems. We obtain globally optimal closed-form solutions for some cases and propose computationally efficient iterative algorithms to obtain stationary points for the other cases. Next, we compare the computational complexity for optimizing the phase shifts and the optimal average channel power of the double-IRS cooperatively assisted system with those of a counterpart single-IRS-assisted system at a large number of reflecting elements in the three regimes. Finally, we numerically demonstrate notable gains of the proposed solutions over the existing solutions at different system parameters. To our knowledge, this is the first work that optimizes the quasi-static phase shift design of a double-IRS cooperatively assisted system and characterizes its advantage over the optimal quasi-static phase shift design of the counterpart single-IRS-assisted system.

Index Terms

Intelligent reflecting surface (IRS), double IRSs, cooperation, quasi-static phase shift design, coordinate descent, optimization.

The authors are with the Department of Electronic Engineering, Shanghai Jiao Tong University, Shanghai 200240, China. The paper has been submitted in part to ICC 2022 [1].

I. INTRODUCTION

Stringent requirements for future wireless networks, such as ultra-high data rate and energy efficiency, cannot be fully achieved with the existing wireless communication technologies. Intelligent reflecting surface (IRS), which consists of nearly passive, low-cost, reflecting elements with reconfigurable parameters, has been recently recognized as a promising solution for improving spectrum and energy efficiency [2], [3]. There have been extensive studies on IRS. In what follows, we restrict our attention to the optimization of base station (BS) beamforming and IRS phase shifts for an IRS-assisted single-cell network. The optimal designs for IRS-assisted multi-cell networks [4]–[7] are out of the scope of this paper. In the existing works on optimal designs for IRS-assisted systems, BS beamforming designs are usually adaptive to instantaneous channel state information (CSI), whereas the phase shift designs can be classified into instantaneous CSI-adaptive phase shift designs [8]–[13] (which adapt to instantaneous CSI) and quasi-static phase shift designs (which adapt to CSI statistics and do not change over time slots during a certain time period) [14]–[18]. Notice that a quasi-static (also termed statistical) phase shift design yields a low phase adjustment cost at some performance sacrifice compared with an instantaneous CSI-adaptive phase shift design. Considering the practical implementation issue, a quasi-static phase shift design may be more valuable [6], [7], [14]–[18].

Early research on IRS investigates the optimal design for an IRS-assisted system with a single IRS. For example, in [8]–[11], [14]–[16], the authors optimize the BS beamformer and IRS phase shifts to minimize the transmit power [8], outage probability [15], and average transmit power [16] and maximize the weighted sum rate [9], secrecy rate [10], energy efficiency [11], and ergodic rate [14]. Specifically, [8]–[11] adopt instantaneous CSI-adaptive phase shift designs, whereas [14]–[16] consider quasi-static phase shift designs.

Later study regarding IRS concentrates on the optimal design for an IRS-assisted system with more than one IRS. For instance, in [12], [13], [17], [18], the authors optimize the BS beamformer and IRS phase shifts to minimize the outage probability [17] and maximize the sum secrecy rate [12], received signal power [13], and ergodic achievable rate [18]. In particular, [12], [13] adopt instantaneous CSI-adaptive phase shift designs, whereas [17], [18] consider quasi-static phase shift designs. Notice that the abovementioned works on multi-IRS-assisted systems [12], [13], [17], [18] ignore channels between any two IRSs, referred to as inter-IRS channels, and hence cannot capture their interaction. To achieve the full potential of multi-IRS-assisted

systems, [19]–[25] explicitly model the inter-IRS channel in a double-IRS-assisted system and consider the cooperation between them. Specifically, [21] and [22] propose cascaded channel estimation methods for a double-IRS-assisted SISO system [21] and a double-IRS-assisted MIMO system [22], respectively. In [19], [20], the authors show that the power gain with respect to (w.r.t.) the total number of reflecting elements of a double-IRS-assisted system is higher in order than that of the counterpart single-IRS-assisted system. In [23]–[25], the authors optimize the BS beamformer and IRS phase shifts to maximize the signal-to-interference-plus-noise ratio (SINR) [23], capacity [24], and secrecy rate [25].

There are two main limitations for the existing works on double-IRS cooperatively assisted systems [19]–[25]. Firstly, [19]–[25] simply assume that the direct link between the BS and user is entirely blocked for tractability. Secondly, [19]–[25] solely consider instantaneous CSI-adaptive phase shift designs, which have higher phase adjustment costs and are more difficult to implement in practice. Therefore, the analysis and optimization of a double-IRS cooperatively assisted system with a general channel model and a quasi-static phase shift design remains open.

In this paper, we shall shed some light on the above issue. Specifically, we consider a double-IRS cooperatively assisted downlink system, where a multi-antenna BS serves a single-antenna user with the help of two multi-element IRSs connected by an inter-IRS channel. The antennas at the BS and the reflecting elements at the IRSs are arranged in uniform rectangular arrays (URAs). The channel between any two nodes in the system is modeled with Rician fading. In particular, the line of sight (LoS) components do not change during the considered time, and the non-line of sight (NLoS) components vary from time slot to time slot. The BS adopts the instantaneous CSI-adaptive maximum-ratio transmission (MRT) beamformer, and the two IRSs adopt a cooperative quasi-static phase shift design, to improve the average achievable rate at a low phase adjustment cost and computational complexity. As the average achievable rate can be approximately reflected by the average channel power of the equivalent channel between the BS and user with a negligible approximation error, this paper focuses on the analysis and optimization of the average channel power¹ rather than the average achievable rate. The main contributions of this paper are summarized as follows.

- **Analysis of Average Channel Power:** First, we characterize the influences of the phase

¹If not specified otherwise, the average channel power means the average channel power of the equivalent channel between the BS and user.

shifts of the two IRSs on the average channel power and divide the channel conditions into four cases accordingly. Then, we obtain the tractable expressions of the average channel power in the general Rician factor, pure LoS, and pure NLoS regimes, respectively.

- **Optimization of Average Channel Power:** First, we jointly optimize the phase shifts of the two IRSs to maximize the average channel power in the general Rician factor and pure LoS regimes, respectively. The corresponding optimization problems are challenging non-convex problems. We obtain globally optimal closed-form solutions for some cases and propose computationally efficient iterative algorithms to obtain stationary points for the other cases based on the coordinate descent (CD) and block coordinate descent (BCD) methods. Then, in each Rician factor regime, we characterize the optimal average channel power when the total number of the reflecting elements is large.
- **Comparison with Single-IRS-Assisted System:** First, we analyze and optimize the average channel power of a counterpart single-IRS-assisted system. Then, we compare the computational complexities for calculating the quasi-static phase shift designs and optimal average channel powers of the double-IRS cooperatively assisted system and the single-IRS-assisted system. Specifically, we show that the double-IRS cooperatively assisted system can achieve a better performance and computational complexity tradeoff in practice.
- **Numerical Results:** We numerically demonstrate notable gains of the proposed solutions over the existing quasi-static phase designs for the single-IRS-assisted systems with the IRS located at different positions and the corresponding double-IRS-assisted system without the inter-IRS channel. Furthermore, we numerically show that for the double-IRS cooperatively assisted system, the proposed quasi-static phase shift design is more desirable than the respective instantaneous CSI-adaptive phase shift designs as long as the LoS components are sufficiently large.

Notation: Boldface lower-case letters (e.g., \mathbf{x}), boldface upper-case letters (e.g., \mathbf{X}), non-boldface letters (e.g., x), and calligraphic upper-case letters (e.g., \mathcal{X}) denote vectors, matrices, scalars, and sets, respectively. \mathbf{X}^H , \mathbf{X}^T , $\text{tr}(\mathbf{X})$, and $\|\mathbf{X}\|_F$ denote the conjugate transpose, transpose, trace, and Frobenius norm of a matrix, respectively. $\text{vec}(\mathbf{X})$ denotes the vectorization of a matrix. $\text{diag}(\mathbf{x})$ denotes a square diagonal matrix with the elements in \mathbf{x} on its main diagonal. $\text{Diag}(\mathbf{X})$ denotes the leading diagonal of matrix \mathbf{X} . $\|\mathbf{x}\|_2$ denotes the Euclidean norm of a vector. $\Re\{x\}$ and $|x|$ denote the real part and modulus of a complex number, respectively.

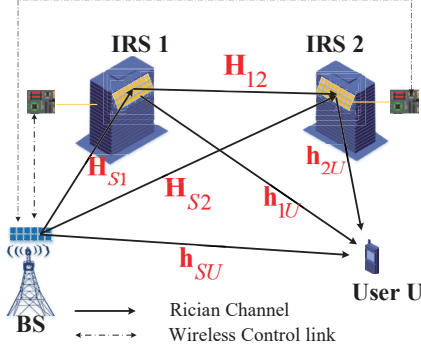


Fig. 1: Double-IRS cooperatively assisted system.

$\angle(\mathbf{x})$ denotes the argument of each element of \mathbf{x} . $\mathbb{E}[\cdot]$ denotes the expectation w.r.t. all random variables in the brackets. \otimes denotes the kronecker product. $\mathbb{C}^{a \times b}$ and $\mathbb{R}^{a \times b}$ denote the space of $a \times b$ complex-valued and real-valued matrices, respectively. $\mathcal{CN}(\mu, \sigma^2)$ denotes a circularly symmetric complex Gaussian random variable with mean μ and variance σ^2 . $\mathbf{1}_T$ and $\mathbf{0}_T$ denote the T dimensional vectors with all elements being 1 and 0, respectively. $X \stackrel{d}{\sim} Y$ represents that random variables X and Y follow the same distribution.

II. SYSTEM MODEL

As shown in Fig. 1, we consider a double-IRS cooperatively assisted downlink system where a multi-antenna BS, represented by S , communicates to a single-antenna user, represented by U , with the help of two multi-element IRSs, indexed by 1 and 2, which are connected by an inter-IRS channel. Let $\mathcal{L} \triangleq \{1, 2\}$ denote the set of IRS indices. The locations of the BS and IRSs are fixed, and the user is static during a certain period. The BS is equipped with a URA of $M_S \times N_S$ antennas. Each IRS $l \in \mathcal{L}$ is equipped with a URA of $M_l \times N_l$ reflecting elements. Let $T_i \triangleq M_i N_i$, $i = S, 1, 2$, denote the numbers of the BS's antennas and IRSs' reflecting elements. Let $T \triangleq T_1 + T_2$ denote the total number of reflecting elements in the system. Let $\mathcal{M}_i \triangleq \{1, 2, \dots, M_i\}$, $\mathcal{N}_i \triangleq \{1, 2, \dots, N_i\}$, and $\mathcal{T}_i \triangleq \{1, 2, \dots, T_i\}$ denote the corresponding sets of indices. The phase shifts of each IRS's reflecting elements can be determined by a smart controller attached to it. The BS communicates to the two IRS controllers to configure the two IRSs' phase shifts via separate reliable wireless links so that both IRSs jointly assist the downlink transmission from the BS to the user.

We consider a narrow-band system and adopt the block-fading model for small-scale fading. Let $\mathbf{H}_{Sl} \in \mathbb{C}^{T_l \times T_S}$, $\mathbf{H}_{12} \in \mathbb{C}^{T_2 \times T_1}$, $\mathbf{h}_{SU}^H \in \mathbb{C}^{1 \times T_S}$, and $\mathbf{h}_{lU}^H \in \mathbb{C}^{1 \times T_l}$ represent the channel matrix between the BS and IRS $l \in \mathcal{L}$, the channel matrix between IRS 1 and IRS 2, the

channel vector between the BS and user, and the channel vector between IRS $l \in \mathcal{L}$ and the user, respectively. Notice that in contrast with the existing works on double-IRS cooperatively assisted systems [19]–[25], we consider the direct channel between the BS and user. As the BS and IRSs are usually far above the ground where scattering is relatively weak, we adopt the Rician fading model² for all small-scale fading channels [6], [7], [14]–[18]. Specifically,

$$\mathbf{H}_{ab} = \sqrt{\alpha_{ab}} \left(\sqrt{\frac{K_{ab}}{K_{ab} + 1}} \bar{\mathbf{H}}_{ab} + \sqrt{\frac{1}{K_{ab} + 1}} \tilde{\mathbf{H}}_{ab} \right), ab \in \{S1, S2, 12\}, \quad (1)$$

$$\mathbf{h}_{ab}^H = \sqrt{\alpha_{ab}} \left(\sqrt{\frac{K_{ab}}{K_{ab} + 1}} \bar{\mathbf{h}}_{ab}^H + \sqrt{\frac{1}{K_{ab} + 1}} \tilde{\mathbf{h}}_{ab}^H \right), ab \in \{1U, 2U, SU\}, \quad (2)$$

where $\alpha_{ab} \geq 0$ represents the large-scale fading power; $K_{ab} \geq 0$ represents the Rician factor; $\bar{\mathbf{H}}_{ab} \in \mathbb{C}^{T_b \times T_a}$ and $\tilde{\mathbf{h}}_{ab}^H \in \mathbb{C}^{1 \times T_a}$ represent the random normalized NLoS components in a slot with elements independently and identically distributed (i.i.d.) according to $\mathcal{CN}(0, 1)$; $\bar{\mathbf{H}}_{ab} \in \mathbb{C}^{T_b \times T_a}$ and $\bar{\mathbf{h}}_{ab}^H \in \mathbb{C}^{1 \times T_a}$ represent the deterministic normalized LoS components with unit-modulus elements. Note that $\bar{\mathbf{H}}_{ab}$ and $\bar{\mathbf{h}}_{ab}^H$ do not change during the considered period, as the locations of the BS, IRSs, and user are assumed to be invariant [6], [7], [14], [15], [17].

Let λ and d ($\leq \frac{\lambda}{2}$) denote the wavelength of transmission signals and the distance between two adjacent reflecting elements or antennas in each row and each column of the URAs. Define $f(x^{(h)}, x^{(v)}, m, n) \triangleq 2\pi \frac{d}{\lambda} \sin x^{(v)}((m-1) \cos x^{(h)} + (n-1) \sin x^{(h)})$, $\mathbf{A}(x^{(h)}, x^{(v)}, M, N) \triangleq \left(e^{j f(x^{(h)}, x^{(v)}, m, n)} \right)_{m=1, \dots, M, n=1, \dots, N}$, and $\mathbf{a}(x^{(h)}, x^{(v)}, M, N) \triangleq \text{vec}(\mathbf{A}(x^{(h)}, x^{(v)}, M, N)) \in \mathbb{C}^{MN}$. Then, $\bar{\mathbf{H}}_{ab}$ and $\bar{\mathbf{h}}_{ab}$ are modeled as [6], [7], [14], [15]:

$$\bar{\mathbf{H}}_{ab} = \mathbf{a}_{A,ab} \mathbf{a}_{D,ab}^H, ab \in \{S1, S2, 12\}, \quad (3)$$

$$\bar{\mathbf{h}}_{ab} = \mathbf{a}_{D,ab}, ab \in \{1U, 2U, SU\}, \quad (4)$$

where $\mathbf{a}_{A,ab} \triangleq \mathbf{a}(\delta_{ab}^{(h)} \delta_{ab}^{(v)}, M_b, N_b)$ and $\mathbf{a}_{D,ab} \triangleq \mathbf{a}(\varphi_{ab}^{(h)}, \varphi_{ab}^{(v)}, M_a, N_a)$. Here, $f(\theta^{(h)}, \theta^{(v)}, m, n)$ represents the difference of the corresponding phase changes over the LoS component; $\delta_{ab}^{(h)} \left(\delta_{ab}^{(v)} \right)$ represents the azimuth (elevation) angle of arrival (AoA) of a signal from node a to the URA at node b ; $\varphi_{ab}^{(h)} \left(\varphi_{ab}^{(v)} \right)$ represents the azimuth (elevation) angle of departure (AoD) of a signal from the URA at node a to node b .

To reduce the cost for phase adjustment, we consider a quasi-static phase shift design [6], [7], [14]–[18]. To be specific, the phase shifts of the two IRSs do not change with the NLoS components from slot to slot and remain constant during the considered period. Let $\boldsymbol{\theta}_l \triangleq (\theta_{l,m,n})_{m \in \mathcal{M}_l, n \in \mathcal{N}_l} \in \mathbb{R}^{M_l \times N_l}$ denote the constant phase shifts of IRS l , where the phase shift

²The Rician fading model is more general than the Rayleigh fading model.

of its (m, n) -th element satisfies $\theta_{l,m,n} \in [0, 2\pi)$. For notation convenience, we introduce $\phi_l \triangleq (\phi_{l,t})_{t \in \mathcal{T}_l} = \text{vec}(\boldsymbol{\theta}_l) \in \mathbb{R}^{T_l}$ to represent the phase shifts of IRS l , where its t -th element satisfies:

$$\phi_{l,t} \in [0, 2\pi), t \in \mathcal{T}_l, l \in \mathcal{L}. \quad (5)$$

The equivalent channel between the BS and user, denoted by $\mathbf{h}_e^H(\boldsymbol{\phi}_1, \boldsymbol{\phi}_2) \in \mathbb{C}^{1 \times T_S}$, can be expressed as:

$$\mathbf{h}_e^H(\boldsymbol{\phi}_1, \boldsymbol{\phi}_2) = \mathbf{h}_{SU}^H + \sum_{l \in \mathcal{L}} \mathbf{h}_{lU}^H \text{diag}(\mathbf{v}_l^H) \mathbf{H}_{Sl} + \mathbf{h}_{2U}^H \text{diag}(\mathbf{v}_2^H) \mathbf{H}_{12} \text{diag}(\mathbf{v}_1^H) \mathbf{H}_{S1}, \quad (6)$$

where $\mathbf{v}_l \triangleq (e^{-j\phi_{l,t}})_{t \in \mathcal{T}_l} \in \mathbb{C}^{T_l}$. Note that $\mathbf{h}_{lU}^H \text{diag}(\mathbf{v}_l^H) \mathbf{H}_{Sl}$ represents the cascaded channel (Sl, lU) , and $\mathbf{h}_{2U}^H \text{diag}(\mathbf{v}_2^H) \mathbf{H}_{12} \text{diag}(\mathbf{v}_1^H) \mathbf{H}_{S1}$ represents the cascaded channel $(S1, 12, 2U)$. The BS serves the user via linear beamforming. Let $\mathbf{w} \in \mathbb{C}^{T_S}$ with $\|\mathbf{w}\|_2^2 = 1$ represent the normalized linear beamforming vector at the BS. Then, the received signal at the user can be expressed as:

$$Y = \mathbf{h}_e^H(\boldsymbol{\phi}_1, \boldsymbol{\phi}_2) \mathbf{w} \sqrt{P_S} X_S + Z, \quad (7)$$

where P_S represents the transmit power of the BS, $X_S \in \mathbb{C}$ with $\mathbb{E}[|X_S|^2] = 1$ represents an information symbol for the user, and $Z \sim \mathcal{CN}(0, \sigma^2)$ denotes the additive white gaussian noise (AWGN).

We assume that $\mathbf{h}_e(\boldsymbol{\phi}_1, \boldsymbol{\phi}_2)$ is perfectly known to the BS and user, once $\boldsymbol{\phi}_1$ and $\boldsymbol{\phi}_2$ are given. We consider coding within each slot. To maximize the achievable rate (singal-to-noise ratio, SNR) at each slot, we adopt the instantaneous CSI-adaptive MRT beamformer at the BS [6], [7], [14]–[16], [18]:³

$$\mathbf{w} = \frac{\mathbf{h}_e(\boldsymbol{\phi}_1, \boldsymbol{\phi}_2)}{\|\mathbf{h}_e(\boldsymbol{\phi}_1, \boldsymbol{\phi}_2)\|_2}. \quad (8)$$

Thus, for given $\boldsymbol{\phi}_1$ and $\boldsymbol{\phi}_2$, the average achievable rate of the double-IRS cooperatively assisted system over slots, $C(\boldsymbol{\phi}_1, \boldsymbol{\phi}_2)$ (bit/s/Hz), is given by:

$$C(\boldsymbol{\phi}_1, \boldsymbol{\phi}_2) \triangleq \mathbb{E} \left[\log_2 \left(1 + \frac{P_S}{\sigma^2} \|\mathbf{h}_e(\boldsymbol{\phi}_1, \boldsymbol{\phi}_2)\|_2^2 \right) \right]. \quad (9)$$

We would like to analyze and maximize $C(\boldsymbol{\phi}_1, \boldsymbol{\phi}_2)$, which is considerably more involved than that in a single-IRS assisted system [6]. For tractability, we approximate $C(\boldsymbol{\phi}_1, \boldsymbol{\phi}_2)$ with its upper bound, $\log_2 \left(1 + \frac{P_S}{\sigma^2} \gamma(\boldsymbol{\phi}_1, \boldsymbol{\phi}_2) \right)$, obtained based on Jensen's inequality as in [6], [7], [14]. Here, $\gamma(\boldsymbol{\phi}_1, \boldsymbol{\phi}_2) \triangleq \mathbb{E}[\|\mathbf{h}_e(\boldsymbol{\phi}_1, \boldsymbol{\phi}_2)\|_2^2]$ represents the average channel power. Later in Section VI, equivalently, we will numerically show that the upper bound is a good approximation of $C(\boldsymbol{\phi}_1, \boldsymbol{\phi}_2)$. In the rest of the paper, we analyze and maximize $\gamma(\boldsymbol{\phi}_1, \boldsymbol{\phi}_2)$ instead of $\log_2 \left(1 + \frac{P_S}{\sigma^2} \gamma(\boldsymbol{\phi}_1, \boldsymbol{\phi}_2) \right)$,

³It is obvious that \mathbf{w} in (8) is optimal for the maximization of the instantaneous SNR w.r.t. \mathbf{w} under $\|\mathbf{w}\|_2^2 = 1$ at each slot and hence is optimal for the average rate maximization.

which is an increasing function of $\gamma(\phi_1, \phi_2)$. Note that in what follows, we let ab , \overline{ab} , and \tilde{ab} represent the Rician channel, LoS channel, and NLoS channel between node a and node b , respectively. The Rician channel ab can be viewed as the composition of the LoS channel \overline{ab} and NLoS channel \tilde{ab} .

III. ANALYSIS

In this section, we analyze the average channel power in the general and special Rician factor regimes, respectively.

A. Analysis in General Rician Factor Regime

In this part, we consider the analysis of the average channel power in the general Rician factor regime. First, we characterize the influences of ϕ_1 and ϕ_2 on $\gamma(\phi_1, \phi_2)$.

Lemma 1. (i) If $K_{S1}(K_{1U} + K_{12}) = 0$ (i.e., $K_{S1} = 0$ or $K_{1U} = K_{12} = 0$), then $\gamma(\phi_1, \phi_2)$ does not change with ϕ_1 . (ii) If $K_{2U}(K_{12} + K_{S2}) = 0$ (i.e., $K_{2U} = 0$ or $K_{12} = K_{S2} = 0$), then $\gamma(\phi_1, \phi_2)$ does not change with ϕ_2 .

Proof: Please refer to Appendix A. ■

Based on Lemma 1, we can divide the channel conditions into four cases according to the values of Rician factors.

- **Case 0** ($K_{S1} = 0$ or $K_{1U} = K_{12} = 0$ and $K_{12} = K_{S2} = 0$ or $K_{2U} = 0$): $\gamma(\phi_1, \phi_2)$ does not change with ϕ_1 or ϕ_2 and hence is rewritten as $\gamma^{(0)}$.
- **Case 1** ($K_{S1} > 0$, $K_{1U} + K_{12} > 0$, and $K_{12} = K_{S2} = 0$ or $K_{2U} = 0$): $\gamma(\phi_1, \phi_2)$ changes only with ϕ_1 and hence is rewritten as $\gamma^{(1)}(\phi_1)$.
- **Case 2** ($K_{S1} = 0$ or $K_{1U} = K_{12} = 0$, $K_{12} + K_{S2} > 0$, and $K_{2U} > 0$): $\gamma(\phi_1, \phi_2)$ changes only with ϕ_2 and hence is rewritten as $\gamma^{(2)}(\phi_2)$.
- **Case 3** ($K_{S1} > 0$, $K_{1U} + K_{12} > 0$, $K_{12} + K_{S2} > 0$, and $K_{2U} > 0$): $\gamma(\phi_1, \phi_2)$ changes with both ϕ_1 and ϕ_2 and is also written as $\gamma^{(3)}(\phi_1, \phi_2)$.

Then, we characterize the average channel power in the four cases of channel conditions. For ease of exposition, we introduce several new notations. Firstly, for $ab \in \{S1, S2, 12, 1U, 2U, SU\}$, we define $L_{\overline{ab}} \triangleq \frac{K_{ab}\alpha_{ab}}{K_{ab}+1}$ and $L_{\tilde{ab}} \triangleq \frac{\alpha_{ab}}{K_{ab}+1}$, which can be interpreted as the large-scale fading powers of the LoS channel \overline{ab} and NLoS channel \tilde{ab} , respectively. Obviously, $L_{\overline{ab}}$ and $L_{\tilde{ab}}$ both increase with α_{ab} , $L_{\overline{ab}}$ increases with K_{ab} , and $L_{\tilde{ab}}$ decreases with K_{ab} . Secondly,

we define $L_{a_1 b_1, a_2 b_2} \triangleq \prod_{i=1}^2 L_{a_i b_i}, (a_1 b_1, a_2 b_2) \in \bigcup_{l \in \mathcal{L}} \left(\{\overline{Sl}, \widetilde{Sl}\} \times \{\overline{lU}, \widetilde{lU}\} \right)$ and $L_{a_1 b_1, a_2 b_2, a_3 b_3} \triangleq \prod_{i=1}^3 L_{a_i b_i}, (a_1 b_1, a_2 b_2, a_3 b_3) \in \{\overline{S1}, \widetilde{S1}\} \times \{\overline{12}, \widetilde{12}\} \times \{\overline{2U}, \widetilde{2U}\}$, which can be interpreted as the large-scale fading powers of the cascaded channel $(a_1 b_1, a_2 b_2)$ and cascaded channel $(a_1 b_1, a_2 b_2, a_3 b_3)$, respectively. Thirdly, for $a \in \{S, 1\}, l \in \mathcal{L}, b \in \{2, U\}$, we define:

$$\Delta_{\overline{al}, \overline{lb}} \triangleq \angle(\text{diag}(\mathbf{a}_{D,lb}^H) \mathbf{a}_{A,al}) \in \mathbb{R}^{T_l}, \quad (10)$$

$$r_{\overline{al}, \overline{ab}} \triangleq \mathbf{a}_{D,al}^H \mathbf{a}_{D,ab} \in \mathbb{C}, \quad (11)$$

$$r_{\overline{ab}, \overline{lb}} \triangleq \mathbf{a}_{A,ab}^H \mathbf{a}_{A,lb} \in \mathbb{C}. \quad (12)$$

Note that $\Delta_{\overline{al}, \overline{lb}}$ represents the sum of the phase changes over the LoS channel \overline{al} and LoS channel \overline{lb} ; $r_{\overline{al}, \overline{ab}}$ depends on $\varphi_{al}^{(h)}, \varphi_{al}^{(v)}, \varphi_{ab}^{(h)}$, and $\varphi_{ab}^{(v)}$, which are determined only by the placement of the URA at node a and the locations of IRS l and node b ; $r_{\overline{12}, \overline{S2}}$ depends on $\delta_{12}^{(h)}, \delta_{12}^{(v)}, \delta_{S2}^{(h)}$, and $\delta_{S2}^{(v)}$, which are determined only by the placement of the URA at IRS 2 and the locations of the BS and IRS 1. Finally, we define:

$$\mathbf{A}_{11} \triangleq \text{diag}(\bar{\mathbf{h}}_{1U}^H) \bar{\mathbf{H}}_{S1} \bar{\mathbf{H}}_{S1}^H \text{diag}(\bar{\mathbf{h}}_{1U}) \in \mathbb{C}^{T_1 \times T_1}, \mathbf{A}_{12} \triangleq \text{diag}(\mathbf{a}_{D,12}^H) \bar{\mathbf{H}}_{S1} \bar{\mathbf{H}}_{S1}^H \text{diag}(\mathbf{a}_{D,12}) \in \mathbb{C}^{T_1 \times T_1},$$

$$\mathbf{A}_{21} \triangleq \text{diag}(\bar{\mathbf{h}}_{2U}^H) \bar{\mathbf{H}}_{S2} \bar{\mathbf{H}}_{S2}^H \text{diag}(\bar{\mathbf{h}}_{2U}) \in \mathbb{C}^{T_2 \times T_2}, \mathbf{A}_{22} \triangleq \text{diag}(\bar{\mathbf{h}}_{2U}^H) \bar{\mathbf{H}}_{12} \bar{\mathbf{H}}_{12}^H \text{diag}(\bar{\mathbf{h}}_{2U}) \in \mathbb{C}^{T_2 \times T_2},$$

$$\mathbf{A}_3 \triangleq \text{diag}(\bar{\mathbf{h}}_{2U}^H) \bar{\mathbf{H}}_{12} \text{diag}(\mathbf{a}_{A,S1}) \in \mathbb{C}^{T_2 \times T_1},$$

$$\mathbf{b}_{11} \triangleq \text{diag}(\bar{\mathbf{h}}_{1U}^H) \bar{\mathbf{H}}_{S1} \bar{\mathbf{h}}_{SU} \in \mathbb{C}^{T_1}, \mathbf{b}_{12} \triangleq \text{diag}(\mathbf{a}_{D,12}^H) \bar{\mathbf{H}}_{S1} \bar{\mathbf{H}}_{S2}^H \mathbf{a}_{A,12} \in \mathbb{C}^{T_1},$$

$$\mathbf{b}_{21} \triangleq \text{diag}(\bar{\mathbf{h}}_{2U}^H) \bar{\mathbf{H}}_{S2} \bar{\mathbf{h}}_{SU} \in \mathbb{C}^{T_2}, \mathbf{b}_{22} \triangleq \text{diag}(\bar{\mathbf{h}}_{2U}^H) \bar{\mathbf{H}}_{12} \bar{\mathbf{h}}_{1U} \in \mathbb{C}^{T_2},$$

$$\mathbf{B}_1 \triangleq \text{diag}(\bar{\mathbf{h}}_{2U}^H) \bar{\mathbf{H}}_{12} \in \mathbb{C}^{T_2 \times T_1},$$

$$\mathbf{B}_2 \triangleq \bar{\mathbf{H}}_{S1} \bar{\mathbf{H}}_{S1}^H \text{diag}(\bar{\mathbf{h}}_{1U}) \in \mathbb{C}^{T_1 \times T_1}, \mathbf{B}_3 \triangleq \bar{\mathbf{H}}_{S1} \bar{\mathbf{H}}_{S2}^H \text{diag}(\bar{\mathbf{h}}_{2U}) \in \mathbb{C}^{T_1 \times T_2},$$

$$\mathbf{B}_4 \triangleq \text{diag}(\bar{\mathbf{h}}_{2U}^H) \bar{\mathbf{H}}_{12} \text{diag}(\bar{\mathbf{H}}_{S1} \bar{\mathbf{h}}_{SU}) \in \mathbb{C}^{T_2 \times T_1}, \mathbf{B}_5 \triangleq \text{diag}(\bar{\mathbf{h}}_{2U}^H) \bar{\mathbf{H}}_{S2} \bar{\mathbf{H}}_{S1}^H \text{diag}(\bar{\mathbf{h}}_{1U}) \in \mathbb{C}^{T_2 \times T_1}.$$

Based on the above notations, the average channel powers in the four cases are summarized as follows.

Theorem 1 (Average Channel Power in General Rician Factor Regime).

$$\begin{aligned} \gamma^{(0)} = & \alpha_{SU} T_S + \sum_{l=1}^2 (L_{\widetilde{Sl}, \overline{lU}} + L_{\overline{Sl}, \widetilde{lU}} + L_{\widetilde{Sl}, \widetilde{lU}}) T_S T_l \\ & + (L_{\widetilde{S1}, \overline{12}, \widetilde{2U}} + L_{\overline{S1}, \widetilde{12}, \overline{2U}} + L_{\overline{S1}, \widetilde{12}, \widetilde{2U}} + L_{\widetilde{S1}, \widetilde{12}, \overline{2U}} + L_{\widetilde{S1}, \widetilde{12}, \widetilde{2U}}) T_S T_1 T_2, \\ \gamma^{(1)}(\phi_1) = & \mathbf{v}_1^H \left(L_{\overline{S1}, \overline{lU}} \mathbf{A}_{11} + L_{\overline{S1}, \overline{12}, \widetilde{2U}} T_2 \mathbf{A}_{12} \right) \mathbf{v}_1 \end{aligned} \quad (13)$$

$$+ 2\Re \left\{ \mathbf{v}_1^H \left(\sqrt{L_{\overline{SU}} L_{\overline{S1}, \overline{1U}}} \mathbf{b}_{11} + \sqrt{L_{\overline{S2}, \overline{2U}} L_{\overline{S1}, \overline{12}, \overline{2U}}} \mathbf{b}_{12} \right) \right\} + \gamma^{(0)}, \quad (14)$$

$$\begin{aligned} \gamma^{(2)}(\phi_2) = & \mathbf{v}_2^H \left(L_{\overline{S2}, \overline{2U}} \mathbf{A}_{21} + L_{\overline{S1}, \overline{12}, \overline{2U}} T_S \mathbf{A}_{22} \right) \mathbf{v}_2 \\ & + 2\Re \left\{ \mathbf{v}_2^H \left(\sqrt{L_{\overline{SU}} L_{\overline{S2}, \overline{2U}}} \mathbf{b}_{21} + \sqrt{L_{\overline{S1}, \overline{1U}} L_{\overline{S1}, \overline{12}, \overline{2U}}} T_S \mathbf{b}_{22} \right) \right\} + \gamma^{(0)}, \end{aligned} \quad (15)$$

$$\begin{aligned} \gamma^{(3)}(\phi_1, \phi_2) = & \gamma^{(1)}(\phi_1) + \gamma^{(2)}(\phi_2) - \gamma^{(0)} + L_{\overline{S1}, \overline{12}, \overline{2U}} T_S \mathbf{v}_2^H \mathbf{A}_3 \mathbf{v}_1^* \mathbf{v}_1^T \mathbf{A}_3^H \mathbf{v}_2 \\ & + 2\Re \left\{ \mathbf{v}_1^H \text{diag}(\mathbf{v}_2^H \mathbf{B}_1) \left(\sqrt{L_{\overline{S1}, \overline{1U}} L_{\overline{S1}, \overline{12}, \overline{2U}}} \mathbf{B}_2 \mathbf{v}_1 + \sqrt{L_{\overline{S2}, \overline{2U}} L_{\overline{S1}, \overline{12}, \overline{2U}}} \mathbf{B}_3 \mathbf{v}_2 \right) \right. \\ & \left. + \mathbf{v}_2^H \left(\sqrt{L_{\overline{SU}} L_{\overline{S1}, \overline{12}, \overline{2U}}} \mathbf{B}_4 \mathbf{v}_1^* + \sqrt{L_{\overline{S1}, \overline{1U}} L_{\overline{S2}, \overline{2U}}} \mathbf{B}_5 \mathbf{v}_1 \right) \right\}. \end{aligned} \quad (16)$$

Proof: Please refer to Appendix B. ■

Theorem 1 indicates that the average channel power in Case 0 does not depend on ϕ_1 or ϕ_2 , and hence a quasi-static phase shift design is void in Case 0 of the general Rician factor regime.

B. Analysis in Pure LoS Regime

In this part, we analyze the average channel power when the Rician factors go to infinity, corresponding to the regime of pure LoS channels. Apparently, Cases 0, 1, and 2 are void in the pure LoS regime, and the pure LoS regime can be regarded as a special case of Case 3 of the general Rician factor regime. Based on Theorem 1, we have the following result.

Corollary 1 (Average Channel Power in Pure LoS Regime). *As K_{S1} , K_{S2} , K_{12} , K_{SU} , K_{1U} , and $K_{2U} \rightarrow \infty$, $\gamma^{(3)}(\phi_1, \phi_2) \rightarrow \bar{\gamma}^{(3)}(\phi_1, \phi_2)$, where*

$$\begin{aligned} \bar{\gamma}^{(3)}(\phi_1, \phi_2) \triangleq & \alpha_{SU} T_S + \alpha_{S1} \alpha_{1U} \mathbf{v}_1^H \mathbf{A}_{11} \mathbf{v}_1 + \alpha_{S2} \alpha_{2U} \mathbf{v}_2^H \mathbf{A}_{21} \mathbf{v}_2 + \alpha_{S1} \alpha_{12} \alpha_{2U} T_S \mathbf{v}_2^H \mathbf{A}_3 \mathbf{v}_1^* \mathbf{v}_1^T \mathbf{A}_3^H \mathbf{v}_2 \\ & + 2\Re \left\{ \sqrt{\alpha_{SU} \alpha_{S1} \alpha_{1U}} \mathbf{v}_1^H \mathbf{b}_{11} + \sqrt{\alpha_{SU} \alpha_{S2} \alpha_{2U}} \mathbf{v}_2^H \mathbf{b}_{21} \right. \\ & \left. + \mathbf{v}_1^H \text{diag}(\mathbf{v}_2^H \mathbf{B}_1) \left(\sqrt{\alpha_{S1} \alpha_{1U} \alpha_{S1} \alpha_{12} \alpha_{2U}} \mathbf{B}_2 \mathbf{v}_1 + \sqrt{\alpha_{S2} \alpha_{2U} \alpha_{S1} \alpha_{12} \alpha_{2U}} \mathbf{B}_3 \mathbf{v}_2 \right) \right. \\ & \left. + \mathbf{v}_2^H \left(\sqrt{\alpha_{SU} \alpha_{S1} \alpha_{12} \alpha_{2U}} \mathbf{B}_4 \mathbf{v}_1^* + \sqrt{\alpha_{S1} \alpha_{1U} \alpha_{S2} \alpha_{2U}} \mathbf{B}_5 \mathbf{v}_1 \right) \right\}. \end{aligned} \quad (17)$$

As the Rician factors go to infinity, the large-scale fading power of each channel or cascaded channel which consists of at least one NLoS channel goes zero. Thus, Theorem 1 readily implies Corollary 1.

C. Analysis in Pure NLoS Regime

In this part, we analyze the average channel power when the Rician factors are zero, corresponding to the regime of pure NLoS channels. Obviously, Cases 1, 2, and 3 are void in the

pure NLoS regime, and the pure NLoS regime can be regarded as a special case of Case 0 of the general Rician factor regime. From Theorem 1, we have the following result.

Corollary 2 (Average Channel Power in Pure NLoS Regime). *If $K_{S1} = K_{S2} = K_{12} = K_{SU} = K_{1U} = K_{2U} = 0$, then $\gamma^{(0)} = \tilde{\gamma}^{(0)}$, where*

$$\tilde{\gamma}^{(0)} \triangleq \alpha_{SU}T_S + \alpha_{S1}\alpha_{1U}T_ST_1 + \alpha_{S2}\alpha_{2U}T_ST_2 + \alpha_{S1}\alpha_{12}\alpha_{2U}T_ST_1T_2. \quad (18)$$

When the Rician factors become zero, the large-scale fading power of each channel or cascaded channel which consists of at least one LoS channel becomes zero. As a result, Theorem 1 readily implies Corollary 2. Besides, Corollary 2 indicates that the average channel power in Case 0 of the pure NLoS regime does not rely on ϕ_1 or ϕ_2 . This fact further indicates that a quasi-static phase shift design is ineffective in the pure NLoS regime.

IV. OPTIMIZATION

In this section, we maximize the average channel power w.r.t. the phase shifts in the general and special Rician factor regimes, respectively.

A. Optimization in General Rician Factor Regime

In this part, we maximize the average channel power w.r.t. the phase shifts in the general Rician factor regime. As shown in Theorem 1, $\gamma^{(0)}$ is irrelevant to ϕ_1 and ϕ_2 in the general Rician factor regime. Thus, in the sequel, we optimize the phase shifts only for Cases 1, 2, and 3 in the general Rician factor regime.

1) *Optimization for Case $l = 1, 2$:* For $l = 1, 2$, as $\gamma^{(l)}(\phi_l)$ depends only on ϕ_l , we optimize ϕ_l in Case l .

Problem 1 (Optimization for Case $l = 1, 2$ in General Rician Factor Regime). *For Case $l = 1, 2$,*

$$\begin{aligned} \gamma^{(l)\star} &\triangleq \max_{\phi_l} \quad \gamma^{(l)}(\phi_l) \\ \text{s.t.} \quad \phi_{l,t} &\in [0, 2\pi), t \in \mathcal{T}_l, \end{aligned} \quad (19)$$

where $\gamma^{(1)}(\phi_1)$ and $\gamma^{(2)}(\phi_2)$ are given by (14) and (15), respectively. Let ϕ_l^* denote an optimal solution for Case l , where $l \in \mathcal{L}$.

Problem 1 is a challenging non-convex problem with a very complex objective function and T_l optimization variables. However, by the triangle inequality and Cauchy-Schwartz inequality,

we can obtain globally optimal closed-form solutions of Problem 1 for Case 1 with $K_{1U} = 0$ or $K_{12} = 0$ and Case 2 with $K_{S2} = 0$ or $K_{12} = 0$, respectively.

For ease of exposition, define $\Lambda(x) = x - 2\pi\lfloor\frac{x}{2\pi}\rfloor \in [0, 2\pi)$, $x \in \mathbb{R}$. Note that $\Lambda(\cdot)$ can be used to provide phase shifts ϕ_l , $l \in \mathcal{L}$ satisfying (5) [6].

Theorem 2 (Optimal Solution of Problem 1). (i) *The unique optimal solution of Problem 1 for Case 1 with $K_{1U} = 0$ or $K_{12} = 0$ is given by:*

$$\phi_1^* = \begin{cases} \Lambda(-\Delta_{\overline{S1}, \overline{12}} - \angle(r_{\overline{S1}, \overline{S2}} r_{\overline{S2}, \overline{12}}) \mathbf{1}_{T_1}), & K_{1U} = 0, \\ \Lambda(-\Delta_{\overline{S1}, \overline{1U}} - \angle(r_{\overline{S1}, \overline{SU}}) \mathbf{1}_{T_1}), & K_{12} = 0. \end{cases} \quad (20)$$

(ii) *The unique optimal solution of Problem 1 for Case 2 with $K_{S2} = 0$ or $K_{12} = 0$ is given by:*

$$\phi_2^* = \begin{cases} \Lambda(-\Delta_{\overline{12}, \overline{2U}} - \angle(r_{\overline{12}, \overline{1U}}) \mathbf{1}_{T_2}), & K_{S2} = 0, \\ \Lambda(-\Delta_{\overline{S2}, \overline{2U}} - \angle(r_{\overline{S2}, \overline{SU}}) \mathbf{1}_{T_2}), & K_{12} = 0. \end{cases} \quad (21)$$

Proof: Please refer to Appendix C. ■

From Theorem 2, we can draw the following conclusions. Firstly, in Case 1 with $K_{1U} = 0$, the optimal phase changes over the cascaded LoS channel $(\overline{S1}, \overline{12})$ are identical to the phase changes over the LoS channel $\overline{S2}$. Secondly, in Case 2 with $K_{S2} = 0$, the optimal phase changes over the cascaded LoS channel $(\overline{12}, \overline{2U})$ are identical to the phase changes over the LoS channel $\overline{1U}$. Finally, in Case 1 and Case 2 both with $K_{12} = 0$, the optimal phase changes over the cascaded LoS channel $(\overline{S1}, \overline{1U})$ are equivalent to the phase changes over the LoS channel \overline{SU} .

However, for Case 1 with $K_{12} > 0$ and $K_{1U} > 0$ and Case 2 with $K_{S2} > 0$ and $K_{12} > 0$, we cannot derive a globally optimal solution with the same method. Instead, we propose a computationally efficient iterative algorithm to obtain stationary points of Problem 1 for Case 1 with $K_{12} > 0$ and $K_{1U} > 0$ and Case 2 with $K_{S2} > 0$ and $K_{12} > 0$, respectively, based on the coordinate descent method. The idea is that at each step of one iteration, $\phi_{l,t}, t \in \mathcal{T}_l$ are sequentially updated by analytically solving the coordinate optimizations, each with a single variable. Specifically, in each coordinate optimization, we maximize $\gamma^{(l)}(\phi_l)$ w.r.t. the phase shift $\phi_{l,t}$ for some $t \in \mathcal{T}_l$ with the other phase shifts being fixed. For ease of exposition, we rewrite ϕ_l as $(\phi_{l,t}, \phi_{l,-t})$, where $\phi_{l,-t}$ represents the elements of ϕ_l except for $\phi_{l,t}$. Then, given $\phi_{l,-t}$ obtained in the previous step, the coordinate optimizations w.r.t. $\phi_{l,t}$ for Case 1 with $K_{12} > 0$ and $K_{1U} > 0$ and Case 2 with $K_{S2} > 0$ and $K_{12} > 0$ are formulated as follows.

Problem 2 (Coordinate Optimization w.r.t. $\phi_{l,t}$ for Case $l = 1, 2$ in General Rician Factor

Regime). For Case $l = 1, 2$ and for all $t \in \mathcal{T}_l$,

$$\phi_{l,t}^\dagger \triangleq \operatorname{argmax}_{\phi_{l,t} \in [0, 2\pi]} \gamma^{(l)}(\phi_{l,t}, \phi_{l,-t}).$$

Problem 2 is a single variable optimization problem and hence is much simpler than Problem 1.

Define:

$$\mathbf{A}_1 \triangleq L_{\overline{S1}, \overline{U}} \mathbf{A}_{11} + L_{\overline{S1}, \overline{12}, \widetilde{2U}} T_2 \mathbf{A}_{12}, \quad \mathbf{A}_2 \triangleq L_{\overline{S2}, \overline{2U}} \mathbf{A}_{21} + L_{\widetilde{S1}, \overline{12}, \overline{2U}} T_S \mathbf{A}_{22}, \quad (22)$$

$$\mathbf{b}_1 \triangleq \sqrt{L_{\overline{S1}} L_{\overline{S1}, \overline{1U}}} \mathbf{b}_{11} + \sqrt{L_{\overline{S2}, \widetilde{2U}} L_{\overline{S1}, \overline{12}, \widetilde{2U}}} \mathbf{b}_{12}, \quad \mathbf{b}_2 \triangleq \sqrt{L_{\overline{S2}} L_{\overline{S2}, \overline{2U}}} \mathbf{b}_{21} + \sqrt{L_{\widetilde{S1}, \overline{1U}} L_{\widetilde{S1}, \overline{12}, \overline{2U}}} T_S \mathbf{b}_{22}. \quad (23)$$

After some basic algebraic manipulations, we can derive a closed-form optimal solution of Problem 2.

Lemma 2 (Optimal Solution of Problem 2). *For Case $l = 1, 2$ and for all $t \in \mathcal{T}_l$, the unique optimal solution of Problem 2 is given by:*

$$\phi_{l,t}^\dagger = \Lambda \left(-\angle \left(\sum_{k \in \mathcal{T}_l, k \neq t} A_{l,t,k} e^{-j\phi_{l,k}} + b_{l,t} \right) \right), \quad (24)$$

where $A_{l,t,k}$ and $b_{l,t}$ represent the (t, k) -th element of \mathbf{A}_l given by (22) and the t -th element of \mathbf{b}_l given by (23), respectively.

Proof: Please refer to Appendix D. ■

The details of the coordinate descent-based algorithm for Case 1 with $K_{12} > 0$ and $K_{1U} > 0$ and Case 2 with $K_{S2} > 0$ and $K_{12} > 0$ are summarized in Algorithm 1. Since Problem 2 can be solved analytically, the computation time of Algorithm 1 is relatively short. Specifically, the computational complexity of Step 4 of Algorithm 1 is $\mathcal{O}(T_l)$. Hence the overall computational complexity of each iteration of Algorithm 1 is $\mathcal{O}(T_l^2)$. Furthermore, we know that every limit point generated by Algorithm 1 is a stationary point of Problem 2, as Problem 2 has a unique optimal solution [26, Proposition 2.7.1].

2) *Optimization for Case 3:* As $\gamma^{(3)}(\phi_1, \phi_2)$ depends on ϕ_1 and ϕ_2 , we jointly optimize ϕ_1 and ϕ_2 in Case 3.

Problem 3 (Optimization for Case 3 in General Rician Factor Regime). *For Case 3,*

$$\begin{aligned} \gamma^{(3)*} &\triangleq \max_{\phi_1, \phi_2} \gamma^{(3)}(\phi_1, \phi_2) \\ &\text{s.t.} \quad (5), \end{aligned}$$

where $\gamma^{(3)}(\phi_1, \phi_2)$ is given by (16). Let (ϕ_1^*, ϕ_2^*) denote an optimal solution.

Algorithm 1 Coordinate Descent Algorithm for Obtaining A Stationary Point of Problem 2 in General Rician Factor Regime

```

1: Initialization: Select  $\phi_l$  satisfying the constraints in (5) as the initial point.
2: repeat
3:   for  $t = 1, \dots, T_l$  do
4:     Calculate  $\phi_{l,t}^\dagger$  according to (24), and set  $\phi_{l,t} = \phi_{l,t}^\dagger$ .
5:   end for
6: until some convergence criterion is met.
  
```

Apparently, Problem 3 is a more challenging non-convex problem than Problem 1, as it has a more complex objective function and more optimization variables. However, by the triangle inequality and Cauchy-Schwartz inequality, we can still obtain a globally optimal closed-form solution of Problem 3 for Case 3 with $K_{S2} = K_{1U} = 0$ or $K_{12} = K_{SU} = 0$.

Theorem 3 (Optimal Solution of Problem 3). (i) For Case 3 with $K_{S2} = K_{1U} = 0$, any (ϕ_1^*, ϕ_2^*) with $\phi_1^* = \Lambda(-\Delta_{\overline{S1}, \overline{12}} + \psi \mathbf{1}_{T_1} - \frac{1}{2}\angle(r_{\overline{S1}, \overline{SU}}) \mathbf{1}_{T_1})$ and $\phi_2^* = \Lambda(-\Delta_{\overline{12}, \overline{2U}} - \psi \mathbf{1}_{T_2} - \frac{1}{2}\angle(r_{\overline{S1}, \overline{SU}}) \mathbf{1}_{T_2})$, for all $\psi \in \mathbb{R}$, is an optimal solution of Problem 3. (ii) For Case 3 with $K_{12} = K_{SU} = 0$, any (ϕ_1^*, ϕ_2^*) with $\phi_1^* = \Lambda(-\Delta_{\overline{S1}, \overline{1U}} + \psi \mathbf{1}_{T_1})$, $\phi_2^* = \Lambda(-\Delta_{\overline{S2}, \overline{2U}} + \psi \mathbf{1}_{T_2} + \angle(r_{\overline{S1}, \overline{S2}}) \mathbf{1}_{T_2})$, for all $\psi \in \mathbb{R}$, is an optimal solution of Problem 3.

Proof: Please refer to Appendix E. ■

Theorem 3 indicates two facts in the general Rician factor regime. Firstly, in Case 3 with $K_{S2} = K_{1U} = 0$, the optimal phase changes over the cascaded LoS channel $(\overline{S1}, \overline{12}, \overline{2U})$ are the same as the phase changes over the LoS channel \overline{SU} . Secondly, in Case 3 with $K_{12} = K_{SU} = 0$, the optimal phase changes over the cascaded LoS channels $(\overline{S1}, \overline{1U})$ and $(\overline{S2}, \overline{2U})$ are identical.

However, for Case 3 with $K_{S2} > 0$, $K_{1U} > 0$, and $K_{12} + K_{SU} > 0$, we cannot derive a globally optimal solution with the same method. Instead, we propose a computationally efficient iterative algorithm for Case 3 with $K_{S2} > 0$, $K_{1U} > 0$, and $K_{12} + K_{SU} > 0$, based on the coordinate descent method. The idea is that at each iteration, $\phi_{l,t}, t \in \mathcal{T}_l, l \in \mathcal{L}$ are sequentially updated by analytically solving the coordinate optimizations. Specifically, in each coordinate optimization, we maximize $\gamma(\phi_1, \phi_2)$ w.r.t. phase shift $\phi_{l,t}$ for some $t \in \mathcal{T}_l, l \in \mathcal{L}$ with the other phase shifts being fixed. For ease of exposition, we rewrite (ϕ_1, ϕ_2) as $(\phi_{l,t}, \phi_{l,-t}, \phi_{-l})$, where $\phi_{l,-t}$ represents the elements of ϕ_l except $\phi_{l,t}$, and $-l$ represents the element in $\mathcal{L} \setminus \{l\}$. Then, given $\phi_{l,-t}$ and ϕ_{-l} obtained in the previous step, the coordinate optimization w.r.t. $\phi_{l,t}$

is formulated as follows.

Problem 4 (Coordinate Optimization w.r.t. $\phi_{l,t}$ for Case 3 in General Rician Factor Regime).

For Case 3 and for all $t \in \mathcal{T}_l, l \in \mathcal{L}$,

$$\phi_{l,t}^\dagger \triangleq \underset{\phi_{l,t} \in [0, 2\pi]}{\operatorname{argmax}} \gamma(\phi_{l,t}, \phi_{l,-t}, \phi_{-l}).$$

Problem 4 is a single variable non-convex optimization problem and hence is much simpler than Problem 3. Define:

$$\mathbf{C}_1 \triangleq \mathbf{A}_1 + L_{\overline{S1}, \overline{12}, \overline{2U}} T_S \mathbf{A}_3^T \mathbf{v}_2^* \mathbf{v}_2^T \mathbf{A}_3^* + 2\sqrt{L_{\overline{S1}, \overline{1U}} L_{\overline{S1}, \overline{12}, \overline{2U}}} \Re\{\operatorname{diag}(\mathbf{v}_2^H \mathbf{B}_1) \mathbf{B}_2\} \in \mathbb{C}^{T_1 \times T_1}, \quad (25a)$$

$$\mathbf{C}_2 \triangleq \mathbf{A}_2 + L_{\overline{S1}, \overline{12}, \overline{2U}} T_S \mathbf{A}_3 \mathbf{v}_1^* \mathbf{v}_1^T \mathbf{A}_3^H + 2\sqrt{L_{\overline{S2}, \overline{2U}} L_{\overline{S1}, \overline{12}, \overline{2U}}} \Re\{\mathbf{B}_1 \operatorname{diag}(\mathbf{v}_1^H) \mathbf{B}_3\} \in \mathbb{C}^{T_2 \times T_2}, \quad (25b)$$

$$\begin{aligned} \mathbf{d}_1 &\triangleq \mathbf{b}_1 + \sqrt{L_{\overline{S2}, \overline{2U}} L_{\overline{S1}, \overline{12}, \overline{2U}}} \operatorname{diag}(\mathbf{v}_2^H \mathbf{B}_1) \mathbf{B}_3 \mathbf{v}_2 \\ &\quad + \sqrt{L_{\overline{S1}, \overline{1U}} L_{\overline{S2}, \overline{2U}}} \mathbf{B}_4^T \mathbf{v}_2^* + \sqrt{L_{\overline{S1}, \overline{1U}} L_{\overline{S2}, \overline{2U}}} \mathbf{B}_5^H \mathbf{v}_2 \in \mathbb{C}^{T_1}, \end{aligned} \quad (26a)$$

$$\begin{aligned} \mathbf{d}_2 &\triangleq \mathbf{b}_2 + \sqrt{L_{\overline{S1}, \overline{1U}} L_{\overline{S1}, \overline{12}, \overline{2U}}} \mathbf{B}_1 \operatorname{diag}(\mathbf{v}_1^H) \mathbf{B}_2 \mathbf{v}_1 \\ &\quad + \sqrt{L_{\overline{S1}, \overline{1U}} L_{\overline{S1}, \overline{12}, \overline{2U}}} \mathbf{B}_4 \mathbf{v}_1^* + \sqrt{L_{\overline{S1}, \overline{1U}} L_{\overline{S2}, \overline{2U}}} \mathbf{B}_5 \mathbf{v}_1 \in \mathbb{C}^{T_2}. \end{aligned} \quad (26b)$$

After some basic algebraic manipulations, we can derive a closed-form optimal solution of Problem 4.

Lemma 3 (Optimal Solution of Problem 4). *For Case 3 and all $t \in \mathcal{T}_l, l \in \mathcal{L}$, the unique optimal solution of Problem 4 is given by:*

$$\phi_{l,t}^\dagger = \Lambda \left(-\angle \left(\sum_{k \in \mathcal{T}_l, k \neq t} C_{l,t,k} e^{-j\phi_{l,k}} + d_{l,t} \right) \right), \quad (27)$$

where $C_{l,t,k}$ represents the (t, k) -th element of \mathbf{C}_l given by (25), and $d_{l,t}$ represents the t -th element of \mathbf{d}_l given by (26).

Proof: Please refer to Appendix F. ■

The details of the coordinate descent-based algorithm are summarized in Algorithm 2. The computational complexities of Step 4 and Step 6 of Algorithm 2 are $\mathcal{O}(T_1 T_2 T_l)$ and $\mathcal{O}(T_l)$, $l \in \mathcal{L}$, as $T_1, T_2 \rightarrow \infty$. Hence, the computational complexity of each iteration of Algorithm 2 is $\mathcal{O}(T_1^2 T_2 + T_2^2 T_1)$, as $T_1, T_2 \rightarrow \infty$. If $T_1 = cT$ and $T_2 = (1 - c)T$ for some $c \in (0, 1)$, then the computational complexity of each iteration of Algorithm 2 becomes $\mathcal{O}(T^3)$, as $T \rightarrow \infty$. As Problem 4 can be solved analytically, the computation efficiency of Algorithm 2 is relatively high. Furthermore, we know that every limit point generated by Algorithm 2 is a stationary point

Algorithm 2 Coordinate Descent Algorithm for Obtaining A Stationary Point of Problem 3 in General Rician Factor Regime

```

1: Initialization: Select  $\phi_1$  and  $\phi_2$  satisfying the con-      5:   for  $t = 1, \dots, T_l$  do
       straints in (5) as the initial point.          6:     Calculate  $\phi_{l,t}^\dagger$  according to (27), and set
2: repeat                                         7:     end for
3:   for  $l = 1, 2$  do                         8:   end for
4:     Calculate  $\mathbf{C}_l$  and  $\mathbf{d}_l$  according to (25) and          9:   until some convergence criterion is met.
       (26), respectively.
  
```

of Problem 3, as Problem 4 has a unique optimal solution [26, Proposition 2.7.1].

3) *Optimal Average Channel Power in General Rician Factor Regime at Large Number of Reflecting Elements:* We characterize the average channel power in Case 0 and the optimal average channel power in Cases 1, 2, and 3 of the general Rician factor regime at large T_1 , T_2 , and T .

Theorem 4 (Optimal Average Channel Power at Large T_1 , T_2 , and T). (i) $\gamma^{(0)} \xrightarrow{T_1, T_2 \rightarrow \infty} (L_{\widetilde{S}1, \widetilde{12}, \widetilde{2U}} + L_{\overline{S}1, \widetilde{12}, \overline{2U}} + L_{\overline{S}1, \widetilde{12}, \widetilde{2U}} + L_{\widetilde{S}1, \widetilde{12}, \overline{2U}} + L_{\widetilde{S}1, \widetilde{12}, \widetilde{2U}})T_1 T_2$, $\gamma^{(1)*} \xrightarrow{T_1, T_2 \rightarrow \infty} L_{\overline{S}1, \widetilde{12}, \widetilde{2U}} T_1 T_2$, $\gamma^{(2)*} \xrightarrow{T_1, T_2 \rightarrow \infty} L_{\widetilde{S}1, \widetilde{12}, \overline{2U}} T_1 T_2$, and $\gamma^{(3)*} \xrightarrow{T_1, T_2 \rightarrow \infty} L_{\overline{S}1, \widetilde{12}, \overline{2U}} T_1 T_2^2$. (ii) If $T_1 = cT$ and $T_2 = (1 - c)T$ for some $c \in (0, 1)$, then $\gamma^{(0)} \xrightarrow{T \rightarrow \infty} (L_{\widetilde{S}1, \widetilde{12}, \widetilde{2U}} + L_{\overline{S}1, \widetilde{12}, \overline{2U}} + L_{\overline{S}1, \widetilde{12}, \widetilde{2U}} + L_{\widetilde{S}1, \widetilde{12}, \overline{2U}} + L_{\widetilde{S}1, \widetilde{12}, \widetilde{2U}})c(1 - c)T_1 T_2$, $\gamma^{(1)*} \xrightarrow{T \rightarrow \infty} L_{\overline{S}1, \widetilde{12}, \widetilde{2U}} c^2(1 - c)T_1 T_2^2$, $\gamma^{(2)*} \xrightarrow{T \rightarrow \infty} L_{\widetilde{S}1, \widetilde{12}, \overline{2U}} c(1 - c)^2 T_1 T_2^3$, and $\gamma^{(3)*} \xrightarrow{T \rightarrow \infty} L_{\overline{S}1, \widetilde{12}, \overline{2U}} c^2(1 - c)^2 T_1 T_2^4$.

Proof: Please refer to Appendix G. ■

Theorem 4 (i) indicates that as $T_1, T_2 \rightarrow \infty$, $\gamma^{(0)}$ increases linearly with T_1 and T_2 , $\gamma^{(1)*}$ increases quadratically with T_1 and linearly with T_2 , $\gamma^{(2)*}$ increases linearly with T_1 and quadratically with T_2 , and $\gamma^{(3)*}$ increases quadratically with T_1 and T_2 . Theorem 4 (ii) indicates that as $T \rightarrow \infty$, $\gamma^{(0)}$ increases quadratically with T , $\gamma^{(1)*}$ and $\gamma^{(2)*}$ increase cubically with T , and $\gamma^{(3)*}$ increases quartically with T . Surprisingly, for the double-IRS cooperatively assisted system, the optimal quasi-static phase shift design for Case 3 achieves the same average power gain in order w.r.t the total number of reflecting elements T as the optimal instantaneous CSI-adaptive phase shift design in [23] but with a lower phase adjustment cost.

⁴ $f(x, y) \xrightarrow{x, y \rightarrow \infty} g(x, y)$ means $\lim_{x, y \rightarrow \infty} \frac{f(x, y)}{g(x, y)} = 1$, and $f(x) \xrightarrow{x \rightarrow \infty} g(x)$ means $\lim_{x \rightarrow \infty} \frac{f(x)}{g(x)} = 1$.

B. Optimization in Pure LoS Regime

In this part, we maximize the average channel power $\bar{\gamma}^{(3)}(\phi_1, \phi_2)$ w.r.t. the phase shifts (ϕ_1, ϕ_2) in the pure LoS regime.

Problem 5 (Optimization in Pure LoS Regime).

$$\bar{\gamma}^{(3)*} \triangleq \max_{\phi_1, \phi_2} \bar{\gamma}^{(3)}(\phi_1, \phi_2)$$

$$s.t. \quad (5),$$

where $\bar{\gamma}^{(3)}(\phi_1, \phi_2)$ is given by (17). Let $(\bar{\phi}_1^*, \bar{\phi}_2^*)$ denote an optimal solution.

As $\bar{\gamma}^{(3)}(\phi_1, \phi_2)$ has a simpler form than $\gamma^{(3)}(\phi_1, \phi_2)$, Problem 5 is more tractable than Problem 3. We propose a computationally efficient iterative algorithm to obtain a stationary point of Problem 5 using the block coordinate descent method. Specifically, we divide the optimization variables into $T_2 + 1$ disjoint blocks, i.e., $\phi_1, \phi_{2,t}, t \in \mathcal{T}_2$, with the first block consisting of T_1 coordinates and each of the remaining blocks consisting of only one coordinate, and sequentially update each block by analytically solving the corresponding block coordinate and coordinate optimization problems. Here, we treat ϕ_1 as a single block, as the optimization problem w.r.t. ϕ_1 can be analytically solved, with a lower computational complexity than the separate optimization problems w.r.t. $\phi_{1,t}, t \in \mathcal{T}_1$, which will be seen shortly. The block coordinate optimization w.r.t. ϕ_1 and the coordinate optimizations w.r.t. $\phi_{2,t}, t \in \mathcal{T}_2$ are formulated as follows.

Problem 6 (Block Coordinate Optimization w.r.t. ϕ_1 in Pure LoS Regime). *In the pure LoS regime,*

$$\bar{\phi}_1^\dagger \triangleq \operatorname{argmax}_{\phi_1} \bar{\gamma}^{(3)}(\phi_1, \phi_2)$$

$$s.t. \quad \phi_{1,t} \in [0, 2\pi), t \in \mathcal{T}_1.$$

Problem 7 (Coordinate Optimization w.r.t. $\phi_{2,t}$ in Pure LoS Regime). *In the pure LoS regime, for all $t \in \mathcal{T}_2$,*

$$\bar{\phi}_{2,t}^\dagger \triangleq \operatorname{argmax}_{\phi_{2,t} \in [0, 2\pi)} \bar{\gamma}^{(3)}(\phi_{2,t}, \phi_{2,-t}, \phi_1).$$

Define:

$$\begin{aligned} \bar{\mathbf{C}}_2 &\triangleq \alpha_{S2}\alpha_{2U}\mathbf{A}_{21} + \alpha_{S1}\alpha_{12}\alpha_{2U}T_S\mathbf{A}_3\mathbf{v}_1^*\mathbf{v}_1^T\mathbf{A}_3^H \\ &\quad + 2\sqrt{\alpha_{S2}\alpha_{2U}\alpha_{S1}\alpha_{12}\alpha_{2U}}\Re\{\mathbf{B}_1\operatorname{diag}(\mathbf{v}_1^H)\mathbf{B}_3\} \in \mathbb{C}^{T_2 \times T_2}, \end{aligned} \quad (28)$$

Algorithm 3 Block Coordinate Descent Algorithm for Obtaining A Stationary Point of Problem 5 in Pure LoS Regime

```

1: Initialization: Select  $\phi_1$  and  $\phi_2$  satisfying the con-      5:   for  $t = 1, \dots, T_2$  do
       straints in (5) as the initial point.          6:     Calculate  $\bar{\phi}_{2,t}^\dagger$  according to (31), and set
2: repeat          7:     end for
3:   Calculate  $\bar{\phi}_1^\dagger$  according to (30), and set  $\phi_1 = \bar{\phi}_1^\dagger$ .      8: until some convergence criterion is met.
4:   Calculate  $\bar{\mathbf{C}}_2$  and  $\bar{\mathbf{d}}_2$  according to (28) and (29),          respectively.
  
```

$$\begin{aligned}
\bar{\mathbf{d}}_2 &\triangleq \sqrt{\alpha_{SU}\alpha_{S2}\alpha_{2U}}\mathbf{b}_{21} + \sqrt{\alpha_{S1}\alpha_{1U}\alpha_{S1}\alpha_{12}\alpha_{2U}}\mathbf{B}_1\text{diag}(\mathbf{v}_1^H)\mathbf{B}_2\mathbf{v}_1 \\
&\quad + \sqrt{\alpha_{SU}\alpha_{S1}\alpha_{1U}}\mathbf{B}_4\mathbf{v}_1^* + \sqrt{\alpha_{S1}\alpha_{1U}\alpha_{S2}\alpha_{2U}}\mathbf{B}_5\mathbf{v}_1 \in \mathbb{C}^{T_2}.
\end{aligned} \tag{29}$$

After some basic algebraic manipulations, we can derive closed-form optimal solutions of Problem 6 and Problem 7 using the triangle inequality and Cauchy-Schwartz inequality.

Lemma 4 (Optimal Solutions of Problem 6 and Problem 7). (i) *The unique optimal solution of Problem 6 is given by:*

$$\begin{aligned}
\bar{\phi}_1^\dagger &= \Lambda \left(-\angle \left(\text{diag} \left(\sqrt{\alpha_{S1}\alpha_{1U}}\bar{\mathbf{h}}_{1U}^H + \sqrt{\alpha_{S1}\alpha_{1U}\alpha_{S1}\alpha_{12}\alpha_{2U}}\mathbf{v}_2^H\mathbf{B}_1 \right) \mathbf{a}_{A,S1} \right) \right. \\
&\quad \left. - \angle \left(\mathbf{a}_{D,S1}^H \left(\sqrt{\alpha_{SU}}\bar{\mathbf{h}}_{SU} + \sqrt{\alpha_{S2}\alpha_{2U}}\bar{\mathbf{H}}_{S2}^H\text{diag}(\mathbf{v}_2)\bar{\mathbf{h}}_{2U} \right) \right) \mathbf{1}_{T_1} \right). \tag{30}
\end{aligned}$$

(ii) *For all $t \in \mathcal{T}_2$, the unique optimal solution of Problem 7 is given by:*

$$\bar{\phi}_{2,t}^\dagger = \Lambda \left(-\angle \left(\sum_{k \in \mathcal{T}_2, k \neq t} \bar{C}_{2,t,k} e^{-j\phi_{2,k}} + \bar{d}_{2,t} \right) \right), \tag{31}$$

where $\bar{C}_{2,t,k}$ represents the (t, k) -th element of $\bar{\mathbf{C}}_2$ given by (28), and $\bar{d}_{2,t}$ represents the t -th element of $\bar{\mathbf{d}}_2$ given by (29).

Proof: Please refer to Appendix H. ■

The details of the block coordinate descent-based algorithm are summarized in Algorithm 3. The computational complexities of Step 3, Step 4, and Step 6 are $\mathcal{O}(T_1 T_2)$, $\mathcal{O}(T_1 T_2^2)$, and $\mathcal{O}(T_2)$, respectively, as $T_1, T_2 \rightarrow \infty$. Hence the computational complexity of each iteration of Algorithm 3 is $\mathcal{O}(T_1 T_2^2)$. Since Problem 6 and Problem 7 have unique optimal solutions, respectively, every limit point generated by Algorithm 3 is a stationary point of Problem 5 [26, Proposition 2.7.1].

Remark 1 (Comparison between Algorithm 3 and Algorithm 2). *The overall computational*

complexity for updating ϕ_1 in each iteration of Algorithm 3 is $\mathcal{O}(T_1 T_2)$, whereas the overall computational complexity for updating $\phi_{1,t}, t \in \mathcal{T}_1$ in each iteration of Algorithm 2 is $\mathcal{O}(T_1^2 T_2)$. Besides, the overall computational complexity for updating $\phi_{2,t}$ in each iteration of Algorithm 3 is identical to that of Algorithm 2, for all $t \in \mathcal{T}_2$. Thus, the computational complexity of Algorithm 3 is lower than that of Algorithm 2.

The following lemma characterizes how the optimal average channel power of the pure LoS regime scales with T_1 , T_2 , and T , when they are large.

Lemma 5 (Optimal Average Channel Power in Pure LoS Regime at Large T_1 , T_2 , and T). (i) $\bar{\gamma}^{(3)*} \xrightarrow{T_1, T_2 \rightarrow \infty} \alpha_{S1} \alpha_{12} \alpha_{2U} T_S T_1^2 T_2^2$. (ii) If $T_1 = cT$ and $T_2 = (1 - c)T$ for some $c \in (0, 1)$, then $\bar{\gamma}^{(3)*} \xrightarrow{T \rightarrow \infty} \alpha_{S1} \alpha_{12} \alpha_{2U} c^2 (1 - c)^2 T_S T^4$.

Proof: Following the proof of Theorem 4, we can show Lemma 5. \blacksquare

Lemma 5 indicates that as $T_1, T_2 \rightarrow \infty$, $\bar{\gamma}^{(3)*}$ increases quadratically with T_1 and T_2 . Furthermore, as $T \rightarrow \infty$, $\bar{\gamma}^{(3)*}$ increases quartically with T .

C. Optimization in Pure NLoS Regime

As shown in Corollary 2, the average channel power in the pure NLoS regime, i.e., $\tilde{\gamma}^{(0)}$, does not change with ϕ_1 or ϕ_2 . Thus, there is no need to further optimize the phase shifts in this regime. However, the deployment of reflecting elements still influences $\tilde{\gamma}^{(0)}$. The following lemma characterizes how $\tilde{\gamma}^{(0)}$ scales with T_1 , T_2 , and T , when they are large.

Lemma 6 (Average Channel Power in Pure NLoS Regime at Large T_1 , T_2 , and T). (i) $\tilde{\gamma}^{(0)} \xrightarrow{T_1, T_2 \rightarrow \infty} \alpha_{S1} \alpha_{12} \alpha_{2U} T_S T_1 T_2$. (ii) If $T_1 = cT$ and $T_2 = (1 - c)T$ for some $c \in (0, 1)$, then $\tilde{\gamma}^{(0)} \xrightarrow{T \rightarrow \infty} \alpha_{S1} \alpha_{12} \alpha_{2U} c(1 - c) T_S T^2$.

Proof: By showing that $\lim_{T_1, T_2 \rightarrow \infty} \frac{\tilde{\gamma}^{(0)}}{\alpha_{S1} \alpha_{12} \alpha_{2U} T_S T_1 T_2} = 1$ and $\lim_{T_1, T_2 \rightarrow \infty} \frac{\tilde{\gamma}^{(0)}}{\alpha_{S1} \alpha_{12} \alpha_{2U} c(1 - c) T_S T^2} = 1$, we can show $\tilde{\gamma}^{(0)} \xrightarrow{T_1, T_2 \rightarrow \infty} \alpha_{S1} \alpha_{12} \alpha_{2U} T_S T_1 T_2$ and $\tilde{\gamma}^{(0)} \xrightarrow{T \rightarrow \infty} \alpha_{S1} \alpha_{12} \alpha_{2U} c(1 - c) T_S T^2$, respectively. \blacksquare

Lemma 6 indicates that as $T_1, T_2 \rightarrow \infty$, $\tilde{\gamma}^{(0)}$ increases linearly with T_1 and T_2 . Furthermore, as $T \rightarrow \infty$, $\tilde{\gamma}^{(0)}$ increases quadratically with T .

V. COMPARISON

In this section, we compare the proposed optimal quasi-static phase shift design of the double-IRS cooperatively assisted system with that of its counterpart single-IRS-assisted system, where

the same BS serves the same user with the help of one IRS indexed by 0 and equipped with a URA of $M_0 \times N_0$ elements. Define $\mathcal{M}_0 \triangleq \{1, \dots, M_0\}$, $\mathcal{N}_0 \triangleq \{1, \dots, N_0\}$, and $\mathcal{T}_0 \triangleq \{1, \dots, M_0 N_0\}$. Let $\phi_0 \triangleq (\phi_{0,t})_{t \in \mathcal{T}_0} \in \mathbb{R}^{T_0 \times 1}$ denote the constant phase shifts of IRS 0, where its t -th element $\phi_{0,t}$ satisfies:

$$\phi_{0,t} \in [0, 2\pi), t \in \mathcal{T}_0. \quad (32)$$

Accordingly, denote $\mathbf{v}_0 \triangleq (e^{-j\phi_{0,t}})_{t \in \mathcal{T}_0} \in \mathbb{C}^T$. For a fair comparison, we let $M_0 N_0 = T$ and IRS 0 is placed at the same location as IRS 1 in the double-IRS cooperatively assisted system. The other setups remain the same as in the double-IRS cooperatively assisted system. Let $\mathbf{H}_{S0} \in \mathbb{C}^{T \times T_S}$ and $\mathbf{h}_{0U}^H \in \mathbb{C}^{1 \times T_S}$ represent the Rician channel between the BS and IRS 0 and the Rician channel between IRS 0 and the user, respectively. Specifically, we have:

$$\begin{aligned} \mathbf{H}_{S0} &= \sqrt{\alpha_{S0}} \left(\sqrt{\frac{K_{S0}}{K_{S0} + 1}} \bar{\mathbf{H}}_{S0} + \sqrt{\frac{1}{K_{S0} + 1}} \tilde{\mathbf{H}}_{S0} \right), \\ \mathbf{h}_{0U}^H &= \sqrt{\alpha_{0U}} \left(\sqrt{\frac{K_{0U}}{K_{0U} + 1}} \bar{\mathbf{h}}_{0U}^H + \sqrt{\frac{1}{K_{0U} + 1}} \tilde{\mathbf{h}}_{0U}^H \right), \end{aligned}$$

where α_{S0} and α_{0U} represent the large-scale fading powers; K_{S0} and K_{0U} represent the Rician factors; $\tilde{\mathbf{H}}_{S0} \in \mathbb{C}^{T \times T_S}$ and $\tilde{\mathbf{h}}_{0U}^H \in \mathbb{C}^{1 \times T_S}$ represent the random normalized NLoS components in a slot with elements i.i.d. according to $\mathcal{CN}(0, 1)$; $\bar{\mathbf{H}}_{S0} = \mathbf{a}_{A,S0} \mathbf{a}_{D,S0}^H \in \mathbb{C}^{T \times T_S}$ and $\tilde{\mathbf{h}}_{0U}^H = \mathbf{a}_{D,0U}^H \in \mathbb{C}^{1 \times T_S}$ represent the deterministic normalized LoS components with unit-modulus elements. Then, the equivalent channel between the BS and user of the single-IRS-assisted system, i.e., $\mathbf{h}_{e,0}^H(\phi_0) \in \mathbb{C}^{T_S}$, is given by:

$$\mathbf{h}_{e,0}^H(\phi_0) = \mathbf{h}_{SU}^H + \mathbf{h}_{0U}^H \text{diag}(\mathbf{v}_0^H) \mathbf{H}_{S0}.$$

Let $\gamma_0(\phi_0) \triangleq \mathbb{E} [\|\mathbf{h}_{e,0}(\phi_0)\|_2^2]$ represent the average channel power of the equivalent channel of the single-IRS-assisted system.

For ease of illustration, denote $\mathbf{A}_0 \triangleq \text{diag}(\bar{\mathbf{h}}_{0U}^H) \bar{\mathbf{H}}_{S0} \bar{\mathbf{H}}_{S0}^H \text{diag}(\bar{\mathbf{h}}_{0U}) \in \mathbb{C}^{T \times T}$ and $\mathbf{b}_0 \triangleq \text{diag}(\bar{\mathbf{h}}_{0U}^H) \bar{\mathbf{H}}_{S0} \bar{\mathbf{h}}_{SU} \in \mathbb{C}^T$. Now, we characterize the average channel power of the single-IRS-assisted system in the general and special Rician factor regimes.

Lemma 7 (Average Channel Power of Single-IRS-Assisted System). (i) For any $K_{S0}, K_{0U} \geq 0$, $\gamma_0(\phi_0) = L_{\overline{S0},\overline{0U}} \mathbf{v}_0^H \mathbf{A}_0 \mathbf{v}_0 + 2\Re \left\{ \sqrt{L_{SU} L_{\overline{S0},\overline{0U}}} \mathbf{v}_0^H \mathbf{b}_0 \right\} + \alpha_{SU} T_S + (L_{\widetilde{S0},\overline{0U}} + L_{\overline{S0},\widetilde{0U}} + L_{\widetilde{S0},\widetilde{0U}}) T_S T$. (ii) As $K_{S0}, K_{0U} \rightarrow \infty$, $\gamma_0(\phi_0) \rightarrow \bar{\gamma}_0(\phi_0) \triangleq \alpha_{S0} \alpha_{0U} \mathbf{v}_0^H \mathbf{A}_0 \mathbf{v}_0 + \alpha_{SU} T_S + 2\Re \left\{ \sqrt{\alpha_{SU} \alpha_{S0} \alpha_{0U}} \mathbf{v}_0^H \mathbf{b}_0 \right\}$. (iii) If $K_{S0} = K_{0U} = 0$, then $\gamma_0(\phi_0) = \tilde{\gamma}_0 \triangleq \alpha_{SU} T_S + \alpha_{S0} \alpha_{0U} T_S T$.

Proof: Following the proof of Theorem 1, we can show Lemma 7. ■

Noting that $\tilde{\gamma}_0$ for the pure NLoS regime does not change with ϕ_0 , we optimize the phase shifts only in the general Rician factor regime and pure LoS regime. Specifically, in the general Rician factor regime, the maximization of $\gamma_0(\phi_0)$ w.r.t. ϕ_0 is formulated as follows.

$$\begin{aligned} \gamma_0^* &\triangleq \max_{\phi_0} \gamma_0(\phi_0) \\ &\text{s.t. (32).} \end{aligned} \tag{33}$$

Let ϕ_0^* denote an optimal solution of the problem in (33). In the pure LoS regime, the maximization of $\bar{\gamma}_0(\phi_0)$ w.r.t. ϕ_0 is formulated below.

$$\begin{aligned} \bar{\gamma}_0^* &\triangleq \max_{\phi_0} \bar{\gamma}_0(\phi_0) \\ &\text{s.t. (32).} \end{aligned} \tag{34}$$

Let $\bar{\phi}_0^*$ denote an optimal solution of the problem in (34).

Define $\Delta_{\overline{S0},\overline{0U}} \triangleq \angle(\text{diag}(\mathbf{a}_{D,0U}^H)\mathbf{a}_{A,S0}) \in \mathbb{R}^T$ and $r_{\overline{S0},\overline{SU}} \triangleq \mathbf{a}_{D,S0}^H \mathbf{a}_{D,SU} \in \mathbb{C}$. The optimal solutions of the problem in (33) and problem in (34) are given below.

Lemma 8 (Optimal Solutions of Problem in (33) and Problem in (34)). *The unique optimal solutions of the problem in (33) and problem in (34) are given by:*

$$\phi_0^* = \bar{\phi}_0^* = \Lambda(-\Delta_{\overline{S0},\overline{0U}} - \angle(r_{\overline{S0},\overline{SU}}) \mathbf{1}_T). \tag{35}$$

Proof: Following the proof of Theorem 2, we can show Lemma 8. ■

Lemma 8 indicates that in both the general Rician factor and pure LoS regimes, the optimal phase changes over the cascaded LoS channel $(\overline{S0}, \overline{0U})$ are equivalent to the phase changes over the LoS channel \overline{SU} . Furthermore, the computational complexities for calculating ϕ_0^* and $\bar{\phi}_0^*$ based on Lemma 8 is $\mathcal{O}(T)$, as $T \rightarrow \infty$.

Finally, we characterize the average channel power in the pure NLoS regime and the optimal average channel power in the general and pure LoS regimes at large T .

Lemma 9 (Optimal Average Channel Power at Large T). (i) $\gamma_0^* \xrightarrow{T \rightarrow \infty} L_{\overline{S0},\overline{0U}} T_S T^2$. (ii) $\bar{\gamma}_0^* \xrightarrow{T \rightarrow \infty} \alpha_{S0} \alpha_{0U} T_S T^2$. (iii) $\tilde{\gamma}_0 \xrightarrow{T \rightarrow \infty} \alpha_{S0} \alpha_{0U} T_S T$.

Proof: Following the proof of Theorem 4, we can show Lemma 9. ■

Lemma 9 indicates that γ_0^* and $\bar{\gamma}_0^*$ increase quadratically with T , and $\tilde{\gamma}_0$ increases linearly with T , as $T \rightarrow \infty$. Similarly, for the single-IRS-assisted system, the optimal quasi-static phase shift design achieves the same average power gain in order as the optimal instantaneous CSI-adaptive phase shift design in [8].

Remark 2 (Quasi-static Phase Shift Design for Single-IRS-Assisted System). *Lemma 7 and Lemma 8 extend the analysis and optimization results on quasi-static phase shift design for a less general single-IRS-assisted system in [14], where the direct channel is modeled as Rayleigh fading. Moreover, note that the optimal average channel power for the general single-IRS-assisted system with a quasi-static phase shift design and a large number of reflecting elements has not been characterized in the existing literature.*

Based on the optimization and analytical results in Section IV and Section V, we summarize the computational complexities and average channel powers both in order for the optimal quasi-static phase shift designs for the two IRS-assisted systems with a large number of total reflecting elements in the general Rician factor, pure LoS, and pure NLoS regimes in Table I.⁵

- **Computational Complexity:** For each case where the phase shift optimization is necessary, the closed-form optimal quasi-static phase shift design for the double-IRS cooperatively assisted system (if it exists) has the same computational complexity as the closed-form optimal quasi-static phase shift design for the single-IRS-assisted system, whereas the numerical quasi-static phase shift design for the double-IRS cooperatively assisted system has higher computational complexity than the closed-form optimal quasi-static phase shift design for the single-IRS-assisted system.
- **Optimal Average Channel Power:** (i) In the general Rician factor regime, the average channel power in Case 0 of the double-IRS cooperatively assisted system is identical to the average channel power in the single-IRS-assisted system. Besides, for the double-IRS cooperatively assisted system in the general Rician factor and pure LoS regimes, the optimal average channel powers in Case 1 and Case 2 are equivalent and are higher than the average channel power in Case 0 and lower than the average channel power in Case 3. (ii) In the pure LoS regime, the average channel power of the double-IRS cooperatively assisted system is higher than that of the single-IRS-assisted system. Besides, for the double-IRS cooperatively assisted system, the average channel power in the pure LoS regime is identical to the average channel power in Case 3 of the general Rician factor regime. (iii) In the pure NLoS regime, the average channel power of the double-IRS cooperatively assisted system is higher than

⁵The computational complexity results are derived from those in Section IV by letting $T_1 = cT$ and $T_2 = (1 - c)T$ for some $c \in (0, 1)$ and $T \rightarrow \infty$. In some cases, there is no need to optimize the phase shifts, and hence we use $\mathcal{O}(1)$ for the computational complexity and consider the average channel power.

TABLE I: Comparisons as $T \rightarrow \infty$

Regime	System	Computational Complexity		Optimal Average Channel Power
General Rician Factor	Double-IRS	Case 0	$\mathcal{O}(1)$	$\mathcal{O}(T^2)$
		Case 1	$\mathcal{O}(T^2)$ (numerical), $\mathcal{O}(T)$ (analytical)	$\mathcal{O}(T^3)$
		Case 2	$\mathcal{O}(T^2)$ (numerical), $\mathcal{O}(T)$ (analytical)	$\mathcal{O}(T^3)$
		Case 3	$\mathcal{O}(T^3)$ (numerical), $\mathcal{O}(T)$ (analytical)	$\mathcal{O}(T^4)$
	Single-IRS	$\mathcal{O}(T)$ (analytical)		$\mathcal{O}(T^2)$
	Pure LoS	Double-IRS	$\mathcal{O}(T^3)$ (numerical)	$\mathcal{O}(T^4)$
	Single-IRS	$\mathcal{O}(T)$ (analytical)	$\mathcal{O}(T^2)$	
Pure NLoS	Double-IRS	$\mathcal{O}(1)$	$\mathcal{O}(T^2)$	
	Single-IRS	$\mathcal{O}(1)$	$\mathcal{O}(T)$	

that of the single-IRS-assisted system. Besides, for the double-IRS cooperatively assisted system, the average channel power in the pure NLoS regime is equivalent to the average channel power in Case 0 of the general Rician factor regime.

- **Tradeoff:** The double-IRS cooperatively assisted system achieves a better performance and computational complexity tradeoff than the single-IRS-assisted system in some cases and a different performance and computational complexity tradeoff in the other cases. As for quasi-static phase shift designs, phase shifts remain constant during a certain period, the computational complexity for optimizing phase shifts is negligible. Therefore, the double-IRS cooperatively assisted system is more preferable than the single-IRS-assisted system in practice.

VI. NUMERICAL RESULTS

In this section, we numerically evaluate the average rates of the proposed solutions for the double-IRS cooperatively assisted system, where the BS, IRS 1, IRS 2, and user U are located at $(0, 0)$, $(0.5, 1)$, $(49.5, 1)$ and $(50, 0)$ (in m), respectively, as shown in Fig. 2. Specifically, the proposed solutions for the general Rician factor, pure LoS, and pure NLoS regimes are referred to as *D-IRS-Prop-Gen*, *D-IRS-Prop-LoS*, and *D-IRS-Prop-NLoS*, respectively. In the simulation, we set $d = \frac{\lambda}{2}$, $M_S = N_S = 2$, $M_1 = N_1 = M_2 = N_2 = 6$, $P_S = 5$ dBm, $\sigma^2 = -104$ dBm, $\varphi_{S1}^{(h)} = \varphi_{S1}^{(v)} = \pi/6$, $\varphi_{S2}^{(h)} = \varphi_{S2}^{(v)} = \pi/4$, $\varphi_{12}^{(h)} = \varphi_{12}^{(v)} = \pi/5$, $\varphi_{SU}^{(h)} = \varphi_{SU}^{(v)} = \pi/3$, $\varphi_{1U}^{(h)} = \varphi_{1U}^{(v)} = \pi/8$, $\varphi_{2U}^{(h)} = \varphi_{2U}^{(v)} = \pi/9$, $\delta_{S1}^{(h)} = \delta_{S1}^{(v)} = \pi/6$, $\delta_{S2}^{(h)} = \delta_{S2}^{(v)} = \pi/5$, $\delta_{12}^{(h)} = \delta_{12}^{(v)} = \pi/4$, $K_{S1} = K_{S2} = K_{1U} = K_{2U} = K_{SU} = K_{12} = K = 10$ dB, if not specified otherwise. We set $\alpha_{ab} = 1/(1000d_{ab}^{\bar{\alpha}_{ab}})$ (i.e., $-30 + 10\bar{\alpha}_{ab} \log_{10}(d_{ab})$ dB), $ab = S1, S2, 12, 1U, 2U, SU$, where

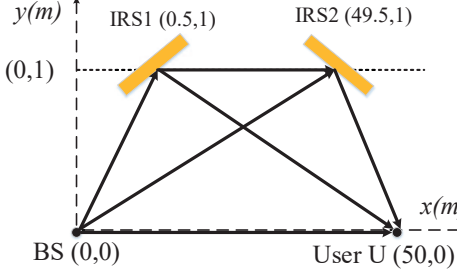


Fig. 2: The double-IRS cooperatively assisted system in Section VI.

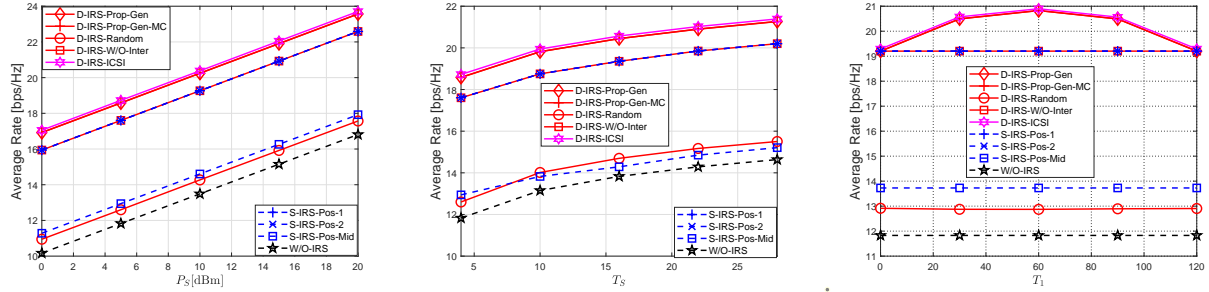


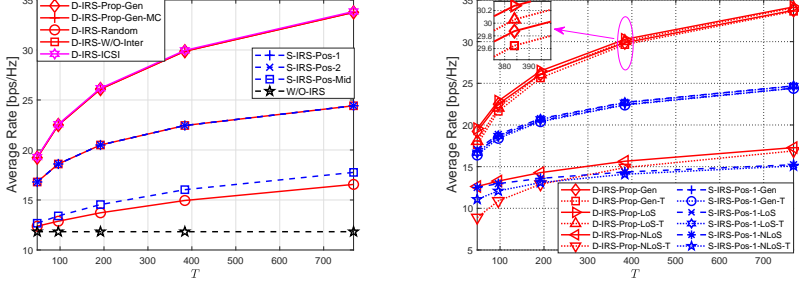
Fig. 3: Average rate versus P_S .

Fig. 4: Average rate versus T_S .

Fig. 5: Average rate versus T_1 .

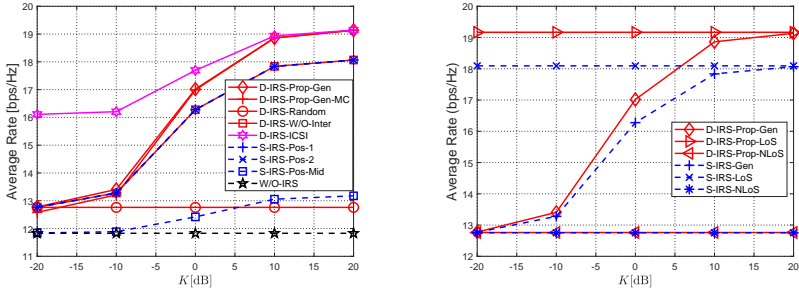
$\bar{\alpha}_{ab}$ represents the corresponding path loss exponent [6], [8], [23]. We set $\bar{\alpha}_{S1} = \bar{\alpha}_{2U} = 2.2$ and $\bar{\alpha}_{SU} = \bar{\alpha}_{S2} = \bar{\alpha}_{1U} = \bar{\alpha}_{12} = 3$ as in [23].

In the simulation, we consider seven baseline schemes which adopt instantaneous CSI-adaptive MRT beamforming as in this paper. Specifically, six of them adopt quasi-static phase shift designs, referred to as *W/O-IRS*, *S-IRS-Pos-1*, *S-IRS-Pos-2*, *S-IRS-Pos-Mid*, *D-IRS-Random*, and *D-IRS-W/O-Inter*, and one adopts an instantaneous CSI-adaptive phase shift design, referred to as *D-IRS-ICSI*. The details of the seven baseline schemes are given below. *W/O-IRS* applies to the counterpart system without any IRS [27]. *S-IRS-Pos-1*, *S-IRS-Pos-2*, and *S-IRS-Pos-Mid* apply to the counterpart single-IRS-assisted systems with the single IRS located at the locations of IRS 1, IRS 2, and the midpoint between IRS 1 and IRS 2, respectively, and adopt the optimal phase shifts obtained by Lemma 8 [14]. More specifically, *S-IRS-Pos-1-Gen*, *S-IRS-Pos-1-LoS*, and *S-IRS-Pos-1-NLoS* represent the quasi-static phase shift design of *S-IRS-Pos-1* in the general Rician factor, pure LoS, and pure NLoS regimes, respectively. *D-IRS-Random*, *D-IRS-W/O-Inter*, and *D-IRS-ICSI* apply to the same double-IRS cooperatively assisted system shown in Fig. 2. Specifically, *D-IRS-Random* chooses the phase shifts uniformly at random [6]; *D-IRS-W/O-Inter* adopts the phase shifts obtained by Algorithm 2 for Problem 3 with $\mathbf{H}_{12} = \mathbf{0}$ (without considering the inter-IRS channel) [17]; *D-IRS-ICSI* adopts the optimal instantaneous



(a) General Rician factor regimes

(b) Special Rician factor regimes

Fig. 6: Average rate versus T 

(a) General Rician factor regimes

(b) Special Rician factor regimes

Fig. 7: Average rate versus K

CSI-adaptive phase shift design as in [23].

Fig. 3, Fig. 4, Fig. 5, Fig. 6, and Fig. 7 illustrate the average rate versus the transmit power P_S , number of antennas at the BS T_S , number of IRS 1's reflecting elements T_1 , total number of reflecting elements in the system T , and Rician factor K , respectively. In these figures, *D-IRS-Prop-Gen-MC* represents the numerical expectation of the rate of *D-IRS-Prop-Gen*, and each other curve represents the analytical upper bound of the average rate of a scheme based on Jensen's inequality. From Fig. 3, Fig. 4, Fig. 5, Fig. 6 (a), and Fig. 7 (a), we can see that *D-IRS-Prop-Gen-MC* and *D-IRS-Prop-Gen* are very close to each other, indicating that the upper bound, $\log_2 (1 + \frac{P_S}{\sigma^2} \gamma(\phi_1, \phi_2))$, is a good approximation of $C(\phi_1, \phi_2)$. In Fig. 6 (b), *D-IRS-Prop-Gen-T* (*S-IRS-Pos-1-Gen-T*), *D-IRS-Prop-LoS-T* (*S-IRS-Pos-1-LoS-T*), and *D-IRS-Prop-NLoS-T* (*S-IRS-Pos-1-NLoS*) represent the asymptotic results for *D-IRS-Prop-Gen* (*S-IRS-Pos-1-Gen*), *D-IRS-Prop-LoS* (*S-IRS-Pos-1-LoS*), and *D-IRS-Prop-NLoS* (*S-IRS-Pos-1-NLoS*) at large T , respectively. For each of them, the gap between the general result at any T and asymptotic result at large T decreases with T , which is in accordance with Theorem 4, Lemma 5, Lemma 6, and Lemma 9. In Fig. 7 (b), the gap between *D-IRS-Prop-Gen* and *D-IRS-Prop-LoS* decreases with K , and the gap

between *D-IRS-Prop-Gen* and *D-IRS-Prop-NLoS* increases with K , which are in accordance with Corollary 1 and Corollary 2. Besides, the gap between *S-IRS-Pos-1-Gen* and *S-IRS-Pos-1-LoS* decreases with K , and the gap between *S-IRS-Pos-1-General* and *S-IRS-Pos-1-NLoS* increases with K , which are in accordance with Lemma 7.

From Fig. 3 and Fig. 4, we see that the average rate of each scheme increases with P_S and T_S , respectively. The increment w.r.t. T_S is due to the increment of the diversity gain. From Fig. 5, we see that the average rate of the proposed solution is maximized when the two IRSs have the same number of elements, mainly due to the symmetric channel setup. From Fig. 6, we observe that the average rate of each scheme for IRS-assisted system increases with T , mainly due to the increment of reflecting signal power. Fig. 7 shows that the average rate of each scheme with quasi-static phase shift design increases with K , mainly due to the increment of the channel power of each LoS component.

From Fig. 3, Fig. 4, Fig. 5, Fig. 6 (a), and Fig. 7 (a), we can see that the proposed solution outperforms the six baseline schemes with quasi-static phase shift designs. Specifically, the gain of the proposed solution over *D-IRS-Random* comes from the optimization of the quasi-static phase shifts and the gain of the proposed solution over *D-IRS-W/O-Inter* derives from the effective utilization of the inter-IRS channel. Furthermore, *D-IRS-ICSI* outperforms the proposed solution at the sacrifice of implementation complexity and computational complexity. Considering both complexity and performance, quasi-static phase shift design is desirable as long as the LoS components are sufficiently large.

VII. CONCLUSION

This paper investigated the analysis and optimization of the quasi-static phase shift design for a double-IRS cooperatively assisted system. Furthermore, this paper compared the computational complexity for optimizing the quasi-static phase shift design and the asymptotically optimal average channel power of the double-IRS cooperatively assisted system at a large number of reflecting elements with those of the counterpart single-IRS-assisted system. Both analytical and numerical results demonstrate notable gains of the proposed cooperative quasi-static phase shift design over the existing solutions and reveal insights into designing practical multi-IRS-assisted systems.

APPENDIX A: PROOF OF LEMMA 1

First, we prove Statement (i). As $\gamma(\phi_1, \phi_2) = \mathbb{E}[\|\mathbf{h}_e(\phi_1, \phi_2)\|_2^2]$, with $\mathbf{h}_e(\phi_1, \phi_2)$ given by (6), it is sufficient to show $\mathbf{h}_e^H(\phi_1, \phi_2) \stackrel{d}{\sim} \mathbf{h}_{SU}^H + \mathbf{h}_{2U}^H \text{diag}(\mathbf{v}_2^H) \mathbf{H}_{S2} + (\mathbf{h}_{1U}^H + \mathbf{h}_{2U}^H \text{diag}(\mathbf{v}_2^H) \mathbf{H}_{12}) \mathbf{H}_{S1}$, which is irrelevant to \mathbf{v}_1 . By (6), it is equivalent to show $\mathbf{H}_{S1} \stackrel{d}{\sim} \text{diag}(\mathbf{v}_1^H) \mathbf{H}_{S1}$ or $\mathbf{H}_{12} \stackrel{d}{\sim} \mathbf{H}_{12} \text{diag}(\mathbf{v}_1^H)$ and $\mathbf{h}_{1U}^H \stackrel{d}{\sim} \mathbf{h}_{1U}^H \text{diag}(\mathbf{v}_1^H)$. First, we show that $\mathbf{H}_{S1} \stackrel{d}{\sim} \text{diag}(\mathbf{v}_1^H) \mathbf{H}_{S1}$ if $K_{S1} = 0$. If $K_{S1} = 0$, then $\mathbf{H}_{S1} = \sqrt{\alpha_{S1}} \tilde{\mathbf{H}}_{S1}$. As all elements of $\tilde{\mathbf{H}}_{S1}$ are i.i.d. $\mathcal{CN}(0, 1)$, $\text{vec}(\mathbf{H}_{S1}) \sim \mathcal{CN}(0, \alpha_{S1} \mathbf{I}_{T_S T_1})$. Besides, we have:

$$\text{vec}(\text{diag}(\mathbf{v}_1^H) \mathbf{H}_{S1}) \stackrel{(a)}{=} (\mathbf{I}_{T_S} \otimes \text{diag}(\mathbf{v}_1^H)) \text{vec}(\mathbf{H}_{S1}) \stackrel{(b)}{\sim} \mathcal{CN}(0, \alpha_{S1} \mathbf{I}_{T_S T_1}). \quad (36)$$

where (a) is due to [28, Theorem 7.16], and (b) is due to [29, (A.26)] and the fact that $\mathbf{I}_{T_S} \otimes \text{diag}(\mathbf{v}_1^H)$ is an unitary matrix (noting that $\text{diag}(\mathbf{v}_1^H)$ is an unitary matrix). Thus, we have $\mathbf{H}_{S1} \stackrel{d}{\sim} \text{diag}(\mathbf{v}_1^H) \mathbf{H}_{S1}$. Next, we show $\mathbf{H}_{12} \stackrel{d}{\sim} \mathbf{H}_{12} \text{diag}(\mathbf{v}_1^H)$ and $\mathbf{h}_{1U}^H \stackrel{d}{\sim} \mathbf{h}_{1U}^H \text{diag}(\mathbf{v}_1^H)$ if $K_{12} = K_{1U} = 0$. If $K_{12} = K_{1U} = 0$, then $\mathbf{H}_{12} = \sqrt{\alpha_{12}} \tilde{\mathbf{H}}_{12}$ and $\mathbf{h}_{1U}^H = \sqrt{\alpha_{1U}} \tilde{\mathbf{h}}_{1U}^H$. As all elements of $\tilde{\mathbf{H}}_{12}$ and $\tilde{\mathbf{h}}_{1U}^H$ are i.i.d. $\mathcal{CN}(0, 1)$, $\text{vec}(\mathbf{H}_{12}) \sim \mathcal{CN}(0, \alpha_{12} \mathbf{I}_{T_1 T_2})$ and $\mathbf{h}_{1U}^H \sim \mathcal{CN}(0, \alpha_{1U} \mathbf{I}_{T_1})$. Besides, we have:

$$\text{vec}(\mathbf{H}_{12} \text{diag}(\mathbf{v}_1^H)) \stackrel{(c)}{=} (\text{diag}(\mathbf{v}_1^H) \otimes \mathbf{I}_{T_2}) \text{vec}(\mathbf{H}_{12}) \stackrel{(d)}{\sim} \mathcal{CN}(0, \alpha_{12} \mathbf{I}_{T_1 T_2}), \quad (37)$$

$$\mathbf{h}_{1U}^H \text{diag}(\mathbf{v}_1^H) \stackrel{(e)}{\sim} \mathcal{CN}(0, \alpha_{1U} \mathbf{I}_{T_1}). \quad (38)$$

where (c) is due to [28, Theorem 7.16], (d) is due to [29, A.26] and the fact that $\text{diag}(\mathbf{v}_1^H) \otimes \mathbf{I}_{T_2}$ is unitary matrix, and (e) is due to the fact that $\text{diag}(\mathbf{v}_1^H)$ is an unitary matrix. Thus, we have $\mathbf{H}_{12} \stackrel{d}{\sim} \mathbf{H}_{12} \text{diag}(\mathbf{v}_1^H)$ and $\mathbf{h}_{1U}^H \stackrel{d}{\sim} \mathbf{h}_{1U}^H \text{diag}(\mathbf{v}_1^H)$. Therefore, we complete the proof of Statement (i).

Next, we prove Statement (ii). Similarly, it is sufficient to show $\mathbf{h}_{2U} \stackrel{d}{\sim} \mathbf{H}_{2U} \text{diag}(\mathbf{v}_2^H)$ or $\mathbf{H}_{12} \stackrel{d}{\sim} \text{diag}(\mathbf{v}_2^H) \mathbf{H}_{12}$ and $\mathbf{H}_{S2} \stackrel{d}{\sim} \text{diag}(\mathbf{v}_2^H) \mathbf{H}_{S2}$. Following the proof for Statement (i), we can show that $\mathbf{h}_{2U} \stackrel{d}{\sim} \mathbf{H}_{2U} \text{diag}(\mathbf{v}_2^H)$ if $K_{2U} = 0$, and $\mathbf{H}_{12} \stackrel{d}{\sim} \text{diag}(\mathbf{v}_2^H) \mathbf{H}_{12}$ and $\mathbf{H}_{S2} \stackrel{d}{\sim} \text{diag}(\mathbf{v}_2^H) \mathbf{H}_{S2}$ if $K_{12} = K_{S2} = 0$. Therefore, we can show Statement (ii).

APPENDIX B: PROOF OF THEOREM 1

In what follows, we derive the expression of $\gamma(\phi_1, \phi_2)$ for all $K_{S1}, K_{S2}, K_{12}, K_{1U}, K_{2U}, K_{SU} \geq 0$, based on which we can readily obtain $\gamma^{(0)}, \gamma^{(1)}(\phi_1), \gamma^{(2)}(\phi_2)$, and $\gamma^{(3)}(\phi_1, \phi_2)$ given by (13), (14), (15), and (16), respectively. Note that for all $K_{S1}, K_{S2}, K_{12}, K_{1U}, K_{2U}, K_{SU} \geq 0$, we have:

$$\begin{aligned} \gamma(\phi_1, \phi_2) &= \mathbb{E}[\|\mathbf{h}_e(\phi_1, \phi_2)\|_2^2] \stackrel{(a)}{=} \mathbb{E} \left[\left\| \underbrace{\mathbf{h}_{SU}^H}_{\triangleq \mathbf{x}_0^H} + \sum_{l \in \mathcal{L}} \underbrace{\mathbf{h}_{lU}^H \text{diag}(\mathbf{v}_l^H) \mathbf{H}_{Sl}}_{\triangleq \mathbf{x}_l^H} + \underbrace{\mathbf{h}_{2U}^H \text{diag}(\mathbf{v}_2^H) \mathbf{H}_{12} \text{diag}(\mathbf{v}_1^H) \mathbf{H}_{S1}}_{\triangleq \mathbf{x}_3^H} \right\|_2^2 \right] \\ &= \sum_{i=0}^3 \mathbb{E}[\|\mathbf{x}_i^H\|_2^2] + 2 \sum_{i=0}^2 \sum_{j=i+1}^3 \mathfrak{R}\{\mathbb{E}[\mathbf{x}_j^H \mathbf{x}_i]\}, \end{aligned} \quad (39)$$

where (a) is due to (6). Thus, it remains to calculate $\mathbb{E}[\|\mathbf{x}_i^H\|_2^2], i = 0, 1, 2, 3$ and $\mathbb{E}[\mathbf{x}_j^H \mathbf{x}_i], i = 0, 1, 2, j = i+1, \dots, 3$. As all elements of $\tilde{\mathbf{h}}_{1U}, \tilde{\mathbf{h}}_{2U}, \tilde{\mathbf{h}}_{SU}, \tilde{\mathbf{H}}_{S1}, \tilde{\mathbf{H}}_{S2}$, and $\tilde{\mathbf{H}}_{12}$ are i.i.d. $\mathcal{CN}(0, 1)$, we can easily show that multiplying any of them with an independent random matrix or a constant matrix producing a random matrix (or vector) with zero mean. This fact will be used in the following proof.

(i) We have:

$$\mathbb{E}[\|\mathbf{x}_0^H\|_2^2] \stackrel{(a)}{=} \mathbb{E}\left[\|\sqrt{L_{SU}}\bar{\mathbf{h}}_{SU}^H + \sqrt{L_{\widetilde{SU}}}\tilde{\mathbf{h}}_{SU}^H\|_2^2\right] \stackrel{(b)}{=} L_{\overline{SU}}\|\bar{\mathbf{h}}_{SU}^H\|_2^2 + L_{\widetilde{SU}}\mathbb{E}\left[\|\tilde{\mathbf{h}}_{SU}^H\|_2^2\right] \stackrel{(c)}{=} \alpha_{SU}T_S, \quad (40)$$

where (a) is due to (2), (b) is due to $\mathbb{E}[\bar{\mathbf{h}}_{SU}^H \tilde{\mathbf{h}}_{SU}] = 0$, and (c) is due to $\|\bar{\mathbf{h}}_{SU}^H\|_2^2 = T_S$ and $\mathbb{E}\left[\|\tilde{\mathbf{h}}_{SU}^H\|_2^2\right] = T_S$.

(ii) For $l \in \mathcal{L}$, we have:

$$\begin{aligned} \mathbb{E}\left[\|\tilde{\mathbf{h}}_{lU}^H \text{diag}(\mathbf{v}_l^H) \bar{\mathbf{H}}_{Sl}\|_2^2\right] &= \mathbb{E}\left[\text{Tr}\left(\tilde{\mathbf{h}}_{lU}^H \text{diag}(\mathbf{v}_l^H) \bar{\mathbf{H}}_{Sl} \bar{\mathbf{H}}_{Sl}^H \text{diag}(\mathbf{v}_l) \tilde{\mathbf{h}}_{lU}\right)\right] \\ &\stackrel{(a)}{=} \mathbb{E}\left[\text{Tr}\left(\bar{\mathbf{H}}_{Sl} \bar{\mathbf{H}}_{Sl}^H \tilde{\mathbf{h}}_{lU} \tilde{\mathbf{h}}_{lU}^H\right)\right] \stackrel{(b)}{=} \text{Tr}\left(\bar{\mathbf{H}}_{Sl} \bar{\mathbf{H}}_{Sl}^H \mathbb{E}\left[\tilde{\mathbf{h}}_{lU} \tilde{\mathbf{h}}_{lU}^H\right]\right) \\ &\stackrel{(c)}{=} \text{Tr}\left(\bar{\mathbf{H}}_{Sl} \bar{\mathbf{H}}_{Sl}^H\right) = T_S T_l, \end{aligned} \quad (41)$$

where (a) is due to $\tilde{\mathbf{h}}_{lU}^H \text{diag}(\mathbf{v}_l^H) \stackrel{d}{\sim} \tilde{\mathbf{h}}_{lU}^H$ (which is shown in Appendix A) and $\text{Tr}(\mathbf{ABC}) = \text{Tr}(\mathbf{BCA})$, and (e) is due to $\mathbb{E}\left[\tilde{\mathbf{h}}_{lU} \tilde{\mathbf{h}}_{lU}^H\right] = \mathbf{I}_{T_l}$. Similarly, we can show:

$$\mathbb{E}\left[\|\bar{\mathbf{h}}_{lU}^H \text{diag}(\mathbf{v}_l^H) \tilde{\mathbf{H}}_{Sl}\|_2^2\right] = T_S T_l, \quad \mathbb{E}\left[\|\tilde{\mathbf{h}}_{lU}^H \text{diag}(\mathbf{v}_l^H) \tilde{\mathbf{H}}_{Sl}\|_2^2\right] = T_S T_l. \quad (42)$$

Thus, we have:

$$\begin{aligned} \mathbb{E}[\|\mathbf{x}_l^H\|_2^2] &\stackrel{(d)}{=} \mathbb{E}\left[\|(\sqrt{L_{lU}}\bar{\mathbf{h}}_{lU}^H + \sqrt{L_{\widetilde{lU}}}\tilde{\mathbf{h}}_{lU}^H)\text{diag}(\mathbf{v}_l^H)(\sqrt{L_{Sl}}\bar{\mathbf{H}}_{Sl}^H + \sqrt{L_{\widetilde{Sl}}}\tilde{\mathbf{H}}_{Sl}^H)\|_2^2\right] \\ &\stackrel{(e)}{=} L_{\overline{Sl}, \overline{lU}}\|\bar{\mathbf{h}}_{lU}^H \text{diag}(\mathbf{v}_l^H) \bar{\mathbf{H}}_{Sl}\|_2^2 + L_{\widetilde{Sl}, \widetilde{lU}}\mathbb{E}\left[\|\tilde{\mathbf{h}}_{lU}^H \text{diag}(\mathbf{v}_l^H) \bar{\mathbf{H}}_{Sl}\|_2^2\right] \\ &\quad + L_{\overline{Sl}, \widetilde{lU}}\mathbb{E}\left[\|\bar{\mathbf{h}}_{lU}^H \text{diag}(\mathbf{v}_l^H) \tilde{\mathbf{H}}_{Sl}\|_2^2\right] + L_{\widetilde{Sl}, \widetilde{lU}}\mathbb{E}\left[\|\tilde{\mathbf{h}}_{lU}^H \text{diag}(\mathbf{v}_l^H) \tilde{\mathbf{H}}_{Sl}\|_2^2\right] \\ &\stackrel{(f)}{=} L_{\overline{Sl}, \overline{lU}}\|\bar{\mathbf{h}}_{lU}^H \text{diag}(\mathbf{v}_l^H) \bar{\mathbf{H}}_{Sl}\|_2^2 + (L_{\widetilde{Sl}, \overline{lU}} + L_{\overline{Sl}, \widetilde{lU}} + L_{\widetilde{Sl}, \widetilde{lU}})T_S T_l \\ &\stackrel{(g)}{=} L_{\overline{Sl}, \overline{lU}}\mathbf{v}_l^H \text{diag}(\bar{\mathbf{h}}_{lU}^H) \bar{\mathbf{H}}_{Sl} \bar{\mathbf{H}}_{Sl}^H \text{diag}(\bar{\mathbf{h}}_{lU}) \mathbf{v}_l + (L_{\widetilde{Sl}, \overline{lU}} + L_{\overline{Sl}, \widetilde{lU}} + L_{\widetilde{Sl}, \widetilde{lU}})T_S T_l, \end{aligned} \quad (43)$$

where (d) is due to (1) and (2), (e) is due to $\mathbb{E}\left[\tilde{\mathbf{h}}_{lU}^H \text{diag}(\mathbf{v}_l^H) \bar{\mathbf{H}}_{Sl}\right] = \mathbf{0}_{1 \times T_S}$, $\mathbb{E}\left[\tilde{\mathbf{h}}_{lU}^H \text{diag}(\mathbf{v}_l^H) \tilde{\mathbf{H}}_{Sl}\right] = \mathbf{0}_{1 \times T_S}$, and $\mathbb{E}\left[\tilde{\mathbf{h}}_{lU}^H \text{diag}(\mathbf{v}_l^H) \tilde{\mathbf{H}}_{Sl}\right] = \mathbf{0}_{1 \times T_S}$, (f) is due to (41) and (42), and (g) is due to $\bar{\mathbf{h}}_{lU}^H \text{diag}(\mathbf{v}_l^H) = \mathbf{v}_l^H \text{diag}(\bar{\mathbf{h}}_{lU}^H)$.

(iii) Similarly to the derivation of (41), we have:

$$\mathbb{E}\left[\|\tilde{\mathbf{h}}_{2U}^H \text{diag}(\mathbf{v}_2^H) \bar{\mathbf{H}}_{12} \text{diag}(\mathbf{v}_1^H) \bar{\mathbf{H}}_{S1}\|_2^2\right] = \|\bar{\mathbf{H}}_{12} \text{diag}(\mathbf{v}_1^H) \bar{\mathbf{H}}_{S1}\|_F^2,$$

$$\begin{aligned}
\mathbb{E} \left[\|\bar{\mathbf{h}}_{2U}^H \text{diag}(\mathbf{v}_2^H) \bar{\mathbf{H}}_{12} \text{diag}(\mathbf{v}_1^H) \tilde{\mathbf{H}}_{S1} \|_2^2 \right] &= T_S \|\bar{\mathbf{h}}_{2U}^H \text{diag}(\mathbf{v}_2^H) \bar{\mathbf{H}}_{12} \|_2^2, \\
\mathbb{E} \left[\|\tilde{\mathbf{h}}_{2U}^H \text{diag}(\mathbf{v}_2^H) \bar{\mathbf{H}}_{12} \text{diag}(\mathbf{v}_1^H) \tilde{\mathbf{H}}_{S1} \|_2^2 \right] &= \mathbb{E} \left[\|\bar{\mathbf{h}}_{2U}^H \text{diag}(\mathbf{v}_2^H) \tilde{\mathbf{H}}_{12} \text{diag}(\mathbf{v}_1^H) \bar{\mathbf{H}}_{S1} \|_2^2 \right] \\
&= \mathbb{E} \left[\|\tilde{\mathbf{h}}_{2U}^H \text{diag}(\mathbf{v}_2^H) \tilde{\mathbf{H}}_{12} \text{diag}(\mathbf{v}_1^H) \bar{\mathbf{H}}_{S1} \|_2^2 \right] = \mathbb{E} \left[\|\tilde{\mathbf{h}}_{2U}^H \text{diag}(\mathbf{v}_2^H) \tilde{\mathbf{H}}_{12} \text{diag}(\mathbf{v}_1^H) \tilde{\mathbf{H}}_{S1} \|_2^2 \right] \\
&= \mathbb{E} \left[\|\tilde{\mathbf{h}}_{2U}^H \text{diag}(\mathbf{v}_2^H) \tilde{\mathbf{H}}_{12} \text{diag}(\mathbf{v}_1^H) \tilde{\mathbf{H}}_{S1} \|_2^2 \right] = T_S T_1 T_2. \tag{44}
\end{aligned}$$

Thus, we have:

$$\begin{aligned}
\mathbb{E} [\|\mathbf{x}_3^H\|_2^2] &\stackrel{(a)}{=} \mathbb{E} \left[\|(\sqrt{L_{2U}} \bar{\mathbf{h}}_{2U}^H + \sqrt{L_{2U}} \tilde{\mathbf{h}}_{2U}^H) \text{diag}(\mathbf{v}_2^H) (\sqrt{L_{12}} \bar{\mathbf{H}}_{12} + \sqrt{L_{12}} \tilde{\mathbf{H}}_{12}) \text{diag}(\mathbf{v}_1^H) (\sqrt{L_{S1}} \bar{\mathbf{H}}_{S1} + \sqrt{L_{S1}} \tilde{\mathbf{H}}_{S1}) \|_2^2 \right] \\
&\stackrel{(b)}{=} L_{\overline{S1}, \overline{12}, \overline{2U}} \|\bar{\mathbf{h}}_{2U}^H \text{diag}(\mathbf{v}_2^H) \bar{\mathbf{H}}_{12} \text{diag}(\mathbf{v}_1^H) \bar{\mathbf{H}}_{S1} \|_2^2 + L_{\overline{S1}, \overline{12}, \widetilde{2U}} \mathbb{E} \left[\|\tilde{\mathbf{h}}_{2U}^H \text{diag}(\mathbf{v}_2^H) \bar{\mathbf{H}}_{12} \text{diag}(\mathbf{v}_1^H) \bar{\mathbf{H}}_{S1} \|_2^2 \right] \\
&\quad + L_{\widetilde{S1}, \overline{12}, \overline{2U}} \mathbb{E} \left[\|\bar{\mathbf{h}}_{2U}^H \text{diag}(\mathbf{v}_2^H) \bar{\mathbf{H}}_{12} \text{diag}(\mathbf{v}_1^H) \tilde{\mathbf{H}}_{S1} \|_2^2 \right] + L_{\widetilde{S1}, \overline{12}, \widetilde{2U}} \mathbb{E} \left[\|\tilde{\mathbf{h}}_{2U}^H \text{diag}(\mathbf{v}_2^H) \bar{\mathbf{H}}_{12} \text{diag}(\mathbf{v}_1^H) \tilde{\mathbf{H}}_{S1} \|_2^2 \right] \\
&\quad + L_{\overline{S1}, \widetilde{12}, \overline{2U}} \mathbb{E} \left[\|\bar{\mathbf{h}}_{2U}^H \text{diag}(\mathbf{v}_2^H) \tilde{\mathbf{H}}_{12} \text{diag}(\mathbf{v}_1^H) \bar{\mathbf{H}}_{S1} \|_2^2 \right] + L_{\overline{S1}, \widetilde{12}, \widetilde{2U}} \mathbb{E} \left[\|\tilde{\mathbf{h}}_{2U}^H \text{diag}(\mathbf{v}_2^H) \tilde{\mathbf{H}}_{12} \text{diag}(\mathbf{v}_1^H) \bar{\mathbf{H}}_{S1} \|_2^2 \right] \\
&\quad + L_{\widetilde{S1}, \widetilde{12}, \widetilde{2U}} \mathbb{E} \left[\|\tilde{\mathbf{h}}_{2U}^H \text{diag}(\mathbf{v}_2^H) \tilde{\mathbf{H}}_{12} \text{diag}(\mathbf{v}_1^H) \tilde{\mathbf{H}}_{S1} \|_2^2 \right] + L_{\widetilde{S1}, \widetilde{12}, \widetilde{2U}} \mathbb{E} \left[\|\tilde{\mathbf{h}}_{2U}^H \text{diag}(\mathbf{v}_2^H) \tilde{\mathbf{H}}_{12} \text{diag}(\mathbf{v}_1^H) \tilde{\mathbf{H}}_{S1} \|_2^2 \right] \\
&\stackrel{(c)}{=} L_{\overline{S1}, \overline{12}, \overline{2U}} \|\bar{\mathbf{h}}_{2U}^H \text{diag}(\mathbf{v}_2^H) \bar{\mathbf{H}}_{12} \text{diag}(\mathbf{v}_1^H) \bar{\mathbf{H}}_{S1} \|_2^2 + L_{\overline{S1}, \overline{12}, \widetilde{2U}} \|\bar{\mathbf{H}}_{12} \text{diag}(\mathbf{v}_1^H) \bar{\mathbf{H}}_{S1} \|_F^2 \\
&\quad + L_{\widetilde{S1}, \overline{12}, \overline{2U}} T_S \|\bar{\mathbf{h}}_{2U} \text{diag}(\mathbf{v}_2^H) \bar{\mathbf{H}}_{12} \|_2^2 \\
&\quad + (L_{\widetilde{S1}, \overline{12}, \widetilde{2U}} L_{\overline{S1}, \widetilde{12}, \overline{2U}} + L_{\overline{S1}, \widetilde{12}, \widetilde{2U}} + L_{\widetilde{S1}, \overline{12}, \overline{2U}} + L_{\widetilde{S1}, \widetilde{12}, \widetilde{2U}}) T_S T_1 T_2 \\
&\stackrel{(d)}{=} L_{\overline{S1}, \overline{12}, \overline{2U}} T_S \mathbf{v}_2^H (\text{diag}(\bar{\mathbf{h}}_{2U}^H) \bar{\mathbf{H}}_{12} \text{diag}(\mathbf{a}_{A,S1})) \mathbf{v}_1^* \mathbf{v}_1^T (\text{diag}(\bar{\mathbf{h}}_{2U}^H) \bar{\mathbf{H}}_{12} \text{diag}(\mathbf{a}_{A,S1}))^H \mathbf{v}_2 \\
&\quad + L_{\overline{S1}, \overline{12}, \widetilde{2U}} T_2 \mathbf{v}_1^H \text{diag}(\mathbf{a}_{D,12}^H) \bar{\mathbf{H}}_{S1} \bar{\mathbf{H}}_{S1}^H \text{diag}(\mathbf{a}_{D,12}) \mathbf{v}_1 + L_{\widetilde{S1}, \overline{12}, \widetilde{2U}} T_S \mathbf{v}_2^H \text{diag}(\bar{\mathbf{h}}_{2U}^H) \bar{\mathbf{H}}_{12} \bar{\mathbf{H}}_{12}^H \text{diag}(\bar{\mathbf{h}}_{2U}) \mathbf{v}_2 \\
&\quad + (L_{\widetilde{S1}, \overline{12}, \widetilde{2U}} + L_{\overline{S1}, \widetilde{12}, \overline{2U}} + L_{\overline{S1}, \widetilde{12}, \widetilde{2U}} + L_{\widetilde{S1}, \overline{12}, \overline{2U}} + L_{\widetilde{S1}, \widetilde{12}, \widetilde{2U}}) T_S T_1 T_2, \tag{45}
\end{aligned}$$

where (a) is due to (1) and (2), (b) is due to

$$\begin{aligned}
\mathbb{E} \left[\tilde{\mathbf{h}}_{2U}^H \text{diag}(\mathbf{v}_2^H) \bar{\mathbf{H}}_{12} \text{diag}(\mathbf{v}_1^H) \tilde{\mathbf{H}}_{S1} \right] &= \mathbb{E} \left[\bar{\mathbf{h}}_{2U}^H \text{diag}(\mathbf{v}_2^H) \bar{\mathbf{H}}_{12} \text{diag}(\mathbf{v}_1^H) \tilde{\mathbf{H}}_{S1} \right] \\
&= \mathbb{E} \left[\tilde{\mathbf{h}}_{2U}^H \text{diag}(\mathbf{v}_2^H) \bar{\mathbf{H}}_{12} \text{diag}(\mathbf{v}_1^H) \tilde{\mathbf{H}}_{S1} \right] = \mathbb{E} \left[\bar{\mathbf{h}}_{2U}^H \text{diag}(\mathbf{v}_2^H) \tilde{\mathbf{H}}_{12} \text{diag}(\mathbf{v}_1^H) \tilde{\mathbf{H}}_{S1} \right] \\
&= \mathbb{E} \left[\tilde{\mathbf{h}}_{2U}^H \text{diag}(\mathbf{v}_2^H) \tilde{\mathbf{H}}_{12} \text{diag}(\mathbf{v}_1^H) \tilde{\mathbf{H}}_{S1} \right] = \mathbf{0}_{1 \times T_S},
\end{aligned}$$

(c) is due to (44), and (d) is due to $\bar{\mathbf{h}}_{2U}^H \text{diag}(\mathbf{v}_2^H) = \mathbf{v}_2^H \text{diag}(\bar{\mathbf{h}}_{2U}^H)$ and $\text{diag}(\mathbf{v}_1^H) \mathbf{a}_{A,S1} = \text{diag}(\mathbf{a}_{A,S1}) \mathbf{v}_1^*$.

(iv) For $l \in \mathcal{L}$, we have:

$$\begin{aligned}
\mathbb{E} [\mathbf{x}_l^H \mathbf{x}_0] &\stackrel{(a)}{=} \mathbb{E} [(\sqrt{L_{lU}} \bar{\mathbf{h}}_{lU}^H + \sqrt{L_{lU}} \tilde{\mathbf{h}}_{lU}^H) \text{diag}(\mathbf{v}_l^H) (\sqrt{L_{Sl}} \bar{\mathbf{H}}_{Sl}^H + \sqrt{L_{Sl}} \tilde{\mathbf{H}}_{Sl}^H) (\sqrt{L_{SU}} \bar{\mathbf{h}}_{SU} + \sqrt{L_{SU}} \tilde{\mathbf{h}}_{SU})] \\
&\stackrel{(b)}{=} \sqrt{L_{SU} L_{Sl, lU}} \bar{\mathbf{h}}_{lU}^H \text{diag}(\mathbf{v}_l^H) \bar{\mathbf{H}}_{Sl} \bar{\mathbf{h}}_{SU} \stackrel{(c)}{=} \sqrt{L_{SU} L_{Sl, lU}} \mathbf{v}_l^H \text{diag}(\bar{\mathbf{h}}_{lU}^H) \bar{\mathbf{H}}_{Sl} \bar{\mathbf{h}}_{SU}, \tag{46}
\end{aligned}$$

where (a) is due to (1) and (2), (b) is due to $\mathbb{E} [\tilde{\mathbf{h}}_{lU}^H \text{diag}(\mathbf{v}_l^H) \bar{\mathbf{H}}_{Sl}] = \mathbb{E} [\bar{\mathbf{h}}_{lU}^H \text{diag}(\mathbf{v}_l^H) \tilde{\mathbf{H}}_{Sl}] =$

$\mathbb{E} \left[\tilde{\mathbf{h}}_{lU}^H \text{diag}(\mathbf{v}_l^H) \tilde{\mathbf{H}}_{Sl} \right] = \mathbf{0}_{1 \times T_S}$ and $\mathbb{E} \left[\tilde{\mathbf{h}}_{SU} \right] = \mathbf{0}_{T_S}$, (c) is due to $\bar{\mathbf{h}}_{lU}^H \text{diag}(\mathbf{v}_l^H) = \mathbf{v}_l^H \text{diag}(\bar{\mathbf{h}}_{lU}^H)$. Similarly, we can show:

$$\begin{aligned} \mathbb{E} \left[\mathbf{x}_3^H \mathbf{x}_0 \right] &= \sqrt{L_{\overline{SU}} L_{\overline{S1}, \overline{12}, \overline{2U}}} \bar{\mathbf{h}}_{2U}^H \text{diag}(\mathbf{v}_2^H) \bar{\mathbf{H}}_{12} \text{diag}(\mathbf{v}_1^H) \bar{\mathbf{H}}_{S1} \bar{\mathbf{h}}_{SU} \\ &= \sqrt{L_{\overline{SU}} L_{\overline{S1}, \overline{12}, \overline{2U}}} \mathbf{v}_2^H \text{diag}(\bar{\mathbf{h}}_{2U}^H) \bar{\mathbf{H}}_{12} \text{diag}(\bar{\mathbf{H}}_{S1} \bar{\mathbf{h}}_{SU}) \mathbf{v}_1^*, \end{aligned} \quad (47)$$

$$\begin{aligned} \mathbb{E} \left[\mathbf{x}_2^H \mathbf{x}_1 \right] &= \sqrt{L_{\overline{S1}, \overline{1U}} L_{\overline{S2}, \overline{2U}}} \bar{\mathbf{h}}_{2U}^H \text{diag}(\mathbf{v}_2^H) \bar{\mathbf{H}}_{S2} \bar{\mathbf{H}}_{S1}^H \text{diag}(\mathbf{v}_1) \bar{\mathbf{h}}_{1U} \\ &= \sqrt{L_{\overline{S1}, \overline{1U}} L_{\overline{S2}, \overline{2U}}} \mathbf{v}_2^H \text{diag}(\bar{\mathbf{h}}_{2U}^H) \bar{\mathbf{H}}_{S2} \bar{\mathbf{H}}_{S1}^H \text{diag}(\bar{\mathbf{h}}_{1U}) \mathbf{v}_1, \end{aligned} \quad (48)$$

$$\begin{aligned} \mathbb{E} \left[\mathbf{x}_3^H \mathbf{x}_1 \right] &= \sqrt{L_{\overline{S1}, \overline{1U}} L_{\overline{S1}, \overline{12}, \overline{2U}}} \bar{\mathbf{h}}_{2U}^H \text{diag}(\mathbf{v}_2) \bar{\mathbf{H}}_{12} \text{diag}(\mathbf{v}_1^H) \bar{\mathbf{H}}_{S1} \bar{\mathbf{H}}_{S1}^H \text{diag}(\mathbf{v}_1) \bar{\mathbf{h}}_{1U} \\ &\quad + \sqrt{L_{\overline{S1}, \overline{1U}} L_{\overline{S1}, \overline{12}, \overline{2U}}} T_S \bar{\mathbf{h}}_{2U}^H \text{diag}(\mathbf{v}_2^H) \bar{\mathbf{H}}_{12} \bar{\mathbf{h}}_{1U} \end{aligned} \quad (49)$$

$$\begin{aligned} &= \mathbf{v}_1^H \text{diag}(\mathbf{v}_2^H \text{diag}(\bar{\mathbf{h}}_{2U}^H) \bar{\mathbf{H}}_{12}) \left(\sqrt{L_{\overline{S1}, \overline{1U}} L_{\overline{S1}, \overline{12}, \overline{2U}}} \bar{\mathbf{H}}_{S1} \bar{\mathbf{H}}_{S1}^H \text{diag}(\bar{\mathbf{h}}_{1U}) \mathbf{v}_1 \right) \\ &\quad + \sqrt{L_{\overline{S1}, \overline{1U}} L_{\overline{S1}, \overline{12}, \overline{2U}}} T_S \mathbf{v}_2^H \text{diag}(\bar{\mathbf{h}}_{2U}^H) \bar{\mathbf{H}}_{12} \bar{\mathbf{h}}_{1U}, \end{aligned} \quad (50)$$

$$\begin{aligned} \mathbb{E} \left[\mathbf{x}_3^H \mathbf{x}_2 \right] &= \sqrt{L_{\overline{S2}, \overline{2U}} L_{\overline{S1}, \overline{12}, \overline{2U}}} \bar{\mathbf{h}}_{2U}^H \text{diag}(\mathbf{v}_2^H) \bar{\mathbf{H}}_{12} \text{diag}(\mathbf{v}_1^H) \bar{\mathbf{H}}_{S1} \bar{\mathbf{H}}_{S2}^H \text{diag}(\mathbf{v}_2) \bar{\mathbf{h}}_{2U} \\ &\quad + \sqrt{L_{\overline{S2}, \overline{2U}} L_{\overline{S1}, \overline{12}, \overline{2U}}} \text{Tr} (\bar{\mathbf{H}}_{12} \text{diag}(\mathbf{v}_1^H) \bar{\mathbf{H}}_{S1} \bar{\mathbf{H}}_{S2}^H) \\ &= \mathbf{v}_1^H \text{diag}(\mathbf{v}_2^H \text{diag}(\bar{\mathbf{h}}_{2U}^H) \bar{\mathbf{H}}_{12}) \left(\sqrt{L_{\overline{S2}, \overline{2U}} L_{\overline{S1}, \overline{12}, \overline{2U}}} \bar{\mathbf{H}}_{S1} \bar{\mathbf{H}}_{S2}^H \text{diag}(\bar{\mathbf{h}}_{2U}) \mathbf{v}_2 \right) \\ &\quad + \sqrt{L_{\overline{S2}, \overline{2U}} L_{\overline{S1}, \overline{12}, \overline{2U}}} \mathbf{v}_1^H \text{diag} (\mathbf{a}_{D,12}^H) \bar{\mathbf{H}}_{S1} \bar{\mathbf{H}}_{S2}^H \mathbf{a}_{A,12}, \end{aligned} \quad (51)$$

Finally, substituting (40)-(51) into (39), we can obtain the expression of $\gamma(\phi_1, \phi_2)$ for all values of the Rician factors. Based on the general expression of $\gamma(\phi_1, \phi_2)$, we can readily obtain $\gamma^{(0)}$, $\gamma^{(1)}(\phi_1)$, $\gamma^{(2)}(\phi_2)$, and $\gamma^{(3)}(\phi_1, \phi_2)$. Therefore, we complete the proof of Theorem 1.

APPENDIX C: PROOF OF THEOREM 2

Before proving Theorem 2, we first show the following lemma.

Lemma 10. Suppose $\mathbf{A} = \mathbf{x}\mathbf{y}^H \in \mathbb{C}^{M \times N}$ with $\mathbf{x} \in \mathbb{C}^M$ and $\mathbf{y} \in \mathbb{C}^N$, $\mathbf{v} \triangleq (e^{-j\phi_n})_{n \in \mathcal{N}} \in \mathbb{C}^N$ with $\mathcal{N} \triangleq \{n = 1, \dots, N\}$, $\mathbf{b} \in \mathbb{C}^M$, and $c_1, c_2 \in \mathbb{R}$. The unique optimal solution of the problem

$$\begin{aligned} \max_{\phi} \quad & c_1 \mathbf{v}^H \mathbf{A}^H \mathbf{A} \mathbf{v} + c_2 \Re \{ \mathbf{v}^H \mathbf{A}^H \mathbf{b} \} \\ \text{s.t.} \quad & \phi_n \in [0, 2\pi), n \in \mathcal{N}, \end{aligned} \quad (52)$$

is $\phi^* = \Lambda(-\angle(\mathbf{y}) - \angle(\mathbf{x}^H \mathbf{b}) \mathbf{1}_N)$.

Proof: We have:

$$\Re \{ \mathbf{v}^H \mathbf{y} \mathbf{x}^H \mathbf{b} \} \stackrel{(a)}{\leq} |\mathbf{v}^H \mathbf{y} \mathbf{x}^H \mathbf{b}| = |\mathbf{v}^H \mathbf{y}| |\mathbf{x}^H \mathbf{b}|, \quad (53)$$

where (a) is due to $\Re\{x\} \leq |x|, x \in \mathbb{C}$ and holds with equality if and only if:

$$\angle(\mathbf{v}^H \mathbf{y}) + \angle(\mathbf{x}^H \mathbf{b}) = 0. \quad (54)$$

Besides, we have:

$$|\mathbf{v}^H \mathbf{y}| = \left| \sum_{n=1}^N e^{j\phi_n} |y_n| e^{j\angle(y_n)} \right| = \left| \sum_{n=1}^N |y_n| e^{j(\phi_n + \angle(y_n))} \right| \stackrel{(b)}{\leq} \sum_{n=1}^N |y_n|, \quad (55)$$

where (b) is due to the triangle inequality and holds with equality if and only if

$$\phi = -\angle(\mathbf{y}) + \psi \mathbf{1}_N, \psi \in \mathbb{R}. \quad (56)$$

Thus, we have:

$$\begin{aligned} c_1 \mathbf{v}^H \mathbf{A}^H \mathbf{A} \mathbf{v} + c_2 \Re\{\mathbf{v}^H \mathbf{A}^H \mathbf{b}\} &\stackrel{(c)}{=} c_1 |\mathbf{v}^H \mathbf{y}|^2 \|\mathbf{x}\|_2^2 + c_2 \Re\{\mathbf{v}^H \mathbf{y} \mathbf{x}^H \mathbf{b}\} \\ &\stackrel{(d)}{\leq} c_1 |\mathbf{v}^H \mathbf{y}|^2 \|\mathbf{x}\|_2^2 + c_2 |\mathbf{v}^H \mathbf{y}| |\mathbf{x}^H \mathbf{b}| \\ &\stackrel{(e)}{\leq} c_1 \left(\sum_{n=1}^N |y_n| \right)^2 \|\mathbf{x}\|_2^2 + c_2 \left(\sum_{n=1}^N |y_n| \right) |\mathbf{x}^H \mathbf{b}|, \end{aligned}$$

where (c) is due to $\mathbf{A} = \mathbf{x} \mathbf{y}^H$, (d) is due to (53), and (e) is due to (55). (d) and (e) both hold with equality if and only if ϕ satisfied (56) and (54). By noting that $\phi_n \in [0, 2\pi), n \in \mathcal{N}$, the optimal solution of the problem in (52) is $\phi^* = \Lambda(-\angle(\mathbf{y}) - \angle(\mathbf{x}^H \mathbf{b}) \mathbf{1}_N)$. \blacksquare

Now, we prove Theorem 2. First, we prove Statement (i). Consider $K_{12} = 0$. By (14), we have:

$$\gamma^{(1)}(\phi_1) = L_{\overline{S1}, \overline{1U}} \mathbf{v}_1^H \mathbf{G}_{11}^H \mathbf{G}_{11} \mathbf{v}_1 + 2 \sqrt{L_{\overline{S1}, \overline{1U}} L_{\overline{S1}, \overline{1U}}} \Re\{\mathbf{v}_1^H \mathbf{G}_{11}^H \mathbf{g}_{11}\} + \gamma^{(0)},$$

where $\mathbf{G}_{11} \triangleq \bar{\mathbf{H}}_{S1}^H \text{diag}(\bar{\mathbf{h}}_{1U})$ and $\mathbf{g}_{11} \triangleq \mathbf{h}_{SU}$. By (3), (4), and Lemma 10, we have $\phi_1^* = \Lambda(-\angle(\text{diag}(\mathbf{a}_{D,1U}^H) \mathbf{a}_{A,S1}) - \angle(\mathbf{a}_{D,S1}^H \mathbf{a}_{D,SU}) \mathbf{1}_{T_1}) \stackrel{(e)}{=} \Lambda(-\Delta_{\overline{S1}, \overline{1U}} - \angle(r_{\overline{S1}, \overline{SU}}) \mathbf{1}_{T_1})$, where (e) is due to (10) and (11). Then, consider $K_{1U} = 0$. By (14), we have:

$$\gamma^{(1)}(\phi_1) = L_{\overline{S1}, \overline{12}, \widetilde{2U}} T_2 \mathbf{v}_1^H \mathbf{G}_{12}^H \mathbf{G}_{12} \mathbf{v}_1 + 2 \sqrt{L_{\overline{S1}, \widetilde{2U}} L_{\overline{12}, \widetilde{2U}}} \Re\{\mathbf{v}_1^H \mathbf{G}_{12}^H \mathbf{g}_{12}\} + \gamma^{(0)},$$

where $\mathbf{G}_{12} \triangleq \bar{\mathbf{H}}_{S1}^H \text{diag}(\mathbf{a}_{D,12})$ and $\mathbf{g}_{12} \triangleq \bar{\mathbf{H}}_{S2}^H \mathbf{a}_{A,12}$. By (3), (4), and Lemma 10, we have $\phi_1^* = \Lambda(-\angle(\text{diag}(\mathbf{a}_{D,12}^H) \mathbf{a}_{A,S1}) - \angle(\mathbf{a}_{D,S1}^H \mathbf{a}_{D,S2} \mathbf{a}_{A,S2}^H \mathbf{a}_{A,12}) \mathbf{1}_{T_1}) \stackrel{(f)}{=} \Lambda(-\Delta_{\overline{S1}, \overline{12}} - \angle(r_{\overline{S1}, \overline{S2}}) \mathbf{1}_{T_1})$, where (f) is due to (10), (11), and (12).

Next, we prove Statement (ii). Consider $K_{12} = 0$. By (15), we have:

$$\gamma^{(2)}(\phi_2) = L_{\overline{S2}, \overline{2U}} \mathbf{v}_2^H \mathbf{G}_{21}^H \mathbf{G}_{21} \mathbf{v}_2 + 2 \sqrt{L_{\overline{S2}, \overline{2U}} L_{\overline{S2}, \overline{2U}}} \Re\{\mathbf{v}_2^H \mathbf{G}_{21}^H \mathbf{g}_{21}\} + \gamma^{(0)},$$

where $\mathbf{G}_{21} \triangleq \bar{\mathbf{H}}_{S2}^H \text{diag}(\bar{\mathbf{h}}_{2U})$ and $\mathbf{g}_{21} \triangleq \mathbf{h}_{SU}$. By (3), (4), and Lemma 10, we have $\phi_2^* = \Lambda(-\angle(\text{diag}(\mathbf{a}_{D,2U}^H) \mathbf{a}_{A,S2}) - \angle(\mathbf{a}_{D,S2}^H \mathbf{a}_{D,SU}) \mathbf{1}_{T_2}) \stackrel{(g)}{=} \Lambda(-\Delta_{\overline{S2}, \overline{2U}} - \angle(r_{\overline{S2}, \overline{SU}}) \mathbf{1}_{T_2})$, where (g) is

due to (10) and (11). Then, consider $K_{S2} = 0$. By (15), we have:

$$\gamma^{(2)}(\phi_2) = L_{\widetilde{S1}, \overline{12}, \overline{2U}} T_S \mathbf{v}_2^H \mathbf{G}_{22}^H \mathbf{G}_{22} \mathbf{v}_2 + 2\sqrt{L_{\widetilde{S1}, \overline{1U}} L_{\widetilde{S1}, \overline{12}, \overline{2U}}} T_S \Re \{ \mathbf{v}_2^H \mathbf{G}_{22}^H \mathbf{g}_{22} \} + \gamma^{(0)},$$

with $\mathbf{G}_{22} \triangleq \bar{\mathbf{H}}_{12}^H \text{diag}(\mathbf{a}_{D,12})$ and $\mathbf{g}_{12} \triangleq \bar{\mathbf{h}}_{1U}$. By (3), (4), and Lemma 10, we have $\phi_1^* = \Lambda(-\angle(\text{diag}(\mathbf{a}_{D,12}^H) \mathbf{a}_{A,12}) - \angle(\mathbf{a}_{D,12}^H \mathbf{a}_{D,1U}) \mathbf{1}_{T_2}) \stackrel{(h)}{=} \Lambda(-\Delta_{\overline{12}, \overline{2U}} - \angle(r_{\overline{12}, \overline{1U}}) \mathbf{1}_{T_2})$, where (h) is due to (10) and (11).

Therefore, we complete the proof of Theorem 2.

APPENDIX D: PROOF OF LEMMA 2

By (14), (15), (22), and (23), we have:

$$\begin{aligned} \gamma^{(l)}(\phi_{l,t}, \phi_{l,-t}) &= \left(\sum_{\substack{k \in \mathcal{T}_l, k \neq t \\ i \in \mathcal{T}_l, i \neq t}} A_{l,k,i} e^{j(\phi_{l,k} - \phi_{l,i})} + A_{l,t,t} \right) + \left(e^{j\phi_{l,t}} \sum_{k \in \mathcal{T}_l, k \neq t} A_{l,t,k} e^{-j\phi_{l,k}} + e^{-j\phi_{l,t}} \sum_{k \in \mathcal{T}_l, k \neq t} A_{l,k,t} e^{j\phi_{l,k}} \right) \\ &\quad + 2\Re \left\{ \left(e^{j\phi_{l,t}} b_{l,t} + \sum_{k \in \mathcal{T}_l, k \neq t} e^{j\phi_{l,k}} b_{l,k} \right) \right\} + \gamma^{(0)} \\ &\stackrel{(a)}{=} 2\Re \left\{ e^{j\phi_{l,t}} \left(\sum_{k \in \mathcal{T}_l, k \neq t} A_{l,t,k} e^{-j\phi_{l,k}} + b_{l,t} \right) + \sum_{k \in \mathcal{T}_l, k \neq t} e^{j\phi_{l,k}} b_{l,k} \right\} + \sum_{\substack{k \in \mathcal{T}_l, k \neq t \\ i \in \mathcal{T}_l, i \neq t}} A_{l,k,i} e^{j(\phi_{l,k} - \phi_{l,i})} + A_{l,t,t} + \gamma^{(0)}, \end{aligned}$$

where (a) is due to $\mathbf{A}_l = \mathbf{A}_l^H$. As $\phi_{l,-t}$ is given, to solve Problem 2 is equivalent to solve:

$$\max_{\phi_{l,t} \in [0, 2\pi)} \Re \left\{ e^{j\phi_{l,t}} \left(\sum_{k \in \mathcal{T}_l, k \neq t} A_{l,t,k} e^{-j\phi_{l,k}} + b_{l,t} \right) \right\}.$$

Besides, we have:

$$\Re \left\{ e^{j\phi_{l,t}} \left(\sum_{k \in \mathcal{T}_l, k \neq t} A_{l,t,k} e^{-j\phi_{l,k}} + b_{l,t} \right) \right\} \stackrel{(b)}{\leq} \left| e^{j\phi_{l,t}} \left(\sum_{k \in \mathcal{T}_l, k \neq t} A_{l,t,k} e^{-j\phi_{l,k}} + b_{l,t} \right) \right| = \left| \sum_{k \in \mathcal{T}_l, k \neq t} A_{l,t,k} e^{-j\phi_{l,k}} + b_{l,t} \right|,$$

where (b) is due to $\Re \{x\} \leq |x|$, $x \in \mathbb{C}$ and holds with equality if and only if $\phi_{l,t} = -\angle \left(\sum_{k \in \mathcal{T}_l, k \neq t} A_{l,t,k} e^{-j\phi_{l,k}} + b_{l,t} \right)$. By noting that $\phi_{l,t} \in [0, 2\pi)$, the unique optimal solution of the equivalent problem is $\phi_{l,t}^\dagger = \Lambda \left(-\angle \left(\sum_{k \in \mathcal{T}_l, k \neq t} A_{l,t,k} e^{-j\phi_{l,k}} + b_{l,t} \right) \right)$. Therefore, we complete the proof of Lemma 2.

APPENDIX E: PROOF OF THEOREM 3

First, we prove statement (i). Consider $K_{S2} = K_{1U} = 0$. We first have:

$$|\mathbf{v}_1^H \text{diag}(\mathbf{a}_{D,12}^H) \mathbf{a}_{A,S1}| \stackrel{(a)}{=} \left| \sum_{t \in \mathcal{T}_1} e^{j(\phi_{1,t} + \Delta_{\overline{S1}, \overline{12}, t})} \right| \stackrel{(b)}{\leq} T_1, \quad (57)$$

$$|\mathbf{v}_2^H \text{diag}(\mathbf{h}_{2U}^H) \mathbf{a}_{A,12}| \stackrel{(c)}{=} \left| \sum_{t \in \mathcal{T}_2} e^{j(\phi_{2,t} + \Delta_{\overline{12}, \overline{2U}, t})} \right| \stackrel{(d)}{\leq} T_2, \quad (58)$$

where (a) and (c) are due to (10), and (b) and (d) are due to the triangle inequality. Note that (b) and (d) hold with equality if and only if:

$$\phi_1 = -\Delta_{\overline{S1},\overline{12}} + \psi_1 \mathbf{1}_{T_1}, \psi_1 \in \mathbb{R}, \quad (59)$$

$$\phi_2 = -\Delta_{\overline{12},\overline{2U}} + \psi_2 \mathbf{1}_{T_2}, \psi_2 \in \mathbb{R}. \quad (60)$$

Then, we have:

$$\begin{aligned} \gamma^{(3)}(\phi_1, \phi_2) &\stackrel{(e)}{=} L_{\overline{S1},\overline{12},\widetilde{2U}} T_S T_2 \left| \mathbf{v}_1^H \text{diag}(\mathbf{a}_{D,12}^H) \mathbf{a}_{A,S1} \right|^2 + L_{\widetilde{S1},\overline{12},\overline{2U}} T_S T_1 \left| \mathbf{v}_2^H \text{diag}(\mathbf{h}_{2U}^H) \mathbf{a}_{A,12} \right|^2 \\ &\quad + L_{\overline{S1},\overline{12},\overline{2U}} T_S \left| \mathbf{v}_2^H \text{diag}(\mathbf{h}_{2U}^H) \mathbf{a}_{A,12} \mathbf{a}_{D,12}^H \text{diag}(\mathbf{a}_{A,S1}) \mathbf{v}_1^* \right|^2 \\ &\quad + 2 \sqrt{L_{\overline{SU}} L_{\overline{S1},\overline{12},\overline{2U}}} \Re \left\{ \mathbf{v}_2^H \text{diag}(\mathbf{h}_{2U}^H) \mathbf{a}_{A,12} \mathbf{a}_{D,12}^H \text{diag}(\mathbf{a}_{A,S1}) \mathbf{v}_1^* r_{\overline{S1},\overline{SU}} \right\} + \gamma^{(0)} \\ &\stackrel{(f)}{\leq} L_{\overline{S1},\overline{12},\widetilde{2U}} T_S T_2 \left| \mathbf{v}_1^H \text{diag}(\mathbf{a}_{D,12}^H) \mathbf{a}_{A,S1} \right|^2 + L_{\widetilde{S1},\overline{12},\overline{2U}} T_S T_1 \left| \mathbf{v}_2^H \text{diag}(\mathbf{h}_{2U}^H) \mathbf{a}_{A,12} \right|^2 \\ &\quad + L_{\overline{S1},\overline{12},\overline{2U}} T_S \left| \mathbf{v}_2^H \text{diag}(\mathbf{h}_{2U}^H) \mathbf{a}_{A,12} \right|^2 \left| \mathbf{v}_1^H \text{diag}(\mathbf{a}_{D,12}^H) \mathbf{a}_{A,S1} \right|^2 \\ &\quad + 2 \sqrt{L_{\overline{SU}} L_{\overline{S1},\overline{12},\overline{2U}}} \left| \mathbf{v}_2^H \text{diag}(\mathbf{h}_{2U}^H) \mathbf{a}_{A,12} \right| \left| \mathbf{v}_1^H \text{diag}(\mathbf{a}_{D,12}^H) \mathbf{a}_{A,S1} \right| \left| r_{\overline{S1},\overline{SU}} \right| + \gamma^{(0)} \\ &\stackrel{(g)}{\leq} L_{\overline{S1},\overline{12},\widetilde{2U}} T_S T_2 T_1^2 + L_{\widetilde{S1},\overline{12},\overline{2U}} T_S T_1 T_2^2 + L_{\overline{S1},\overline{12},\overline{2U}} T_S T_1^2 T_2^2 \\ &\quad + 2 \sqrt{L_{\overline{SU}} L_{\overline{S1},\overline{12},\overline{2U}}} T_1 T_2 \left| r_{\overline{S1},\overline{SU}} \right| + \gamma^{(0)}, \end{aligned} \quad (61)$$

where (e) is due to (16), (f) is due to $\mathbf{a}_{D,12}^H \text{diag}(\mathbf{a}_{A,S1}) \mathbf{v}_1^* = \mathbf{v}_1^H \text{diag}(\mathbf{a}_{D,12}^H) \mathbf{a}_{A,S1}$ and $\Re\{x\} \leq |x|, x \in \mathbb{C}$, and (g) is due to (57) and (58). Note that (f) holds with equality if and only if

$$\angle(\mathbf{v}_2^H \text{diag}(\mathbf{h}_{2U}^H) \mathbf{a}_{A,12}) + \angle(\mathbf{v}_1^H \text{diag}(\mathbf{a}_{D,12}^H) \mathbf{a}_{A,S1}) + \angle(r_{\overline{S1},\overline{SU}}) = 0. \quad (62)$$

Besides, note that (g) holds with equality if and only if (57) and (58) hold with equality, i.e., (59) and (60) hold. Thus, the upper bound in (61) is achieved if and only if (59), (60), and (62) hold simultaneously. By substituting (59) and (60) into (62), we have $\psi_1 + \psi_2 + \angle(r_{\overline{S1},\overline{SU}}) = 0$. By noting that $\phi_{l,t} \in [0, 2\pi], t \in \mathcal{T}_l, l \in \mathcal{L}$ and by choosing $\psi_1 = -\frac{1}{2}\angle(r_{\overline{S1},\overline{SU}}) + \psi$ and $\psi_2 = -\frac{1}{2}\angle(r_{\overline{S1},\overline{SU}}) - \psi$ for all $\psi \in \mathbb{R}$, we can show that any (ϕ_1^*, ϕ_2^*) with $\phi_1^* = \Lambda(-\Delta_{\overline{S1},\overline{12}} + \psi \mathbf{1}_{T_1} - \frac{1}{2}\angle(r_{\overline{S1},\overline{SU}}) \mathbf{1}_{T_1})$ and $\phi_2^* = \Lambda(-\Delta_{\overline{12},\overline{2U}} - \psi \mathbf{1}_{T_2} - \frac{1}{2}\angle(r_{\overline{S1},\overline{SU}}) \mathbf{1}_{T_2})$, $\psi \in \mathbb{R}$ is an optimal solution of Problem 1.

Next, we prove statement (ii). Consider $K_{SU} = K_{12} = 0$. We first have:

$$\left| \mathbf{v}_l^H \text{diag}(\mathbf{h}_{lU}^H) \mathbf{a}_{A,S1} \right| \stackrel{(h)}{=} \left| \sum_{t \in \mathcal{T}_l} e^{j(\phi_{l,t} + \Delta_{\overline{S1},\overline{12},t})} \right| \stackrel{(i)}{\leq} T_l, l \in \mathcal{L}, \quad (63)$$

where (h) is due to (10), (i) is due to the triangle inequality and holds with equality if and only if:

$$\phi_l = \Lambda(-\Delta_{\overline{S1},\overline{12}} + \psi_l), \psi_l \in \mathbb{R}. \quad (64)$$

Then, we have:

$$\begin{aligned}
\gamma^{(3)}(\phi_1, \phi_2) &\stackrel{(j)}{=} \sum_{l=1}^2 L_{\overline{S_l}, \overline{U}} T_S \left| \mathbf{v}_l^H \text{diag}(\bar{\mathbf{h}}_{lU}^H) \mathbf{a}_{A,Sl} \right|^2 \\
&\quad + 2\sqrt{L_{\overline{S1}, \overline{1U}} L_{\overline{S2}, \overline{2U}}} \Re \left\{ \mathbf{v}_2^H \text{diag}(\bar{\mathbf{h}}_{2U}^H) \bar{\mathbf{H}}_{S2} \bar{\mathbf{H}}_{S1}^H \text{diag}(\bar{\mathbf{h}}_{1U}) \mathbf{v}_1 \right\} + \gamma^{(0)} \\
&\stackrel{(k)}{\leq} \sum_{l=1}^2 L_{\overline{S_l}, \overline{U}} T_S \left| \mathbf{v}_l^H \text{diag}(\bar{\mathbf{h}}_{lU}^H) \mathbf{a}_{A,Sl} \right|^2 + \gamma^{(0)} \\
&\quad + 2\sqrt{L_{\overline{S1}, \overline{1U}} L_{\overline{S2}, \overline{2U}}} \left| \mathbf{v}_2^H \text{diag}(\bar{\mathbf{h}}_{2U}^H) \mathbf{a}_{A,S2} \right| \left| \mathbf{v}_1^H \text{diag}(\bar{\mathbf{h}}_{1U}^H) \mathbf{a}_{A,S1} \right| \left| r_{\overline{S1}, \overline{S2}} \right| \\
&\stackrel{(l)}{\leq} \sum_{l=1}^2 L_{\overline{S_l}, \overline{U}} T_S T_l^2 + 2\sqrt{L_{\overline{S1}, \overline{1U}} L_{\overline{S2}, \overline{2U}}} T_1 T_2 \left| r_{\overline{S1}, \overline{S2}} \right| + \gamma^{(0)}, \tag{65}
\end{aligned}$$

where (j) is due to (16), (k) is due to $\Re\{x\} \leq |x|, x \in \mathbb{C}$, and (l) is due to (63). Note that (k) holds with equality if and only if:

$$\angle(\mathbf{v}_1^H \text{diag}(\bar{\mathbf{h}}_{1U}^H) \mathbf{a}_{A,S1}) - \angle(\mathbf{v}_2^H \text{diag}(\bar{\mathbf{h}}_{2U}^H) \mathbf{a}_{A,S2}) + \angle(r_{\overline{S1}, \overline{S2}}) = 0. \tag{66}$$

Besides, note that (l) holds with equality if and only if (63) holds with equality, i.e., (64) holds. Thus, the upper bound in (65) is achieved if and only if (64) and (66) hold simultaneously. By substituting (64) into (66), we have $\psi_1 - \psi_2 + \angle(r_{\overline{S1}, \overline{S2}}) = 0$. By noting that $\phi_{l,t} \in [0, 2\pi), t \in \mathcal{T}_l, l \in \mathcal{L}$ and by choosing $\psi_1 = \psi$ and $\psi_2 = \psi + \angle(r_{\overline{S1}, \overline{S2}})$ for all $\psi \in \mathbb{R}$, we can show that any (ϕ_1^*, ϕ_2^*) with $\phi_1^* = \Lambda(-\Delta_{\overline{S1}, \overline{1U}} + \psi \mathbf{1}_{T_1})$, $\phi_2^* = \Lambda(-\Delta_{\overline{S2}, \overline{2U}} + \psi \mathbf{1}_{T_2} + \angle(r_{\overline{S1}, \overline{S2}}) \mathbf{1}_{T_2})$, $\psi \in \mathbb{R}$ is an optimal solution of Problem 1.

Therefore, we complete the proof of Theorem 3.

APPENDIX F: PROOF OF LEMMA 3

By (16), (25), and (26), we have:

$$\begin{aligned}
\gamma^{(3)}(\phi_{l,t}, \phi_{l,-t}, \phi_{-l}) &= \left(\sum_{\substack{k \in \mathcal{T}_l, k \neq t \\ i \in \mathcal{T}_l, i \neq t}} C_{l,k,i} e^{j(\phi_{l,k} - \phi_{l,i})} + C_{l,t,t} \right) + \left(e^{j\phi_{l,t}} \sum_{k \in \mathcal{T}_l, k \neq t} C_{l,t,k} e^{-j\phi_{l,k}} + e^{-j\phi_{l,t}} \sum_{k \in \mathcal{T}_l, k \neq t} C_{l,k,t} e^{j\phi_{l,k}} \right) \\
&\quad + 2\Re \left\{ \left(e^{j\phi_{l,t}} d_{l,t} + \sum_{k \in \mathcal{T}_l, k \neq t} e^{j\phi_{l,k}} d_{l,k} \right) \right\} + \gamma^{(0)} \\
&\stackrel{(a)}{=} 2\Re \left\{ e^{j\phi_{l,t}} \left(\sum_{k \in \mathcal{T}_l, k \neq t} C_{l,t,k} e^{-j\phi_{l,k}} + d_{l,t} \right) + \sum_{k \in \mathcal{T}_l, k \neq t} e^{j\phi_{l,k}} d_{l,k} \right\} + \sum_{\substack{k \in \mathcal{T}_l, k \neq t \\ i \in \mathcal{T}_l, i \neq t}} C_{l,k,i} e^{j(\phi_{l,k} - \phi_{l,i})} + C_{l,t,t} + \gamma^{(0)},
\end{aligned}$$

where (a) is due to $\mathbf{C}_l = \mathbf{C}_l^H$. As $(\phi_{l,-t}, \phi_{-l})$ is given, to solve Problem 4 is equivalent to solve:

$$\max_{\phi_{l,t} \in [0, 2\pi)} \Re \left\{ e^{j\phi_{l,t}} \left(\sum_{k \in \mathcal{T}_l, k \neq t} C_{l,t,k} e^{-j\phi_{l,k}} + d_{l,t} \right) \right\}.$$

Besides, we have:

$$\Re \left\{ e^{j\phi_{l,t}} \left(\sum_{k \in \mathcal{T}_l, k \neq t} C_{l,t,k} e^{-j\phi_{l,k}} + d_{l,t} \right) \right\} \stackrel{(b)}{\leq} \left| \sum_{k \in \mathcal{T}_l, k \neq t} C_{l,t,k} e^{-j\phi_{l,k}} + d_{l,t} \right|,$$

where (b) is due to $\Re\{x\} \leq |x|$, $x \in \mathbb{C}$ and holds with equality if and only if $\phi_{l,t} = -\angle \left(\sum_{k \in \mathcal{T}_l, k \neq t} C_{l,t,k} e^{-j\phi_{l,k}} + d_{l,t} \right)$. By noting that $\phi_{l,t} \in [0, 2\pi)$, the unique optimal solution of the equivalent problem is $\phi_{l,t}^\dagger = \Lambda \left(-\angle \left(\sum_{k \in \mathcal{T}_l, k \neq t} C_{l,t,k} e^{-j\phi_{l,k}} + d_{l,t} \right) \right)$. Therefore, we complete the proof of Lemma 3.

APPENDIX G: PROOF OF THEOREM 4

Before proving Theorem 4, we first show:

$$\begin{aligned} \|\mathbf{v}_l^H \text{diag}(\bar{\mathbf{h}}_{lU}^H) \bar{\mathbf{H}}_{Sl} \|_2 &= \|\mathbf{v}_l^H \text{diag}(\bar{\mathbf{h}}_{lU}^H) \mathbf{a}_{A,Sl} \mathbf{a}_{D,Sl}^H \|_2 \\ &\stackrel{(a)}{\leq} |\mathbf{v}_l^H \text{diag}(\mathbf{a}_{D,lU}^H) \mathbf{a}_{A,Sl}| \|\mathbf{a}_{D,Sl}^H\|_2 \stackrel{(b)}{\leq} \sqrt{T_S} T_l, \end{aligned} \quad (67)$$

$$\begin{aligned} |\mathbf{v}_2^H \text{diag}(\bar{\mathbf{h}}_{2U}^H) \bar{\mathbf{H}}_{12} \text{diag}(\mathbf{a}_{A,S1}) \mathbf{v}_1^*| &= \|\mathbf{v}_2^H \text{diag}(\mathbf{a}_{D,2U}^H) \mathbf{a}_{A,12} \mathbf{a}_{D,12}^H \text{diag}(\mathbf{a}_{A,S1}) \mathbf{v}_1^* \|_2 \\ &\stackrel{(c)}{\leq} |\mathbf{v}_2^H \text{diag}(\mathbf{a}_{D,2U}^H) \mathbf{a}_{A,12}| \|\mathbf{a}_{D,12}^H \text{diag}(\mathbf{a}_{A,S1}) \mathbf{v}_1^* \|_2 \stackrel{(d)}{\leq} T_1 T_2, \end{aligned} \quad (68)$$

$$\begin{aligned} \|\mathbf{v}_1^H \text{diag}(\mathbf{a}_{D,12}^H) \bar{\mathbf{H}}_{S1} \|_2 &= \|\mathbf{v}_1^H \text{diag}(\mathbf{a}_{D,12}^H) \mathbf{a}_{A,S1} \mathbf{a}_{D,S1}^H \|_2 \\ &\stackrel{(e)}{\leq} |\mathbf{v}_1^H \text{diag}(\mathbf{a}_{D,12}^H) \mathbf{a}_{A,S1}| \|\mathbf{a}_{D,S1}^H\|_2 \stackrel{(f)}{\leq} \sqrt{T_S} T_1, \end{aligned} \quad (69)$$

$$\begin{aligned} \|\mathbf{v}_2^H \text{diag}(\bar{\mathbf{h}}_{2U}^H) \bar{\mathbf{H}}_{12} \|_2 &= \|\mathbf{v}_2^H \text{diag}(\bar{\mathbf{h}}_{2U}^H) \mathbf{a}_{A,12} \mathbf{a}_{D,12}^H \|_2 \\ &\stackrel{(g)}{\leq} |\mathbf{v}_2^H \text{diag}(\bar{\mathbf{h}}_{2U}^H) \mathbf{a}_{A,12}| \|\mathbf{a}_{D,12}^H\|_2 \stackrel{(h)}{\leq} \sqrt{T_1} T_2, \end{aligned} \quad (70)$$

where (a), (c), (e), and (g) are due to Cauchy-Schwartz inequality, and (b), (d), (f), and (h) are due to the triangle inequality. Based on (67), (68), (69), and (70), we prove Theorem 4 below.

First, consider Case 0. As $\lim_{T_1, T_2 \rightarrow \infty} \frac{\gamma^{(0)}}{(L_{\bar{S}1, \bar{12}, \bar{2U}} + L_{\bar{S}1, \bar{12}, \bar{2U}} + L_{\bar{S}1, \bar{12}, \bar{2U}} + L_{\bar{S}1, \bar{12}, \bar{2U}} + L_{\bar{S}1, \bar{12}, \bar{2U}}) T_S T_1 T_2} = 1$, we can show $\gamma^{(0)} \stackrel{T_1, T_2 \rightarrow \infty}{\sim} (L_{\bar{S}1, \bar{12}, \bar{2U}} + L_{\bar{S}1, \bar{12}, \bar{2U}} + L_{\bar{S}1, \bar{12}, \bar{2U}} + L_{\bar{S}1, \bar{12}, \bar{2U}} + L_{\bar{S}1, \bar{12}, \bar{2U}}) T_S T_1 T_2$.

Next, consider Case 1. For all ϕ_1 , we have:

$$\begin{aligned} \gamma^{(1)}(\phi_1) &\stackrel{(i)}{=} L_{\bar{S}1, \bar{1U}} \|\mathbf{v}_1^H \text{diag}(\bar{\mathbf{h}}_{1U}^H) \bar{\mathbf{H}}_{S1} \|_2^2 + L_{\bar{S}1, \bar{12}, \bar{2U}} T_2 \|\mathbf{v}_1^H \text{diag}(\mathbf{a}_{D,12}^H) \bar{\mathbf{H}}_{S1} \|_2^2 + \gamma^{(0)} \\ &\quad + 2\Re \left\{ \mathbf{v}_1^H \left(\sqrt{L_{\bar{S}U} L_{\bar{S}1, \bar{1U}}} \text{diag}(\bar{\mathbf{h}}_{1U}^H) \bar{\mathbf{H}}_{S1} \bar{\mathbf{h}}_{SU} + \sqrt{L_{\bar{S}2, \bar{2U}} L_{\bar{S}1, \bar{12}, \bar{2U}}} \text{diag}(\mathbf{a}_{D,12}^H) \bar{\mathbf{H}}_{S1} \bar{\mathbf{H}}_{S2}^H \mathbf{a}_{A,12} \right) \right\} \\ &\stackrel{(j)}{\leq} L_{\bar{S}1, \bar{1U}} \|\mathbf{v}_1^H \text{diag}(\bar{\mathbf{h}}_{1U}^H) \bar{\mathbf{H}}_{S1} \|_2^2 + L_{\bar{S}1, \bar{12}, \bar{2U}} T_2 \|\mathbf{v}_1^H \text{diag}(\mathbf{a}_{D,12}^H) \bar{\mathbf{H}}_{S1} \|_2^2 + \gamma^{(0)} \\ &\quad + 2\sqrt{L_{\bar{S}U} L_{\bar{S}1, \bar{1U}}} \|\mathbf{v}_1^H \text{diag}(\bar{\mathbf{h}}_{1U}^H) \bar{\mathbf{H}}_{S1} \|_2 \|\mathbf{a}_{D,SU}\|_2 + 2\sqrt{L_{\bar{S}2, \bar{2U}} L_{\bar{S}1, \bar{12}, \bar{2U}}} \|\mathbf{v}_1^H \text{diag}(\mathbf{a}_{D,12}^H) \bar{\mathbf{H}}_{S1} \|_2 \|\mathbf{a}_{D,S2}\|_2 |r_{S2,12}| \\ &\stackrel{(k)}{\leq} L_{\bar{S}1, \bar{1U}} T_S T_1^2 + L_{\bar{S}1, \bar{12}, \bar{2U}} T_S T_1^2 T_2 + 2\sqrt{L_{\bar{S}U} L_{\bar{S}1, \bar{1U}}} T_S T_1 + 2\sqrt{L_{\bar{S}2, \bar{2U}} L_{\bar{S}1, \bar{12}, \bar{2U}}} T_S T_1 T_2 + \gamma^{(0)} \triangleq \gamma_{ub}^{(1)*}, \end{aligned} \quad (71)$$

where (i) is due to (14), (j) is due to $\Re\{x\} \leq |x|, x \in \mathbb{C}$ and Cauchy-Swartz inequality, and (k) is due to (67) and (69). On the other hand, we have:

$$\begin{aligned}
\gamma^{(1)}(\hat{\phi}_1) &= L_{\overline{S1}, \overline{1U}} \|\hat{\mathbf{v}}_1^H \text{diag}(\bar{\mathbf{h}}_{1U}^H) \bar{\mathbf{H}}_{S1}\|_2^2 + L_{\overline{S1}, \overline{12}, \overline{2U}} T_2 \|\hat{\mathbf{v}}_1^H \text{diag}(\mathbf{a}_{D,12}^H) \bar{\mathbf{H}}_{S1}\|_2^2 + \gamma^{(0)} \\
&\quad + 2\Re \left\{ \hat{\mathbf{v}}_1^H \left(\sqrt{L_{\overline{SU}} L_{\overline{S1}, \overline{1U}}} \text{diag}(\bar{\mathbf{h}}_{1U}^H) \bar{\mathbf{H}}_{S1} \bar{\mathbf{h}}_{SU} + \sqrt{L_{\overline{S2}, \overline{2U}}} \text{diag}(\mathbf{a}_{D,12}^H) \bar{\mathbf{H}}_{S1} \bar{\mathbf{H}}_{S2}^H \mathbf{a}_{A,12} \right) \right\} \\
&\stackrel{(l)}{\geq} L_{\overline{S1}, \overline{12}, \overline{2U}} T_2 \|\hat{\mathbf{v}}_1^H \text{diag}(\mathbf{a}_{D,12}^H) \bar{\mathbf{H}}_{S1}\|_2^2 + \gamma^{(0)} - 2\sqrt{L_{\overline{SU}} L_{\overline{S1}, \overline{1U}}} \|\hat{\mathbf{v}}_1^H \text{diag}(\bar{\mathbf{h}}_{1U}^H) \bar{\mathbf{H}}_{S1}\|_2 \|\mathbf{a}_{D,SU}\|_2 \\
&\quad - 2\sqrt{L_{\overline{S2}, \overline{2U}} L_{\overline{S1}, \overline{12}, \overline{2U}}} \|\hat{\mathbf{v}}_1^H \text{diag}(\mathbf{a}_{D,12}^H) \bar{\mathbf{H}}_{S1}\|_2 \|\mathbf{a}_{D,S2}\|_2 |r_{S2,12}| \\
&\stackrel{(m)}{\geq} L_{\overline{S1}, \overline{12}, \overline{2U}} T_S T_1^2 T_2 - 2\sqrt{L_{\overline{SU}} L_{\overline{S1}, \overline{1U}}} T_1 T_S - 2\sqrt{L_{\overline{S2}, \overline{2U}} L_{\overline{S1}, \overline{12}, \overline{2U}}} T_1 T_S T_2 + \gamma^{(0)} \triangleq \gamma_{lb}^{(1)*}, \tag{72}
\end{aligned}$$

where $\hat{\phi}_1 \triangleq \Lambda(-\Delta_{\overline{S1}, \overline{12}} - \angle(r_{\overline{S1}, \overline{S2}} r_{\overline{S2}, \overline{12}}) \mathbf{1}_{T_1})$, $\hat{\mathbf{v}}_1 \triangleq \left(e^{-j\hat{\phi}_{1,t}} \right)_{t \in \mathcal{T}_1}$, (l) is due to $\Re\{x\} \geq -|x|, x \in \mathbb{C}$ and Cauchy-Swartz inequality, and (m) is due to (67), (69), and $\|\hat{\mathbf{v}}_1^H \text{diag}(\mathbf{a}_{D,12}^H) \bar{\mathbf{H}}_{S1}\|_2^2 = T_S \left| \sum_{t=1}^{T_1} e^{j(-\Delta_{\overline{S1}, \overline{12}, t} - \angle(r_{\overline{S1}, \overline{S2}} r_{\overline{S2}, \overline{12}}) + \Delta_{\overline{S1}, \overline{12}, t})} \right|_2^2 = T_S T_1^2$. Clearly, we have $\gamma_{lb}^{(1)*} \leq \gamma^{(1)*} \leq \gamma_{ub}^{(1)*}$. As $\lim_{T_1, T_2 \rightarrow \infty} \frac{\gamma_{ub}^{(1)*}}{L_{\overline{S1}, \overline{12}, \overline{2U}} T_S T_1^2 T_2} = 1$ and $\lim_{T_1, T_2 \rightarrow \infty} \frac{\gamma_{lb}^{(1)*}}{L_{\overline{S1}, \overline{12}, \overline{2U}} T_S T_1^2 T_2} = 1$, by the squeeze theorem, we have $\lim_{T_1, T_2 \rightarrow \infty} \frac{\gamma^{(1)*}}{L_{\overline{S1}, \overline{12}, \overline{2U}} T_S T_1^2 T_2} = 1$. Thus, we can show $\gamma^{(1)*} \xrightarrow{T_1, T_2 \rightarrow \infty} L_{\overline{S1}, \overline{12}, \overline{2U}} T_S T_1^2 T_2$.

Then, consider Case 2. For all ϕ_2 , we have:

$$\begin{aligned}
\gamma^{(2)}(\phi_2) &\stackrel{(o)}{=} L_{\overline{S2}, \overline{2U}} \|\mathbf{v}_2^H \text{diag}(\bar{\mathbf{h}}_{2U}^H) \bar{\mathbf{H}}_{S2}\|_2^2 + L_{\overline{S1}, \overline{12}, \overline{2U}} T_S \|\mathbf{v}_2^H \text{diag}(\bar{\mathbf{h}}_{2U}^H) \bar{\mathbf{H}}_{12}\|_2^2 + \gamma^{(0)} \\
&\quad + 2\Re \left\{ \mathbf{v}_2^H \left(\sqrt{L_{\overline{SU}} L_{\overline{S2}, \overline{2U}}} \text{diag}(\bar{\mathbf{h}}_{2U}^H) \bar{\mathbf{H}}_{S2} \bar{\mathbf{h}}_{SU} + \sqrt{L_{\overline{S1}, \overline{1U}} L_{\overline{S1}, \overline{12}, \overline{2U}}} T_S \text{diag}(\bar{\mathbf{h}}_{2U}^H) \bar{\mathbf{H}}_{12} \bar{\mathbf{h}}_{1U} \right) \right\} \\
&\stackrel{(p)}{\leq} L_{\overline{S2}, \overline{2U}} \|\mathbf{v}_2^H \text{diag}(\bar{\mathbf{h}}_{2U}^H) \bar{\mathbf{H}}_{S2}\|_2^2 + L_{\overline{S1}, \overline{12}, \overline{2U}} T_S \|\mathbf{v}_2^H \text{diag}(\bar{\mathbf{h}}_{2U}^H) \bar{\mathbf{H}}_{12}\|_2^2 + \gamma^{(0)} \\
&\quad + 2\sqrt{L_{\overline{SU}} L_{\overline{S2}, \overline{2U}}} \|\mathbf{v}_2^H \text{diag}(\bar{\mathbf{h}}_{2U}^H) \bar{\mathbf{H}}_{S2}\|_2 \|\mathbf{a}_{D,SU}\|_2 + 2\sqrt{L_{\overline{S1}, \overline{1U}} L_{\overline{S1}, \overline{12}, \overline{2U}}} T_S \|\mathbf{v}_2^H \text{diag}(\bar{\mathbf{h}}_{2U}^H) \bar{\mathbf{H}}_{12}\|_2 \|\mathbf{a}_{D,1U}\|_2 \\
&\stackrel{(q)}{\leq} L_{\overline{S2}, \overline{2U}} T_S T_2^2 + L_{\overline{S1}, \overline{12}, \overline{2U}} T_S T_1 T_2^2 + 2\sqrt{L_{\overline{SU}} L_{\overline{S2}, \overline{2U}}} T_S T_2 + 2\sqrt{L_{\overline{S1}, \overline{1U}} L_{\overline{S1}, \overline{12}, \overline{2U}}} T_S T_1 T_2 + \gamma^{(0)} \triangleq \gamma_{ub}^{(2)*}, \tag{73}
\end{aligned}$$

where (o) is due to (15), (p) is due to $\Re\{x\} \leq |x|, x \in \mathbb{C}$ and Cauchy-Schwartz inequality, and (q) is due to (67) and (70). On the other hand, we have:

$$\begin{aligned}
\gamma^{(2)}(\hat{\phi}_2) &= L_{\overline{S2}, \overline{2U}} \|\hat{\mathbf{v}}_2^H \text{diag}(\bar{\mathbf{h}}_{2U}^H) \bar{\mathbf{H}}_{S2}\|_2^2 + L_{\overline{S1}, \overline{12}, \overline{2U}} T_S \|\hat{\mathbf{v}}_2^H \text{diag}(\bar{\mathbf{h}}_{2U}^H) \bar{\mathbf{H}}_{12}\|_2^2 + \gamma^{(0)} \\
&\quad + 2\Re \left\{ \hat{\mathbf{v}}_2^H \left(\sqrt{L_{\overline{SU}} L_{\overline{S2}, \overline{2U}}} \text{diag}(\bar{\mathbf{h}}_{2U}^H) \bar{\mathbf{H}}_{S2} \bar{\mathbf{h}}_{SU} + \sqrt{L_{\overline{S1}, \overline{1U}} L_{\overline{S1}, \overline{12}, \overline{2U}}} T_S \text{diag}(\bar{\mathbf{h}}_{2U}^H) \bar{\mathbf{H}}_{12} \bar{\mathbf{h}}_{1U} \right) \right\} \\
&\stackrel{(r)}{\geq} L_{\overline{S1}, \overline{12}, \overline{2U}} T_S \|\hat{\mathbf{v}}_2^H \text{diag}(\bar{\mathbf{h}}_{2U}^H) \bar{\mathbf{H}}_{12}\|_2^2 + \gamma^{(0)} \\
&\quad - 2\sqrt{L_{\overline{SU}} L_{\overline{S2}, \overline{2U}}} \|\hat{\mathbf{v}}_2^H \text{diag}(\bar{\mathbf{h}}_{2U}^H) \bar{\mathbf{H}}_{S2}\|_2 \|\mathbf{a}_{D,SU}\|_2 - 2\sqrt{L_{\overline{S1}, \overline{1U}} L_{\overline{S1}, \overline{12}, \overline{2U}}} T_S \|\hat{\mathbf{v}}_2^H \text{diag}(\bar{\mathbf{h}}_{2U}^H) \bar{\mathbf{H}}_{12}\|_2 \|\mathbf{a}_{D,1U}\|_2 \\
&\stackrel{(s)}{\geq} L_{\overline{S1}, \overline{12}, \overline{2U}} T_S T_1 T_2^2 - 2\sqrt{L_{\overline{SU}} L_{\overline{S2}, \overline{2U}}} T_S T_2 - 2\sqrt{L_{\overline{S1}, \overline{1U}} L_{\overline{S1}, \overline{12}, \overline{2U}}} T_S T_1 T_2 + \gamma^{(0)} \triangleq \gamma_{lb}^{(2)*}, \tag{74}
\end{aligned}$$

where $\hat{\phi}_2 \triangleq \Lambda(-\Delta_{\overline{12}, \overline{2U}} - \angle(r_{\overline{12}, \overline{1U}}) \mathbf{1}_{T_2})$, $\hat{\mathbf{v}}_2 \triangleq \left(e^{-j\hat{\phi}_{2,t}} \right)_{t \in \mathcal{T}_2}$, (r) is due to $\Re\{x\} \geq -|x|, x \in \mathbb{C}$ and Cauchy-Schwartz inequality, (s) is due to (67), (70), and $\|\hat{\mathbf{v}}_2^H \text{diag}(\bar{\mathbf{h}}_{2U}^H) \bar{\mathbf{H}}_{12}\|_2^2 = T_1 \left| \sum_{t=1}^{T_2} e^{j(-\Delta_{\overline{12}, \overline{2U}, t} - \angle(r_{\overline{12}, \overline{1U}}) + \Delta_{\overline{12}, \overline{2U}, t})} \right|_2^2 = T_1 T_2^2$. Clearly, we have $\gamma_{lb}^{(2)*} \leq \gamma^{(2)*} \leq \gamma_{ub}^{(2)*}$. As $\lim_{T_1, T_2 \rightarrow \infty}$

$\frac{\gamma_{ub}^{(2)*}}{L_{\overline{S1},\overline{12},\widetilde{2U}}T_ST_1T_2^2} = 1$ and $\lim_{T_1,T_2 \rightarrow \infty} \frac{\gamma_{lb}^{(2)*}}{L_{\overline{S1},\overline{12},\widetilde{2U}}T_ST_1T_2^2} = 1$, by the squeeze theorem, we have $\lim_{T_1,T_2 \rightarrow \infty} \frac{\gamma^{(2)*}}{L_{\overline{S1},\overline{12},\widetilde{2U}}T_ST_1T_2^2} = 1$, Thus, we can show $\gamma^{(2)*} \xrightarrow{T_1,T_2 \rightarrow \infty} L_{\overline{S1},\overline{12},\widetilde{2U}}T_ST_1T_2^2$.

Finally, consider Case 3. For all ϕ_1 and ϕ_2 , we have:

$$\begin{aligned}
\gamma^{(3)}(\phi_1, \phi_2) &\stackrel{(t)}{\leq} \gamma_{ub}^{(1)*} + \gamma_{ub}^{(2)*} - \gamma^{(0)} + L_{\overline{S1},\overline{12},\overline{2U}}|\mathbf{v}_2^H \text{diag}(\bar{\mathbf{h}}_{2U}^H) \bar{\mathbf{H}}_{12} \text{diag}(\mathbf{a}_{A,S1}) \mathbf{v}_1^*|^2 \|\mathbf{a}_{D,S1}^H\|_2^2 \\
&\quad + 2\sqrt{L_{\overline{S1},\overline{1U}}L_{\overline{S1},\overline{12},\overline{2U}}}|\mathbf{v}_2^H \text{diag}(\bar{\mathbf{h}}_{2U}^H) \bar{\mathbf{H}}_{12} \text{diag}(\mathbf{a}_{A,S1}) \mathbf{v}_1^*|\|\mathbf{a}_{D,S1}^H\|_2 \|\mathbf{v}_1^H \text{diag}(\bar{\mathbf{h}}_{1U}^H) \bar{\mathbf{H}}_{S1}\|_2 \\
&\quad + 2\sqrt{L_{\overline{S2},\overline{2U}}L_{\overline{S1},\overline{12},\overline{2U}}}|\mathbf{v}_2^H \text{diag}(\bar{\mathbf{h}}_{2U}^H) \bar{\mathbf{H}}_{12} \text{diag}(\mathbf{a}_{A,S1}) \mathbf{v}_1^*|\|\mathbf{a}_{D,S1}^H\|_2 \|\mathbf{v}_2^H \text{diag}(\bar{\mathbf{h}}_{2U}^H) \bar{\mathbf{H}}_{S2}\|_2 \\
&\quad + 2\sqrt{L_{\overline{S2}}L_{\overline{S1},\overline{12},\overline{2U}}}|\mathbf{v}_2^H \text{diag}(\bar{\mathbf{h}}_{2U}^H) \bar{\mathbf{H}}_{12} \text{diag}(\mathbf{a}_{A,S1}) \mathbf{v}_1^*| |r_{S1,SU}| \\
&\quad + 2\sqrt{L_{\overline{S1},\overline{1U}}L_{\overline{S2},\overline{2U}}} \|\mathbf{v}_2^H \text{diag}(\bar{\mathbf{h}}_{2U}^H) \bar{\mathbf{H}}_{S2}\|_2 \|\mathbf{v}_1^H \text{diag}(\bar{\mathbf{h}}_{1U}^H) \bar{\mathbf{H}}_{S1}\|_2 \\
&\stackrel{(u)}{\leq} \gamma_{ub}^{(1)*} + \gamma_{ub}^{(2)*} - \gamma^{(0)} + L_{\overline{S1},\overline{12},\overline{2U}}T_ST_1T_2^2 + 2\sqrt{L_{\overline{S1},\overline{1U}}L_{\overline{S1},\overline{12},\overline{2U}}}T_ST_1T_2 \\
&\quad + 2\sqrt{L_{\overline{S2},\overline{2U}}L_{\overline{S1},\overline{12},\overline{2U}}}T_ST_1T_2^2 + 2(\sqrt{L_{\overline{S2}}L_{\overline{S1},\overline{12},\overline{2U}}} + \sqrt{L_{\overline{S1},\overline{1U}}L_{\overline{S2},\overline{2U}}})T_ST_1T_2 \triangleq \gamma_{ub}^{(3)*},
\end{aligned}$$

where (t) is due to (71), (73), $\Re\{x\} \leq |x|$, $x \in \mathbb{C}$, and Cauchy-Schwartz inequality, and (u) is due to (67)-(70). On the other hand, we have:

$$\begin{aligned}
\gamma^{(3)}(\hat{\phi}_1, \hat{\phi}_2) &\stackrel{(v)}{\geq} \gamma_{lb}^{(1)*} + \gamma_{lb}^{(2)*} - \gamma^{(0)} + L_{\overline{S1},\overline{12},\overline{2U}}|\hat{\mathbf{v}}_2^H \text{diag}(\bar{\mathbf{h}}_{2U}^H) \bar{\mathbf{H}}_{12} \text{diag}(\mathbf{a}_{A,S1}) \hat{\mathbf{v}}_1^*|^2 \|\mathbf{a}_{D,S1}^H\|_2^2 \\
&\quad - 2\sqrt{L_{\overline{S1},\overline{1U}}L_{\overline{S1},\overline{12},\overline{2U}}}|\hat{\mathbf{v}}_2^H \text{diag}(\bar{\mathbf{h}}_{2U}^H) \bar{\mathbf{H}}_{12} \text{diag}(\mathbf{a}_{A,S1}) \hat{\mathbf{v}}_1^*|\|\mathbf{a}_{D,S1}^H\|_2 \|\hat{\mathbf{v}}_1^H \text{diag}(\bar{\mathbf{h}}_{1U}^H) \bar{\mathbf{H}}_{S1}\|_2 \\
&\quad - 2\sqrt{L_{\overline{S2},\overline{2U}}L_{\overline{S1},\overline{12},\overline{2U}}}|\hat{\mathbf{v}}_2^H \text{diag}(\bar{\mathbf{h}}_{2U}^H) \bar{\mathbf{H}}_{12} \text{diag}(\mathbf{a}_{A,S1}) \hat{\mathbf{v}}_1^*|\|\mathbf{a}_{D,S1}^H\|_2 \|\hat{\mathbf{v}}_2^H \text{diag}(\bar{\mathbf{h}}_{2U}^H) \bar{\mathbf{H}}_{S2}\|_2 \\
&\quad - 2\sqrt{L_{\overline{S2}}L_{\overline{S1},\overline{12},\overline{2U}}}|\hat{\mathbf{v}}_2^H \text{diag}(\bar{\mathbf{h}}_{2U}^H) \bar{\mathbf{H}}_{12} \text{diag}(\mathbf{a}_{A,S1}) \hat{\mathbf{v}}_1^*| |r_{S1,SU}| \\
&\quad - 2\sqrt{L_{\overline{S1},\overline{1U}}L_{\overline{S2},\overline{2U}}} \|\hat{\mathbf{v}}_2^H \text{diag}(\bar{\mathbf{h}}_{2U}^H) \bar{\mathbf{H}}_{S2}\|_2 \|\hat{\mathbf{v}}_1^H \text{diag}(\bar{\mathbf{h}}_{1U}^H) \bar{\mathbf{H}}_{S1}\|_2 \\
&\stackrel{(w)}{\geq} \gamma_{lb}^{(1)*} + \gamma_{lb}^{(2)*} - \gamma^{(0)} + L_{\overline{S1},\overline{12},\overline{2U}}T_ST_1T_2^2 - 2\sqrt{L_{\overline{S1},\overline{1U}}L_{\overline{S1},\overline{12},\overline{2U}}}T_ST_1T_2 \\
&\quad - 2\sqrt{L_{\overline{S2},\overline{2U}}L_{\overline{S1},\overline{12},\overline{2U}}}T_ST_1T_2^2 - 2(\sqrt{L_{\overline{S2}}L_{\overline{S1},\overline{12},\overline{2U}}} + \sqrt{L_{\overline{S1},\overline{1U}}L_{\overline{S2},\overline{2U}}})T_ST_1T_2 \triangleq \gamma_{lb}^{(3)*},
\end{aligned}$$

where (v) is due to (72), (74), $\Re\{x\} \geq -|x|$, $x \in \mathbb{C}$, and Cauchy-Schwartz inequality, and (w) is due to (67)-(70), and $|\hat{\mathbf{v}}_2^H \text{diag}(\bar{\mathbf{h}}_{2U}^H) \bar{\mathbf{H}}_{12} \text{diag}(\mathbf{a}_{A,S1}) \hat{\mathbf{v}}_1^*| = \left| \sum_{t=1}^{T_1} e^{j(-\Delta_{\overline{S1},\overline{12},t} - \angle(r_{\overline{S1},\overline{S2}}r_{\overline{S2},\overline{12}}) + \Delta_{\overline{S1},\overline{12},t})} \right|^2$ $\left| \sum_{t=1}^{T_2} e^{j(-\Delta_{\overline{12},\overline{2U},t} - \angle(r_{\overline{12},\overline{1U}}) + \Delta_{\overline{12},\overline{2U},t})} \right|^2 = T_1^2 T_2^2$. Clearly, we have $\gamma_{lb}^{(3)*} \leq \gamma^{(3)*} \leq \gamma_{ub}^{(3)*}$. As $\lim_{T_1,T_2 \rightarrow \infty} \frac{\gamma_{ub}^{(3)*}}{L_{\overline{S1},\overline{12},\overline{2U}}T_ST_1T_2^2} = 1$ and $\lim_{T_1,T_2 \rightarrow \infty} \frac{\gamma_{lb}^{(3)*}}{L_{\overline{S1},\overline{12},\overline{2U}}T_ST_1T_2^2} = 1$, by the squeeze theorem, we have $\lim_{T_1,T_2 \rightarrow \infty} \frac{\gamma^{(3)*}}{L_{\overline{S1},\overline{12},\overline{2U}}T_ST_1T_2^2} = 1$, Thus, we can show $\gamma^{(3)*} \xrightarrow{T_1,T_2 \rightarrow \infty} L_{\overline{S1},\overline{12},\overline{2U}}T_ST_1T_2^2$.

Therefore, we complete the proof of Statement (i). Furthermore, by substituting $T_1 = cT$ and $T_2 = (1 - c)T$ into Statement (i), we can easily show Statement (ii).

APPENDIX H: PROOF OF LEMMA 4

First, we prove Statement (i). By (17), we have $\bar{\gamma}^{(3)}(\phi_1, \phi_2) = \mathbf{v}_1^H \bar{\mathbf{G}}_1^H \bar{\mathbf{G}}_1 \mathbf{v}_1 + 2\Re\{\bar{\mathbf{G}}_1^H \bar{\mathbf{g}}_1\} + \bar{\mathbf{g}}_1^H \bar{\mathbf{g}}_1$ where $\bar{\mathbf{G}}_1 \triangleq \bar{\mathbf{H}}_{S1}^H \text{diag}(\sqrt{\alpha_{S1}\alpha_{1U}}\bar{\mathbf{h}}_{S1} + \sqrt{\alpha_{S1}\alpha_{12}\alpha_{2U}}\mathbf{B}_1^H \mathbf{v}_2)$ and $\bar{\mathbf{g}}_1^H \triangleq \sqrt{\alpha_{SU}}\bar{\mathbf{h}}_{SU}^H + \sqrt{\alpha_{S2}\alpha_{2U}}\bar{\mathbf{h}}_{2U}^H \text{diag}(\mathbf{v}_2^H)\bar{\mathbf{H}}_{S2}$. By Lemma 10, we can show that the unique optimal solution of Problem 6 is

$$\begin{aligned}\bar{\phi}_1^\dagger = \Lambda & \left(-\angle \left(\text{diag} \left(\sqrt{\alpha_{S1}\alpha_{1U}}\bar{\mathbf{h}}_{1U}^H + \sqrt{\alpha_{S1}\alpha_{1U}\alpha_{S1}\alpha_{12}\alpha_{2U}}\mathbf{v}_2^H \mathbf{B}_1 \right) \mathbf{a}_{A,S1} \right) \right. \\ & \left. - \angle \left(\mathbf{a}_{D,S1}^H \left(\sqrt{\alpha_{SU}}\bar{\mathbf{h}}_{SU} + \sqrt{\alpha_{S2}\alpha_{2U}}\bar{\mathbf{H}}_{S2}^H \text{diag}(\mathbf{v}_2)\bar{\mathbf{h}}_{2U} \right) \right) \mathbf{1}_{T_1} \right).\end{aligned}$$

Next, we prove Statement (ii). By (16), we have:

$$\begin{aligned}\bar{\gamma}^{(3)}(\phi_{2,t}, \phi_{2,-t}, \phi_1) & \stackrel{(a)}{=} 2\Re \left\{ e^{j\phi_{2,t}} \left(\sum_{k \in \mathcal{T}_2, k \neq t} \bar{C}_{2,t,k} e^{-j\phi_{2,k}} + \bar{d}_{2,t} \right) \right\} + \sum_{k \in \mathcal{T}_2, k \neq t} \sum_{i \in \mathcal{T}_2, i \neq t} \bar{C}_{2,k,i} e^{j(\phi_{2,k} - \phi_{2,i})} \\ & + \bar{C}_{2,t,t} + 2\Re \left\{ \sum_{k \in \mathcal{T}_2, k \neq t} e^{j\phi_{2,k}} \bar{d}_{2,k} \right\} + \gamma^{(0)},\end{aligned}$$

where (a) is due to $\bar{\mathbf{C}}_l = \bar{\mathbf{C}}_l^H$. As $(\phi_{2,-t}, \phi_1)$ is given, to solve Problem 7 is equivalent to solve:

$$\max_{\phi_{2,t} \in [0, 2\pi)} \Re \left\{ e^{j\phi_{2,t}} \left(\sum_{k \in \mathcal{T}_2, k \neq t} \bar{C}_{2,t,k} e^{-j\phi_{2,k}} + \bar{d}_{2,t} \right) \right\}.$$

Besides, we have:

$$\Re \left\{ e^{j\phi_{2,t}} \left(\sum_{k \in \mathcal{T}_2, k \neq t} \bar{C}_{2,t,k} e^{-j\phi_{2,k}} + \bar{d}_{2,t} \right) \right\} \stackrel{(b)}{\leq} \left| \sum_{k \in \mathcal{T}_2, k \neq t} \bar{C}_{2,t,k} e^{-j\phi_{2,k}} + \bar{d}_{2,t} \right|,$$

where (b) is due to $\Re\{x\} \leq |x|$, $x \in \mathbb{C}$ and holds with equality if and only if $\phi_{2,t} = -\angle \left(\sum_{k \in \mathcal{T}_2, k \neq t} \bar{C}_{2,t,k} e^{-j\phi_{2,k}} + \bar{d}_{2,t} \right)$. By noting that $\phi_{2,t} \in [0, 2\pi)$, the unique optimal solution of the equivalent problem is $\bar{\phi}_{2,t}^\dagger = \Lambda \left(-\angle \left(\sum_{k \in \mathcal{T}_2, k \neq t} \bar{C}_{2,t,k} e^{-j\phi_{2,k}} + \bar{d}_{2,t} \right) \right)$. Therefore, we complete the proof of Lemma 4.

REFERENCES

- [1] G. Ding, Y. Cui, L. Hu, F. Yang, L. Ding, and X. Xing Chen, “Optimal Quasi-Static phase shift design for a Double-IRS cooperatively assisted system,” *submitted to 2022 IEEE ICC*, Seoul, Korea (South), May., 2022.
- [2] Q. Wu and R. Zhang, “Towards smart and reconfigurable environment: Intelligent reflecting surface aided wireless network,” *IEEE Commun. Mag.*, vol. 58, no. 1, pp. 106–112, Nov., 2020.
- [3] E. Basar, M. Di Renzo, J. De Rosny, M. Debbah, M. S. Alouini, and R. Zhang, “Wireless communications through reconfigurable intelligent surfaces,” *IEEE Access*, vol. 7, pp. 116 753–116 773, sept., 2019.
- [4] C. Pan, H. Ren, K. Wang, W. Xu, M. Elkashlan, A. Nallanathan, and L. Hanzo, “Multicell MIMO communications relying on intelligent reflecting surfaces,” *IEEE Trans. Wireless Commun.*, vol. 19, no. 8, pp. 5218–5233, Aug., 2020.
- [5] H. Xie, J. Xu, and Y.-F. Liu, “Max-Min fairness in IRS-Aided Multi-Cell MISO systems with joint transmit and reflective beamforming,” *IEEE Trans. Wireless Commun.*, vol. 20, no. 2, pp. 1379–1393, Feb., 2021.
- [6] Y. Jia, C. Ye, and Y. Cui, “Analysis and optimization of an intelligent reflecting surface-assisted system with interference,” *IEEE Trans. Wireless Commun.*, vol. 19, no. 12, pp. 8068–8082, Dec., 2020.

- [7] Y. Jia, Y. Cui, and W. Jiang, "Robust optimization of instantaneous beamforming and quasi-static phase shifts in an IRS-assisted multi-cell network," *IEEE Trans. Wireless Commun.*, pp. 1–1, 2021.
- [8] Q. Wu and R. Zhang, "Intelligent reflecting surface enhanced wireless network via joint active and passive beamforming," *IEEE Trans. Wireless Commun.*, vol. 18, no. 11, pp. 5394–5409, Nov., 2019.
- [9] H. Guo, Y. Liang, J. Chen, and E. G. Larsson, "Weighted sum-rate maximization for reconfigurable intelligent surface aided wireless networks," *IEEE Trans. Commun.*, vol. 19, no. 5, pp. 3064–3076, May., 2020.
- [10] X. Yu, D. Xu, and R. Schober, "Enabling secure wireless communications via intelligent reflecting surfaces," in *2019 IEEE GLOBECOM*, Feb., 2019, pp. 1–6.
- [11] C. Huang, A. Zappone, G. C. Alexandropoulos, M. Debbah, and C. Yuen, "Reconfigurable intelligent surfaces for energy efficiency in wireless communication," *IEEE Trans. Wireless Commun.*, vol. 18, no. 8, pp. 4157–4170, Aug., 2019.
- [12] X. Yu, D. Xu, Y. Sun, D. W. K. Ng, and R. Schober, "Robust and secure wireless communications via intelligent reflecting surfaces," *IEEE J. Sel. Areas Commun.*, vol. 38, no. 11, pp. 2637–2652, Nov., 2020.
- [13] P. Wang, J. Fang, X. Yuan, Z. Chen, and H. Li, "Intelligent reflecting surface-assisted millimeter wave communications: Joint active and passive precoding design," *IEEE Trans. Veh. Technol.*, vol. 69, no. 12, pp. 14 960–14 973, Dec., 2020.
- [14] Y. Han, W. Tang, S. Jin, C. K. Wen, and X. Ma, "Large intelligent surface-assisted wireless communication exploiting statistical CSI," *IEEE Trans. Veh. Technol.*, vol. 68, no. 8, pp. 8238–8242, Aug., 2019.
- [15] C. Guo, Y. Cui, F. Yang, and L. Ding, "Outage probability analysis and minimization in intelligent reflecting surface-assisted MISO systems," *IEEE Commun. Lett.*, vol. 24, no. 7, pp. 1563–1567, Feb., 2020.
- [16] M. Zhao, A. Liu, Y. Wan, and R. Zhang, "Two-timescale beamforming optimization for intelligent reflecting surface aided multiuser communication with QoS constraints," *IEEE Trans. Wireless Commun.*, vol. 20, no. 9, pp. 6179–6194, Apr., 2021.
- [17] Z. Zhang, Y. Cui, F. Yang, and L. Ding, "Analysis and optimization of outage probability in multi-intelligent reflecting surface-assisted systems," Sept., 2019. [Online]. Available: <https://arxiv.org/abs/1909.02193>
- [18] Y. Gao, J. Xu, W. Xu, D. W. K. Ng, and M. Alouini, "Distributed IRS with statistical passive beamforming for MISO communications," *IEEE Commun. Lett.*, vol. 10, no. 2, pp. 221–225, Feb., 2021.
- [19] Y. Han, S. Zhang, L. Duan, and R. Zhang, "Cooperative Double-IRS aided communication: Beamforming design and power scaling," *IEEE Commun. Lett.*, vol. 9, no. 8, pp. 1206–1210, Aug., 2020.
- [20] W. Mei, B. Zheng, C. You, and R. Zhang, "Intelligent reflecting surface aided wireless networks: From single-reflection to multi-reflection design and optimization," Sept., 2021. [Online]. Available: <https://arxiv.org/abs/2109.13641>
- [21] C. You, B. Zheng, and R. Zhang, "Wireless communication via double IRS: Channel estimation and passive beamforming designs," *IEEE Commun. Lett.*, vol. 10, no. 2, pp. 431–435, Feb., 2021.
- [22] B. Zheng, C. You, and R. Zhang, "Efficient channel estimation for Double-IRS aided multi-user MIMO system," *IEEE Trans. Commun.*, vol. 69, no. 6, pp. 3818–3832, Jun., 2021.
- [23] B. Zheng, C. You, and R. Zhang, "Double-IRS assisted multi-user MIMO: Cooperative passive beamforming design," *IEEE Trans. Wireless Commun.*, vol. 20, no. 7, pp. 4513–4526, Feb., 2021.
- [24] Y. Han, S. Zhang, L. Duan, and R. Zhang, "Double-IRS aided MIMO communication under LoS channels: Capacity maximization and scaling," Feb., 2021. [Online]. Available: <https://arxiv.org/abs/2102.13537>
- [25] L. Dong, H. Wang, J. Bai, and H. Xiao, "Double intelligent reflecting surface for secure transmission with inter-surface signal reflection," *IEEE Trans. Veh. Technol.*, vol. 70, no. 3, pp. 2912–2916, Mar., 2021.
- [26] D. P. Bertsekas, *Nonlinear programming*. Athena scientific Belmont, MA, 1998.
- [27] K. Zhi, C. Pan, H. Ren, and K. Wang, "Statistical CSI-Based design for reconfigurable intelligent surface-aided massive MIMO systems with direct links," *IEEE Wireless Commun. Lett.*, vol. 10, no. 5, pp. 1128–1132, May., 2021.
- [28] J. R. Schott, *Matrix Analysis for Statistics*. Wiley, New York, 1997.

[29] D. Tse and P. Viswanath, *Fundamentals of Wireless Communication*. Cambridge University Press, 2005.